

Alma Mater Studiorum – Università di Bologna

DOTTORATO DI RICERCA IN  
Meccanica e Scienze Avanzate dell'Ingegneria  
Prog.3 Meccanica Applicata  
Ciclo XXV

**Settore Concorsuale di afferenza: 09/A2**

**Settore Scientifico disciplinare: ING-IND/13**

**Synthesis of Hand Exoskeletons for the  
Rehabilitation of Post-Stroke Patients**

**Presentata da:**

Ing. Mohammad Mozaffari Foumashi

**Coordinatore Dottorato:**

Prof. Vincenzo Parenti Castelli

**Relatore:**

Prof. Vincenzo Parenti Castelli

Ing. Marco Troncossi

**Esame finale anno 2013**



**Alma Mater Studiorum - Universit di Bologna**

**DOTTORATO DI RICERCA IN  
Meccanica e Scienze Avanzate dell'Ingegneria  
Prog.3 Meccanica Applicata  
Ciclo XXV**

**Settore Concorsuale di afferenza: 09/A2**

**Settore Scientifico disciplinare: ING-IND/13**

**SYNTHESIS OF HAND EXOSKELETONS FOR  
THE REHABILITATION OF POST-STROKE  
PATIENTS**

**Presentata da:**

Ing. Mohammad Mozaffari Fomashi

**Coordinatore Dottorato:**

Prof. Vincenzo Parenti Castelli

**Relatore:**

Prof. Vincenzo Parenti Castelli

Ing. Marco Troncosi

**Esame finale anno 2013**

I would like to dedicate this thesis to Neda and my loving parents

## Abstract

This dissertation presents the synthesis of a hand exoskeleton (HE) for the rehabilitation of post-stroke patients. Through the analysis of state-of-the-art, a topological classification was proposed. Based on the proposed classification principles, the rehabilitation HEs were systematically analyzed and classified. This classification is helpful to both understand the reason of proposing certain solutions for specific applications and provide some useful guidelines for the design of a new HE, that was actually the primary motivation of this study.

Further to this classification, a novel rehabilitation HE was designed to support patients in cylindrical shape grasping tasks with the aim of recovering the basic functions of manipulation. The proposed device comprises five planar mechanisms, one per finger, globally actuated by two electric motors. Indeed, the thumb flexion/extension movement is controlled by one actuator whereas a second actuator is devoted to the control of the flexion/extension of the other four fingers. By focusing on the single finger mechanism, intended as the basic model of the targeted HE, the feasibility study of three different 1 DOF mechanisms are analyzed: a 6-link mechanism, that is connected to the human finger only at its tip, an 8-link and a 12-link mechanisms where phalanges and articulations are part of the kinematic chain. The advantages and drawbacks of each mechanism are deeply analyzed with respect to targeted requirements: the 12-link mechanism was selected as the most suitable solution. The dimensional synthesis based on the Burmester theory as well as kinematic and static analyses were separately done for all fingers in order to satisfy the desired specifications. The results of the kinematic and static analysis confirmed the validity of the design.

The HE was finally designed and a prototype was built. The experimental results of the first tests are promising and demonstrate the potential for clinical applications of the proposed device in robot-assisted training of the human hand for grasping functions.

# Contents

<b>Contents</b>	<b>v</b>
<b>List of Figures</b>	<b>viii</b>
<b>List of Tables</b>	<b>xii</b>
<b>1 Introduction</b>	<b>1</b>
<b>2 The Classification</b>	<b>10</b>
2.1 Introduction . . . . .	10
2.2 Classification of Hand Exoskeletons . . . . .	11
2.2.1 Number of DOFs . . . . .	12
2.2.2 Number of MCs . . . . .	13
2.2.3 Mechanism Architecture . . . . .	15
2.2.3.1 External Mechanisms . . . . .	16
2.2.3.2 Lateral Mechanisms . . . . .	18
2.2.3.3 Internal Mechanisms . . . . .	19
2.3 Literature review and Discussion . . . . .	19
<b>3 The Feasibility Study</b>	<b>32</b>
3.1 Introduction . . . . .	32
3.2 Design Specification . . . . .	33
3.3 High level design choices . . . . .	35
3.3.1 Kinematic architectures . . . . .	35
3.3.2 Connection between HE and human fingers . . . . .	36
3.3.3 HE placement relative to the human hand . . . . .	37

3.3.4	Actuation . . . . .	38
3.3.5	Control and sensor equipment . . . . .	39
3.4	Feasibility study of HEs . . . . .	40
3.4.1	Technical specification . . . . .	40
3.4.2	Feasibility study of different architecture . . . . .	45
3.4.2.1	6-linkage mechanism . . . . .	46
3.4.2.2	8-linkage mechanism . . . . .	52
3.4.2.3	12-linkage mechanism . . . . .	54
3.5	Discussion . . . . .	55
<b>4</b>	<b>Synthesis, Analysis and Design of 12-Link mechanism</b>	<b>59</b>
4.1	Introduction . . . . .	59
4.2	Synthesis and Synchronization . . . . .	60
4.3	Kinematic Analysis . . . . .	65
4.4	Mechanical Design . . . . .	66
4.5	B.H.O. Prototype . . . . .	77
<b>5</b>	<b>The Experimental tests</b>	<b>83</b>
5.1	Introduction . . . . .	83
5.2	An EMG-based robotic hand exoskeleton for bilateral training of grasp . . . . .	83
5.2.1	System Description . . . . .	84
5.2.1.1	A graspable force sensorized object for rehabilitation applications . . . . .	84
5.2.1.2	EMG processing subsystem for grasp control . . . . .	84
5.2.2	The EMG-based robotic-assisted bilateral training . . . . .	86
5.2.2.1	Experiment description . . . . .	88
5.2.2.2	Experimental results . . . . .	88
5.3	A Motor Imagery BCI approach to robotic-assisted neuro-motor rehabilitation of reaching and hand grasping in stroke . . . . .	89
5.3.1	System Description . . . . .	90
5.3.1.1	The BRAVO Exoskeleton . . . . .	90
5.3.1.2	The integrated BCI system . . . . .	90

## CONTENTS

---

5.3.1.3	Control . . . . .	90
5.3.2	Experimental Evaluation . . . . .	92
5.3.2.1	Participants . . . . .	92
5.3.2.2	Procedure and methods . . . . .	92
5.3.3	Preliminary Results . . . . .	94
<b>6</b>	<b>Conclusions</b>	<b>98</b>
	<b>Appdx A</b>	<b>101</b>
	<b>References</b>	<b>118</b>

# List of Figures

1.1	BRAVO system architecture scheme. . . . .	7
2.1	Schematics of common mechanism architectures with one or three controlled DOFs and one or three MCs. . . . .	14
2.2	Distribution of the rehabilitation HEs found in literature among the possible solutions identified by the three classification principles. . . . .	26
3.1	A planar 3R serial chain is constrained by two RR chains to define a six-bar linkage. . . . .	47
3.2	Watt kinematic chain and schematic of the watt-chain-based mechanism. . . . .	48
3.3	5 configurations considered as reference for synthesis of 6-link mechanism. . . . .	49
3.4	A 3R chain connected to the human finger phalanges. . . . .	49
3.5	A 3R chain connected to the human finger phalanges. . . . .	50
3.6	A synthesized 6-link mechanism. . . . .	51
3.7	(a)8-link kinematic chain taken as reference for the synthesis of a finger mechanism; (b) schematic of the synthesized 8-link mechanism with revolute and prismatic pairs. . . . .	53
3.8	Schematic of a configuration of the synthesized 8-link mechanism. . . . .	54
3.9	Schematic of a configuration of the synthesized 8-link mechanism. . . . .	54
3.10	Schematic of a configuration of the synthesized 8-link mechanism. . . . .	55
3.11	(a) 12-link mechanism topology; (b) Schematic of the 12-link mechanism. . . . .	56

## LIST OF FIGURES

---

3.12 (a) 8-link mechanism topology; (b) Schematic of the 8-link mechanism for the thumb. . . . .	57
4.1 Index finger Configuration for different size hands (with respect to the height of the person) when grasping cylindrical objects of diameter 55, 70, 90 and 120 [mm] respectively . . . . .	62
4.2 Joint angle $\alpha$ in different size hands when grasping cylindrical objects of diameter 55, 70, 90 and 120 [mm] respectively. . . . .	63
4.3 Joint angle $\beta$ in different size hands when grasping cylindrical objects of diameter 55, 70, 90 and 120 [mm] respectively. . . . .	63
4.4 Joint angle $\gamma$ in different size hands when grasping cylindrical objects of diameter 55, 70, 90 and 120 [mm] respectively. . . . .	64
4.5 The names assigned to each revolute joint. . . . .	66
4.6 The forces between the mechanisms' links at different kinematic pairs. . . . .	67
4.7 The forces between the mechanisms' links at different kinematic pairs. . . . .	68
4.8 The modules and x,y components of the force in the joints Q and M.	69
4.9 The modules and x,y components of the force in the joints K and G.	70
4.10 The forces exerted to the human finger phalanges with respect to input link angle $\alpha$ [Degree].. . . .	71
4.11 The velocities [m/s] of each joint with respect to input link angle $\alpha$ [Degree]. . . . .	72
4.12 The velocities [m/s] of each joint of the mechanism with respect to input link angle $\alpha$ [Degree]. . . . .	73
4.13 The accelerations [m/s <sup>2</sup> ] of each joint of the mechanism with respect to input link angle $\alpha$ [Degree]. . . . .	74
4.14 The accelerations [m/s <sup>2</sup> ] of each joint of the mechanism with respect to input link angle $\alpha$ [Degree]. . . . .	75
4.15 Schematic CAD model of the B.H.O. hand exoskeleton . . . . .	77
4.16 Schematic CAD model of the B.H.O. hand exoskeleton . . . . .	78
4.17 Schematic CAD model of the B.H.O. hand exoskeleton . . . . .	79
4.18 The manufactured prototype of the B.H.O. hand exoskeleton . . . .	80

## LIST OF FIGURES

---

4.19	The manufactured prototype of the B.H.O. hand exoskeleton . . .	81
4.20	The manufactured prototype of the B.H.O. hand exoskeleton . . .	82
5.1	Conceptual scheme of the proposed system, (a) schematic overview (b) the captured picture. . . . .	85
5.2	The sensorized cylindrical object (left) showing the correspondance between each FSR and the fingers (right). . . . .	86
5.3	The sensor location of the EMG electrodes on the arm. Anterior surface (a.) and posterior surface (b.) of the left arm. . . . .	87
5.4	The setup for the experimental evaluation of the proposed system: side view (left) and top view (right). . . . .	87
5.5	Global data flow of the system. Dotted lines indicate either train- ing or evaluation information. . . . .	88
5.6	Grasping forces acquired by the sensorized objects during the ex- periment exerted by the left (dominant/healthy) and right (wear- ing the hand orthosis) hands. . . . .	89
5.7	The BRAVO hand exoskeleton . . . . .	91
5.8	Conceptual scenario for the reaching and grasping tasks proposed to the patients. . . . .	93
5.9	The grasping sequence. . . . .	94
5.10	Trajectories executed during the rehabilitation session for one patient	95
5.11	Sequence of movements performed by one patient under BCI con- trol: a→b reaching, c→d grasping, e return movement, f release .	96
1	A planar 3R serial chain is constrained by two RR chains to define a six-bar linkage. . . . .	101
2	A schematic of a planar 3R serial chain. The graph of this chain forms a straight line with a vertex for each link in the manipulator.	102
3	Examples of constrained 3R serial chain. . . . .	103
4	The Watt and Stephenson six-bar chains, and the different forms obtained by selecting different links as the base. . . . .	104
5	The linkage graphs show the synthesis sequence for the three con- strained 3R chains in which the two RR chains are attached inde- pendently. . . . .	105

## LIST OF FIGURES

---

6	The linkage graphs show the synthesis sequence for the four constrained 3R chains in which the second RR chain connects to the first RR chain. . . . .	106
7	The joint angle and link length parameters for the Watt Ia six-bar linkage. . . . .	111

# List of Tables

2.1	Current rehabilitation HEs classified according the three proposed principles. . . . .	20
2.2	Current rehabilitation HEs classified according the three proposed principles. . . . .	21
2.3	Current rehabilitation HEs classified according the three proposed principles. . . . .	22
2.4	Current rehabilitation HEs classified according the three proposed principles. . . . .	23
2.5	Current rehabilitation HEs classified according the three proposed principles. . . . .	24
2.6	Current rehabilitation HEs classified according the three proposed principles. . . . .	25
3.1	Thumb Joint Flexion (degrees) . . . . .	42
3.2	Index finger joint Flexion (degrees) . . . . .	42
3.3	Middle finger joint Flexion (degrees) . . . . .	43
3.4	Ring finger joint Flexion (degrees) . . . . .	43
3.5	Little finger joint Flexion (degrees) . . . . .	43
3.6	Coupling Ratio of DIP and PIP Joints . . . . .	44
3.7	Topology elements for 1 DOF planar mechanisms. . . . .	46
5.1	Results of the rehabilitation session . . . . .	96

# Chapter 1

## Introduction

The hand is an organ of grasp as well as of sensation, fine discrimination and exquisite dexterity. Unfortunately hand injuries are very common and the number of people suffering from that is considerable. These injuries include traumatic injuries, problems related to the aging (e.g. arthritic conditions), congenital deformities and the problems of a weak control of movement and force due to neurological diseases. The corresponding malfunctioning of the hand results in limitation in activities of daily living (ADLs). The importance of having a normally functioning hand for an independent and active life needs no emphasis. At the rehabilitation phase, well-established rehabilitation techniques rely on thorough and constant exercise (Diller [2000]). Early initiation of active movements by means of repetitive training proved its efficacy in guaranteeing a good level of recovery (Bütefisch et al. [1995]). The recovery of hand functioning is generally assisted by physical therapists that make the patients perform some exercises. These exercises are mainly concentrated on basic gross mobility skills such as moving specific joints and strengthening specific muscles. Further exercises, more complicated, can possibly be executed in order to allow the patient to recover the ability in ADLs. Quite often a few months are required to achieve acceptable improvement in finger movement and autonomous control. Therefore, the rehabilitation procedure is generally time consuming and costly. Moreover, due to the complexity of the neurological aspects involved in the upper-extremity control, permanent disabilities may unfortunately persist in the chronic phase (Olsen [1990]).

In the attempt to solve part of these problems, robot-assisted rehabilitation has known a significant growing in the last two decades. Many studies seem to demonstrate that robotic-aided therapy is more efficient and effective if compared to conventional therapy (see e.g. Prange et al. [2006], Brewer et al. [2007], Krebs et al. [2008], Kwakkel et al. [2008] and Mehrholz et al. [2009]). Although it is not still completely clear which factors specifically enhance recovery, it is commonly accepted that the success of robot-assisted therapy likely relies on the possibility offered by robotic systems to automate training exercises (that can prove exhausting for physical therapists), to deliver them in a highly repeatable way and to objectively estimate the rehabilitation progress by a number of reliable measurements (e.g. range of motion, strength, responsiveness to stimulation,...).

According to various types of hand problems, different rehabilitation protocols have been proposed. Obviously, also the design of the robotic systems strictly depends on the functions to be accomplished and the rehabilitation procedure to be implemented. Considering the implications on the exoskeleton design issues, three aspects of the rehabilitation protocols could be pointed out that can lead to completely different solutions: -global complexity of exercises: basic movements of the finger joints vs execution of ADLs; -complexity of the hand movements: gross motion of all the fingers vs single finger dexterity; -Rehabilitation environment: real environment vs virtual reality. It is worth noting that among the various strategies that have been clinically tested so far, the paradigm known as "assist-as-needed" seems to have received the greatest success. In a few words, the robotic device should provide as much force/movement assistance as needed to accomplish a given task, whereas, in order to maximize the patient's voluntary participation, it should enable the subject who does not need power assistance to move autonomously.

Since the 80's, many researchers have been attempting to develop robotic devices aiming at replicating the functions of the human hand, in the fields of industrial robotics, tele-manipulation, humanoid robotics, and upper limb prosthetics. A special kind of robotic hand is the active orthosis, also known as hand exoskeleton (HE). With respect to other kinds of robotic hands, a HE is an actuated mechanical system that is directly attached to the human hand, so that the movements of the two systems(HE and human hand) are coupled and forces/moments are

exchanged between them. In practice, a HE can apply forces to the fingers in order to (i) constrain them to perform a given trajectory, (ii) improve the forces that would be naturally exerted or (iii) reflect external forces. In the design of such devices, a number of critical issues related to the human-machine interaction must be considered. For instance, the control of the transmitted forces is mandatory for safety reasons, the motion of the HE links must be consistent with that of the human fingers, etc.

Depending on the specific applications, HEs exist that are extremely different, in both architectures and technological characteristics. For instance, some exoskeletons control the motion of each finger or group of linked fingers by coupling the movement of the anatomical joints together (Takahashi et al. [2005], Loureiro and Harwin [2007] and Hasegawa et al. [2008]), whereas others achieve the control of 4 DOFs per single finger, and up to 5 fingers (Wege and Hommel [2005] and Kitada et al. [1997]). A recent survey on the state-of-the-art about HEs is available in Mozaffari-Foumashi et al. [2011], Balasubramanian et al. [2010] and Mozaffari-Foumashi et al. [2010], with focus being placed on the kinematic description, the actuator systems, the transmission components and the control schemes. From the functional point of view, the HEs can be divided into 3 groups:

- Rehabilitation HEs
- Haptic Devices
- Assistive devices

Rehabilitation HEs (Takahashi et al. [2008], Loureiro and Harwin [2007], Wege and Hommel [2005], Yamaura et al. [2009], Kawasaki et al. [2007], Worsnopp et al. [2007], Fu et al. [2008], Mulas et al. [2005], Lucas et al. [2004], Chiri et al. [2009], Wang et al. [2009], Ertas et al. [2009], Ho et al. [2011], Burton et al. [2011], Li et al. [2011] and Wolbrecht et al. [2011]) are devices specifically developed to perform certain exercises for recovering the function lost by the hand. Haptic devices (Kitada et al. [1997], Choi and Choi [1999], Fontana et al. [2009], Simoncini et al. [2007], Fang et al. [2009], Nakagawara et al. [2005], Stergiopoulos et al. [2003], Lelieveld and Maeno [2006], Bouzit et al. [2002], Turki and Coiffet [1995], Sun et al. [2009] and Lord et al. [2011]) have two main functions: tracking

the wearer's hand movements for controlling some other device and providing a force feedback to the user's hand. These devices can be employed in a number of applications. Among them, it is worth recalling the use in Virtual Reality (VR) applications for rehabilitation purposes, where the patient controls a slave virtual device that can interact with an environment generated by a software simulator (Jack et al. [2001], and Cardoso et al. [2006]). The forces calculated from the VR model are reflected to the operator's human fingers by means of the exoskeleton actuators, thus causing a realistic human sensation of touch and force sensing. Assistive devices (Hasegawa et al. [2008], Sasaki et al. [2004], Kline et al. [2005], Shields et al. [1997], Tadano et al. [2010], and In et al. [2011]) are tools used by patients with hand diseases in everyday life, in order to perform activities that would be difficult or impossible to carry out without a supportive aid. Because of their specific application, they must be particularly lightweight and comfortable to wear. They may be also used for rehabilitation purposes.

In this study, the main focus is on the rehabilitation devices. Several research studies focused recently on both the development of novel robotic rehabilitation HE and the use of Virtual Reality technologies for rehabilitation. The former may overcome some of the major limitations that manual assisted movement training suffers from, i.e. lack of repeatability, lack of objective estimation of rehabilitation progress, and high dependence on specialized personnel availability. On the other hand, VR-based rehabilitation protocols may significantly improve the quality of rehabilitation by offering strong functional motivations to the patient, who can therefore be more attentive to the movement to be performed. Several studies (Jack et al. [2001]) have demonstrated positive effects of VR on rehabilitation, which enhances cognitive and executive functions of stroke patients (Cardoso et al. [2006]) by allowing them to receive enhanced feedback on the outcome of the rehabilitation tasks he/she is performing. Moreover, VR can provide an even more stimulating video game-like rehabilitation environment when integrated with force feedback devices and more specifically exoskeletons interfaces, thus enhancing the quality of the rehabilitation. However, VR presents the limit of not being able to guarantee a coherent alignment of visual and proprioceptive sensory stimulation. Stereoscopy, due to issues of patient's usability, is still not employed in rehabilitation training, and so the perception of depth

in the visual representation of the task should rely only on visual cues such as perspective, shadows and occlusions among objects. It has not been studied yet how this misalignment of sensory modalities can affect the functional recovery in stroke, since a quick adaptability of patients to such a sensory misalignment is observed as well.

For this reason and for accelerating the transfer in ADLs, it becomes more and more interesting being able to propose to the patient rehabilitation tasks in a real setting, with the active assistance provided by the robot. But in this scenario how is it possible to actively guide the impaired limb toward the object to be reached and grasped? In this context, the BRAVO project ("Brain computer interfaces for Robotic enhanced Action in Visuo-motOr tasks"), a project funded by IIT (Italian Institute of Technology), and developed by a number of partners, among which the PERCRO lab (Scuole Superiori S. Anna of Pisa) and GRAB laboratory (Department of Industrial Engineering, University of Bologna), aimed at enhancing the classical feedback control schemes through a novel neuro-feedback generated by a model of user's attention and gaze. Such additional feedbacks are introduced for predicting the intended action of the patient.

In this context, the BRAVO system proposes a new paradigm shift in the control of exoskeletons and active orthoses for rehabilitation and assistance in ADLs. The classical approach to rehabilitation and assistive robotics is based on a robot, whose action is activated by the user's movement detected by means of force and position sensing. This is not a reliable way of controlling the robot when the user is motor impaired and so can present spasticity, tremor, reduced motor function, muscle weakness. Current limitations of existing devices rely on the lack or reduced capability to predict the intended action of the patient. The innovative approach of BRAVO makes use of the information arising from the user's attention and intention, detected by means of eye-tracking, scene analysis and BCI, to enhance the motor assist by the prediction of user's intended movement.

Since sight normally anticipates movement, and movements of the eye are normally performed directing the gaze on the target before beginning the arm/hand's movement (Pfurtscheller and Lopes da Silva [1999]), this information can be used to enhance, ahead of the real start of movement, the user's bio-feedback to obtain and adaptable robot to user's behavior. In this respect, the robotic systems

developed within BRAVO are extremely innovative compared to already existing assistive technologies. Indeed, these systems are based on state of the art robotic technologies, e.g. exoskeletons, where classical feedback control schemes are adopted based on movement and force detection, but enhanced through a novel neuro-feedback generated by a model of user's attention and gaze and guided by user's eye-tracking.

The innovative approach proposed in BRAVO consists in using BCI and Eye Gaze Tracking (input systems) for predicting the user intentions and a robotic arm exoskeleton and hand orthosis (output systems) for assisting the user in performing the tasks. The final objective is to allow the use of robotic systems also to patients that suffer from hard neurological injuries that cannot be treated with traditional controlled robotic devices.

In Fig. 1.1 the architecture of the overall system is presented. The working principle is based on a set of input devices: eye tracking and cameras, position and force sensors and BCI. Such inputs are properly processed in order to recognize the object that the user has planned to grasp, the position of the object and the intention of starting the grasp closure. As for output, two output devices are used for assisting the user movements. The first one is an arm exoskeleton (Frisoli et al. [2009]) and the second one is a novel hand orthosis (Mozaffari-Foumashi et al. [2013]).

The system functionalities can be illustrated with reference to Fig. 1.1 through the following sequence of operations:

1. the user sits on a chair in front of a table with several objects that can be grasped with one hand
2. the user decides to grasp and move an object
3. the user looks toward the object that he/she is going to grasp
4. the eye tracking system will get the direction of gaze
5. the camera mounted on the user's head will identify the object

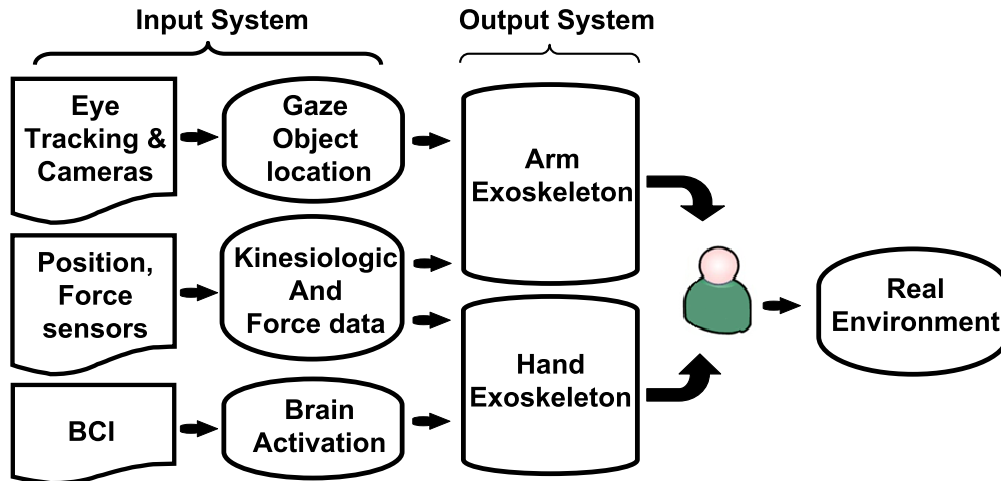


Figure 1.1: BRAVO system architecture scheme.

6. a second camera will detect the object position
7. the arm exoskeleton will be controlled in order to assist the user in reaching the object and orienting the hand for preparing the grasping phase
8. the user decides to close his hand
9. his intention is detected by the BCI
10. the hand orthosis will assist the user in the grasping movement

Object placing and hand opening will be assisted with analogous procedure. The development plan for the achievement of the complete system has divided into the following phases:

- Development of Reaching Control arm exoskeleton based on the eye gaze tracking
- Development of Grasping Control of the hand orthosis based on BCI
- Development of a novel hand orthosis

- Integration of the control and the robotic devices in a single multipurpose system

Within this framework, we were involved in the development of a rehabilitation HE. The analysis of the state-of-the-art was the first step of our activity, preceding the design phase. We therefore, proposed a systematic classification of the reviewed systems based on three main key issues, namely the number of controlled Degree of Freedoms (DOFs), the number of mechanical connections (MCs) with the human phalanges and the mechanism architecture. This classification is helpful to understand the reason of proposing certain solutions for the different applications and the advantages and drawbacks of the different designs proposed in the literature. In addition to this classification, many other design issues such as type of connection between HE and human fingers, safety factors, actuations/motors, control issues, sensor and encoder equipments are deeply discussed.

Returning to the primary motivation of this study, a novel HE device, called Bologna Hand Orthosis (B.H.O) was developed for the rehabilitation of the hand for post-stroke patients to support a cylindrical shape grasping tasks with the aim of recovering the basic functions of manipulation. Through the design phase, some preliminary decisions are made among a number of high level design specifications. Based on these decisions, the rehabilitation HE comprises five planar mechanisms, one per finger, globally actuated by two motors equipped with incremental encoders for implementing position/velocity control schemes. Indeed, the thumb flexion/extension movement along a certain plane is controlled by one actuator (motor and speed reducer) whereas a second actuator is devoted to the control of the flexion/extension of the other four fingers (being the four corresponding mechanisms connected to the same driving shaft). As for HE's finger mechanism, the feasibility study of three different 1 DOF mechanisms, intended as the basic model of the targeted hand exoskeleton, was developed, namely: a 6-link mechanism based on the Watt chain connected to the human finger only at his tip, an 8-link mechanism where phalanges and articulations are part of the kinematic chain (with three MCs points between the exoskeleton and the human finger, being these necessary to close the chain), and a 12-link mechanism where, again, all phalanges and finger articulations are part of the kinematic chain. The

advantages and drawbacks of each mechanism are deeply analyzed and, based on targeted requirements, the 12-link mechanism was selected as a suitable candidate for the single finger exoskeleton. After selecting the mechanism topology, the dimensional synthesis was done for 5 fingers in order to satisfy the desired constraints. As the same topology is used for the group of 4 fingers and all four fingers are actuated by the same 1 DOF actuator, the finger synchronization issue is taken into account in the synthesis procedure in order to guaranty the correct grasping. The kinematic and static analyses are also done in order to verify the kinematic constraints.

Eventually, the mechanical design (CAD model) and the manufactured prototype are presented. After designing and manufacturing the hand exoskeleton at Bologna University, the HE was delivered to PERCRO laboratory of the Scuola Superiore Sant'Anna in Pisa (Italy) for experimental tests. Two experimental tests are reported in this dissertation: the first one is testing the application of HE by using the EMG(Electromyography) signals for bilateral active training of grasp motion in stroke, and the second test is verifying the application of HE connecting to the arm exoskeleton for motor rehabilitation of reaching and hand grasping motion in stroke. The results show how manufactured HE can be successfully used, and how patients are able to perform assisted grasping tasks of simple objects successively.

# Chapter 2

## The Classification

### 2.1 Introduction

The literature proposes a number of rehabilitation HEs, which generally present some common characteristics and several special peculiarities concerning their mechanics, electronics (control) and working principles. Understanding the rationale at the basis of the solutions proposed so far, would help designers of new devices to take important decisions, even though it could result pretty difficult in a number of cases. Indeed, depending on the specific applications, HEs exist that are extremely different in both architectures and technological characteristics. For instance, from the kinematic point of view, in some exoskeletons only 1 or 2 DOFs result controllable (Mulas et al. [2005], WaveFlex-Hand [2011], Kinetec-Maestra-Hand [2011], Iqbal et al. [2010], Schabowsky et al. [2010], Ren et al. [2009], Kutner et al. [2010], Takahashi et al. [2008], Ertas et al. [2009], Rosati et al. [2009], Wolbrecht et al. [2011], Wu et al. [2010] and Yamaura et al. [2009]), being some fingers linked together and/or the movement of the anatomical joints coupled, whereas other systems achieve the control of 4 DOFs per single finger and for up to 5 fingers (Wege and Hommel [2005]), and still others leave some joints uncontrolled (resulting in under-actuated mechanisms)(Chiri et al. [2009]). The driving power is typically generated by electric or pneumatic actuators (Heo et al. [2012]), and transmitted in several different ways such as by cables and pulleys, linkage with rigid members, tendon-driven mechanisms, geared systems, etc. Also the control

strategies and the sensor systems can be extremely different, the most important issue likely being the sensing method to catch the user's intention (e.g. from EMG or EEG signals) as comprehensively illustrated in [Heo et al. \[2012\]](#).

Due to this variability, a methodical analysis of the literature can help to identify useful guidelines: from this standpoint the surveys presented by [Balasubramanian et al. \[2010\]](#) and [Heo et al. \[2012\]](#) respectively focus on the technical specifications and clinical applications of rehabilitation HEs and on actuators and control strategies of rehabilitation and assistive HEs. Complementary to these works, the present chapter proposes a systematic classification of the exoskeletons based on their kinematic characteristics and their coupling with the human hand, i.e. on those topological aspects that have a major influence on the synthesis of the exoskeleton mechanisms. This analysis, focused on rehabilitation HEs though significant also for assistive and haptic devices, is helpful to understand both the reasons of proposing certain solutions for the different applications and the advantages and drawbacks of the diverse designs proposed in the literature. The final purpose of the proposed classification is then to provide guidelines useful for the design of new HEs on the basis of a systematic analysis.

### 2.2 Classification of Hand Exoskeletons

From the literature analysis it emerges that the best possible device probably does not exist, because the complexity of the overall problem prevents unique design principles to be determined and unambiguous design guidelines to be defined. Depending on the specific application, the designer of a new HE must face a wide range of interconnected choices ([Troncossi et al. \[2012\]](#)), such as the number of DOFs, the mechanism topology, the transmission system, the control strategy and sensor system, etc. A certain decision on each issue entails both advantages and drawbacks and also it affects other aspects of the design. Moreover, since several design specifications and objectives are often in contrast, a trade-off must be defined, with weighting factors depending on both the specific application and the designers' sensitivity and experience. Design choices can be effectively done if they are supported by a methodical analysis of the main problems and the cor-

responding solutions, also considering what solutions other designers/researchers have already proposed. In this perspective, focusing on the kinematics of the exoskeleton, the authors present a topological classification of the widely heterogeneous solutions that can be theoretically proposed (illustrated in this Section) and review the existent literature based on it. The exoskeleton mechanism of a single finger is considered as the basic unit to analyze, thus making it possible to systematically categorize all the possible solutions achievable to form a HE. In particular, the attention is placed on the index finger mechanism since it is the only finger present in all the rehabilitation HEs, and the other finger mechanisms generally have the same kinematic characteristics. Three main key issues selected as discriminating characteristics for distinguishing different solutions are systematically investigated since they correspond to the high-level design choices that have the major consequences on the topological and dimensional synthesis of the exoskeleton mechanisms. They are:

- the number of controlled DOFs;
- the number of mechanical connections (MCs) with the human phalanges;
- the mechanism architecture.

### 2.2.1 Number of DOFs

From the mechanical design viewpoint, the first specification to define concerns the kinematics of the system. Indeed, the designer must firstly choose:

- how many finger mechanisms will form the overall HE, and how many of them must be controlled independently;
- the number of active DOFs of the mechanism that guides the functions of a single finger (that is, from the dual viewpoint, the number of articulation movements that can be possibly coupled or left free in each finger).

Indeed, according to the human hand anatomy, a HE can fully control a human hand only if it has 20 actuated DOFs (4 DOFs per finger). On the other side, it should be taken into account that both the hardware and control procedure

of the resulting device could be very complex. Alternative solutions can be thus obtained by accepting a worsening of the system versatility and by controlling less DOFs of the hand/fingers, thus reducing the global complexity of the system. The choice about this fundamental feature depends on the trajectories to be followed, the force(s) to be applied and/or measured on the human fingers, the required versatility, and the control strategies to be implemented. The possible combinations of DOFs are uncountable and the literature offers a wide range of solutions, ranging from a passive device where no actuator is present [Brokaw et al. \[2011\]](#) to a HE able to fully control the movements of the five fingers with its 20 DOFs ([Wege and Hommel \[2005\]](#)). Intermediate solutions foresee to possibly couple the movements of phalanges and fingers and/or leaving them free (i.e. uncontrolled). In order to define a systematic criterion of classification, the attention can be placed on the number of controlled DOFs of the index finger mechanism, thus providing five different groups of HEs, with 0 (for passive devices) to 4 DOFs per finger.

Figure 2.1 shows some schemes that illustrate the topological differences of finger exoskeleton mechanisms: from the mobility viewpoint, the reported solutions have 1 or 3 controlled DOFs (the star symbol representing an actuated joint). For the sake of graphical simplicity, the possibility of actuating the abduction/adduction movement is not reported among the schemes. It is worth noting that the mechanisms in Fig. 2.1 (e, i, k) are under-actuated, i.e. the number of DOFs controlled with actuators is smaller than the kinematic DOFs of the mechanism (as counted e.g. by the Grubler-Kutzbach formula).

### 2.2.2 Number of MCs

The HEs are connected to the human finger phalanges to control the movement of fingers and to exert force/moment on them. For safety reasons, the imposed movements must be consistent with the physiological ones (i.e. the natural range of motion of the human articulations must be respected) and the loads transmitted to the human finger must be limited. In this respect, the most important decision concerns the number of connections of the HE with each finger. Based

## 2. The Classification

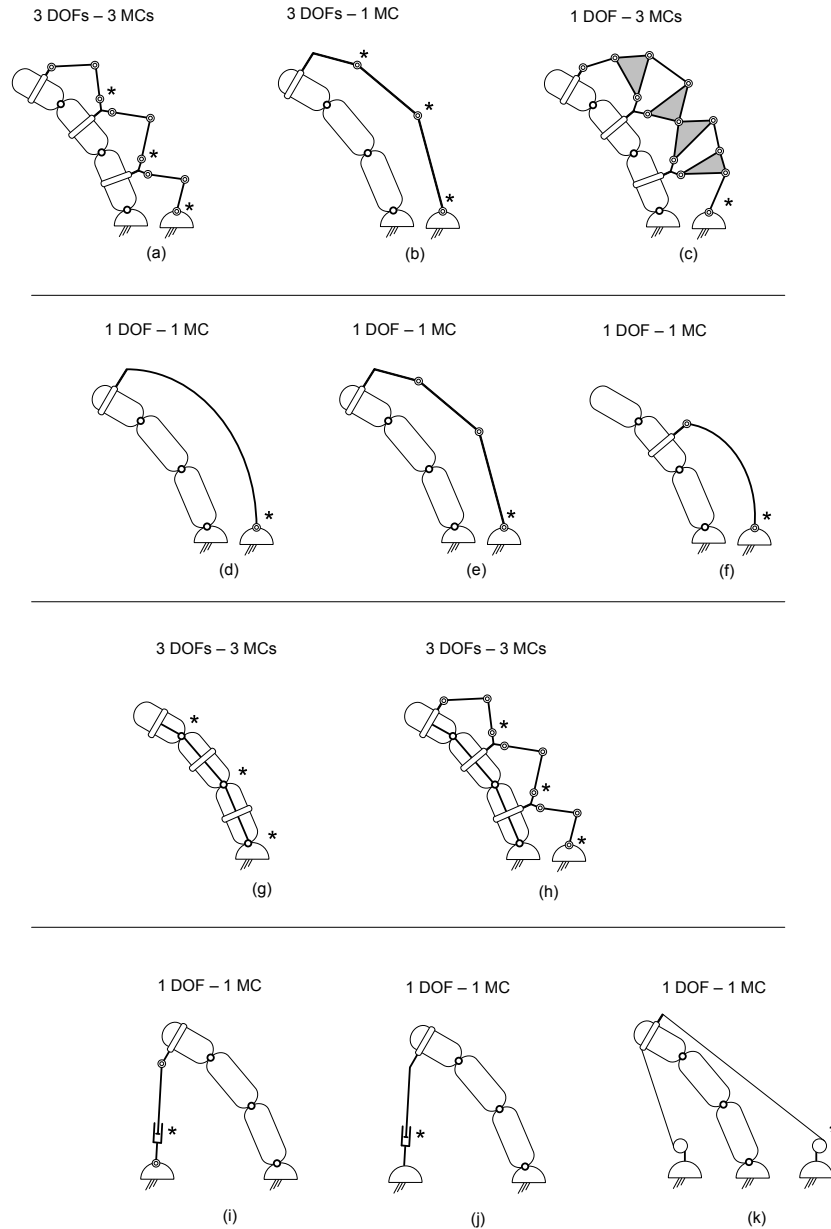


Figure 2.1: Schematics of common mechanism architectures with one or three controlled DOFs and one or three MCs. The star symbols indicated actuated joints. (a) External/Integrated; (b) External/Stand-Alone; (c) External/Integrated; (d) External/Stand-Alone; (e) External/Integrated (this mechanism is under-actuated); (f) External/Integrated; (g, h) Lateral; (i-k) Internal (being the first case an under-actuated mechanism).

on the number of MCs, three different groups can be identified, i.e. HEs with 1, 2 or 3 MCs per finger. This classification principle is mainly important for the topological synthesis of the mechanisms in the design phase as well as for control issues and for practical aspects, e.g. the easiness of wearability during the initial fitting. In Fig. 2.1 solutions with 1 or 3 MCs are reported as examples, showing the variety that can be achieved by differently combining DOFs and MCs.

The exoskeleton can be attached to the finger by different means. The most common and simple methods are attaching the mechanism to human finger by using flexible straps or rigid links wrapped around the phalanges, and/or thimbles fixed to the human fingertip. Another possible solution is using a glove as an intermediate mean. In this case, the user wears the glove (possibly instrumented with sensors) and the HE is connected to the glove ([Festo-Company \[2012\]](#)). It is worth noting that the stiffness of the connection can be a significant factor in different perspectives. A flexible strap can slightly move with respect to the phalanx, thus determining variable contact areas that can negatively affect the controllability and the accuracy of the system when following certain trajectories. On the other hand, a flexible strap is easier to fix during the initial fitting with respect to a stiffer solution (e.g. a metal ring), it is inherently safer (the compliance can play as a mechanical filter of forces) and, due to its intrinsic adaptability, it lets the HE accommodate slightly different hand sizes without the possible need to change the HE geometry.

### 2.2.3 Mechanism Architecture

With "architecture" we mean the topology and geometry of a mechanism as well as some main characteristics of the power transmission chain. When observing a HE, the general impression is dominated by the global features of the mechanism architecture, that show the main designers' choices. Reviewing the literature based on the analysis of the mechanism architecture could be difficult due to the several variable aspects involved, e.g. the solutions adopted to transmit/reduce motion, the placement of the actuators, the position of the mechanism links relative to the human finger 2.1.

For systematically classifying the extremely different kinds of mechanism that can be adopted as hand/finger exoskeletons, the placement of the mechanisms with respect to human fingers is here considered as the most significant issue. The main reason is the strong impact of this factor (i) on topological and dimensional synthesis of the mechanism and (ii) on the solution to transmit power from the exoskeleton actuators to the human fingers. In addition, the boundary conditions and the constraints that arise from the placement of the mechanism (e.g. interference avoidance) play an important role in the design phase. The HEs can be thus categorized according to the finger mechanism placement with respect to human finger in three groups, conventionally denoted as (i) External Mechanisms (placed externally to the hand backside, Fig. 2.1 (a-f)), (ii) Lateral Mechanisms (located at the side of the finger, Fig. 2.1 (g-h)), and (iii) Internal Mechanisms (placed in the internal side of the hand palm, Fig. 2.1 (i-k)).

### 2.2.3.1 External Mechanisms

With this expression, exoskeletons placed externally to the hand backside are intended, i.e. mechanisms whose links remain above the human finger phalanges for the full range of motion in order to avoid interference with both the human counterparts and the grasped object. This means that in the synthesis of the mechanism important geometrical constraints are fixed (e.g. the links must stay in the finger backside semi-space and avoid interference with the human phalanges), with obvious consequences and limitations. Two approaches can be adopted to make the finger follow targeted trajectories, and a corresponding "sub-classification" can be thus proposed for this group: (i) Integrated Mechanisms, where the human finger phalanges and articulations are integrating parts of the system kinematic scheme, i.e. they serve as links and joints of the resulting mechanisms, as for instance the case of Fig. 2.1 (a) and (ii) Stand-Alone Mechanisms, where the human finger phalanges are attached to some moving links of a mechanism that works autonomously, as for instance in Fig. 2.1(b).

- Integrated Mechanisms

The HE moves the fingers by means of mechanisms which include the human fingers themselves as integrating parts in the kinematic scheme. The concept can be easily explained referring to Fig. 2.1 (f), where the control of the distal phalanx motion is not of interest (i.e. it is kept free) whereas the movements of the proximal and middle phalanges are coupled, being part of a four-bar linkage made of the 2 phalanges themselves, 2 artificial links, 2 artificial revolute joints and 2 human articulations (considered as revolute joints as well). Many other linkage can be formed in a similar way (e.g. see Fig. 2.1 (a, c, e, f)), as those proposed for the rehabilitation HEs presented in [Mulas et al. \[2005\]](#), [Schabowsky et al. \[2010\]](#), [Iqbal et al. \[2010\]](#), [Sarakoglou et al. \[2004\]](#), [Yamaura et al. \[2009\]](#), [Ito et al. \[2011\]](#), [Wege and Hommel \[2005\]](#) and [Wang et al. \[2009\]](#).

A special care must be taken in order to respect the natural range of motion of the human articulations (e.g. hyperextension must be avoided), for safety reasons. This means that in the mechanism synthesis the phalanx poses should be checked all along the resulting trajectory.

- Stand-Alone Mechanisms

The kinematic chain of the stand-alone mechanisms is completely determined without the need of human finger parts. One or more phalanges are fixed to some link of the mechanism without introducing further DOFs or further constraints. An example easy to illustrate is reported in Fig. 2.1 (b): the end-effector of a planar four-link serial manipulator with 3 DOFs controls the pose of the human fingertip that is attached to it. The introduction of the human finger in the kinematic scheme of the mechanism (two additional links and three revolute joints) does not change the mobility of the system (see also Fig. 2.1 (d)). From a mechanical point of view, things are more complex when there are more MCs so that intermediate links of the mechanism are connected to two or three phalanges (while remaining always external to the hand backside) and must make them rotate around their natural motion axis according to given trajectories. In other words, it is necessary to make the relative rotation axes of the artificial links coincide with the relative rotation axes of the corresponding phalanges. The

so-called remote center of motions mechanisms (RCMs) can be used to solve the problem. These mechanisms are able to implement the rotation of a body around a fixed axis that is remotely located from the structure of the joint while avoiding interference. Different mechanism topologies are available to achieve this task (Zong et al. [2008]) and are used in several applications. Existent rehabilitation HEs that include these kind of mechanisms use linkage-based RCMs (Wolbrecht et al. [2011] and Fu et al. [2008]), geared systems (Wang et al. [2009]) or circular prismatic joints (Ho et al. [2011]).

It is worth mentioning another -completely different- kind of External Mechanisms, namely the devices where deformable bodies are pneumatically actuated and drive the finger motion. The actuators (artificial muscles) are connected to the human hand and the deformation of the flexible body provides the human fingers with movement. Depending on the presence or absence of an artificial structure connected to the artificial muscles, this architecture can be either Stand-Alone or Integrated (in the last case the human fingers provide the skeletal structure). The main characteristics of this solution are a fairly poor accuracy in spite of a great simplicity and lightness (two aspects particularly important for assistive devices(Wu et al. [2010])). Currently, no rehabilitation HE presents this architecture.

### 2.2.3.2 Lateral Mechanisms

The simplest way to make the rotation axes of the artificial links and human phalanges coincide is to place the physical revolute joints of the exoskeleton at the level of the human articulations, beside the finger (as shown in Fig. 2.1 (g, h), so that no RCM mechanism is required, for the sake of the superior simplicity of this architecture with respect to the other solutions. The distinction between Integrated and Stand-Alone Mechanisms would be theoretically possible, but it makes no practical sense since the good qualities of this architecture are relative to stand-alone mechanisms only.

### 2.2.3.3 Internal Mechanisms

In this kind of architecture, some exoskeleton components are situated in the user's palm region. The distinction between Integrated and Stand-Alone Mechanisms would be theoretically possible also in this case, but it not very significant since the main advantage of this option is the possibility to use cables (or linear actuators) and pull (and/or push) the fingertips to provide the fingers with motion in a very simple way (Fig. 2.1 (i-k)): therefore the human segments are integrating parts of the system.

## 2.3 Literature review and Discussion

Table 2.1 provides the survey of the existent rehabilitation HEs organized according to the three proposed classification principles. Information relative to the number of finger mechanisms forming the HE and the total number of DOFs of the overall system are also reported as well as some notable remarks. Fig. 2.2 reports the same data arranged in such a way to appreciate the variability and the distribution of the numerous combinations of DOFs, MCs and mechanism architectures present in the literature.

The number of active DOFs is probably the main aspect characterizing a certain solution. From the literature analysis summarized in table 2.1 and Fig. 2.2 it emerges that:

- index finger mechanism with 1 active DOF is the most widespread adopted solution. In particular the quantities of rehabilitation HEs classified based on the number of controlled DOFs are one (Brokaw et al. [2011]), thirteen (WaveFlex-Hand [2011], Kinetec-Maestra-Hand [2011], Mulas et al. [2005], Ho et al. [2011], Iqbal et al. [2010], Schabowsky et al. [2010], Chiri et al. [2009], Ren et al. [2009], Kutner et al. [2010], Takahashi et al. [2008], Ertas et al. [2009], Rosati et al. [2009] and Wolbrecht et al. [2011]), seven (Fu et al. [2008], Sarakoglou et al. [2004], Wu et al. [2010], Yamaura et al. [2009], Loureiro and Harwin [2007], Burton et al. [2011] and Festo-Company

## 2. The Classification

Table 2.1: Current rehabilitation HEs classified according the three proposed principles.

References	Index Finger active DOFs	MCs	Mechanism Architecture	Fingers per HE	HE active DOFs	Notes
Brokaw et al. [2011]	0	2	Lateral Mechanisms	2	0	The mechanism actuates the flexion/extension movement of index MCP joint and thumb CMC joint
WaveFlex-Hand [2011]	1	1	External Mechanisms - Stand alone	1	1	The mechanism actuates the flexion/extension movement of MCP and PIP joints of all fingers one by one (not simultaneously)
Kinetec-Maestra-Hand [2011]	1	1	External Mechanisms - Stand alone	4	1	The mechanism actuates the flexion/extension movement of 4 fingers simultaneously
Mulas et al. [2005]	1	1	External Mechanisms - Stand alone	5	2	The mechanism actuates the flexion/extension movement of 4 fingers simultaneously (fingertip of all fingers are connected rigidly together)

## 2. The Classification

Table 2.2: Current rehabilitation HEs classified according the three proposed principles.

References	Index Finger active DOFs	MCs	Mechanism Architecture	Fingers per HE	HE active DOFs	Notes
Ho et al. [2011]	1	1	External Mechanisms - Stand alone	5	5	The movement of MCP and PIP are coupled.
Iqbal et al. [2010]	1	1	External Mechanisms - Integrated Mechanisms	2	2	4 link serial manipulator
Schabowsky et al. [2010]	1	2	External Mechanisms - Integrated Mechanisms	5	2	The combination of 4 fingers is controlled with 1 motor, The movement of MCP and PIP joints are coupled.
Chiri et al. [2009]	1	3	External Mechanisms - Integrated Mechanisms (MCP joint) and Lateral Mechanisms (PIP and DIP joints)	5	5	The movement of the finger joints are coupled and actuated by 1 motor (elastic under-actuated mechanism)

## 2. The Classification

Table 2.3: Current rehabilitation HEs classified according the three proposed principles.

References	Index Finger active DOFs	MCs	Mechanism Architecture	Fingers per HE	HE active DOFs	Notes
Rosenstein et al. [2008]	1	1	Lateral Mechanisms	4	1	
Takahashi et al. [2005]	1	1	Lateral Mechanisms	5	2	
Ertas et al. [2009]	1	3	External Mechanisms - Stand alone	1	1	
Oboe et al. [2010]	1	1	External Mechanisms - Stand alone	4	1	
Wolbrecht et al. [2011]	1	2	External Mechanisms - Stand alone	1	1	
Fu et al. [2008]	2	3	External Mechanisms - Stand alone	4	8	-The flexion/extension movement of DIP,PIP and MCP joints are coupled -The abduction/adduction of MCP joint is actuated by another motor

## 2. The Classification

Table 2.4: Current rehabilitation HEs classified according the three proposed principles.

References	Index Finger active DOFs	MCs	Mechanism Architecture	Fingers per HE	HE active DOFs	Notes
Wu et al. [2010]	2	2	External Mechanisms - Integrated Mechanisms	4	2	The flexion movement provided by pneumatic actuator and the extension movement provided by torsion spring
Yamaura et al. [2009]	2	3	External Mechanisms - Integrated Mechanisms	1	2	The movement of DIP and PIP joints are coupled
Loureiro and Harwin [2007]	2	2	Lateral Mechanisms	5	3	2 DOFs (flexion/extension of MCP and PIP joints), the DIP joints of fingers are kept free
Burton et al. [2011]	2	3	External Mechanisms - Integrated Mechanisms (MCP joint) and Lateral Mechanisms (PIP and DIP joints)	5	10	The joints that are actuated with one motor and different pulleys: -MCP joints of index and middle - DIP and PIP joints of index and middle -MCP joints of ring and little - DIP and PIP joints of ring and little

## 2. The Classification

---

Table 2.5: Current rehabilitation HEs classified according the three proposed principles.

References	Index Finger active DOFs	MCs	Mechanism Architecture	Fingers per HE	HE active DOFs	Notes
Festo-Company [2012]	2	3	External Mechanisms - Stand alone	5	8	2 DOFs for thumb, 2 DOFs for index(1 flexion/extension and 1 abduction/adduction), 1 DOF for middle, 1 DOF for ring and 1 DOF for little finger
Ito et al. [2011]	3	3	External Mechanisms - Integrated Mechanisms	5	15	2 DOFs flexion/extension (MCP and PIP joints), 1 DOF abduction/adduction movement
Worsnopp et al. [2007]	3	3	Lateral Mechanisms	1	3	6 motors per finger, 3 for the flexion and 3 for the extension movement
Wege and Hommel [2005]	4	3	External Mechanisms - Integrated Mechanisms	5	20	

## 2. The Classification

Table 2.6: Current rehabilitation HEs classified according the three proposed principles.

References	Index Finger active DOFs	MCs	Mechanism Architecture	Fingers per HE	HE active DOFs	Notes
Li et al. [2011]	4	3	External Mechanisms - Integrated Mechanisms	2	8	
Wang et al. [2009]	4	3	External Mechanisms - Integrated Mechanisms	1	4	
Fu et al. [2011]	4	3	External Mechanisms - Stand alone	2	8	
Sarakoglou et al. [2004]	2	2	External Mechanisms - Integrated Mechanisms	5	9	2 DOFs for each finger and 1 DOF for thumb
Ren et al. [2009]	1	1	Lateral Mechanisms	5	2	The mechanism of a four-bar linkage used to generate hand opening and closing motion

## 2. The Classification

		DOFs					
		1	2	3	4		
<b>External Mechanisms</b>	<b>Integrated</b>	MCs	1	2 devices Mulas et al. [2005] Iqbal et al. [2010]			
			2	1 device Schabowsky et al. [2010]	2 devices Sarakoglou et al. [2004] Wu et al. [2010]		
			3		1 device Yamaura et al. [2009]	1 device Ito et al. [2011]	3 devices Wege and Hommel [2005] Li et al. [2011] Fu et al. [2011]
<b>Stand-Alone</b>		MCs	1	3 devices WaveFlex-Hand Kinetec-Maestra-Hand Rosati et al. [2009]			
			2	2 devices Song and Tong [2005] Wolbrecht et al. [2011]			
			3		1 device Wang et al. [2009]		1 device Fu et al. [2011].
<b>Internal Mechanisms</b>		MCs	1	1 device Bouzit et al. [2002]			
			2				
			3				
<b>Lateral Mechanisms</b>		MCs	1	3 devices Ren et al. [2009] Kutner et al. [2010] Takahashi et al. [2008]			
			2		1 device Loureiro and Harwin [2007]		
			3	2 devices Chiri et al. [2009] Ertas et al. [2009]	2 devices Burton et al. [2011] Festo-ExoHand	1 device Worsnopp et al. [2007]	

Figure 2.2: Distribution of the rehabilitation HEs found in literature among the possible solutions identified by the three classification principles.

[2012]), two (Ito et al. [2011] and Worsnopp et al. [2007]), and four (Wege and Hommel [2005], Li et al. [2011], Wang et al. [2009] and Fu et al. [2011]) for the five groups ranging from 0 to 4 DOFs respectively;

- apart from the four HEs conceived to fully control the movement of the human finger (Wege and Hommel [2005], Li et al. [2011], Wang et al. [2009] and Fu et al. [2011]), the abduction/adduction of the first phalanx is actuated in very few cases (Fu et al. [2008], Festo-Company [2012] and Ito et al. [2011]);
- the last phalanx is left free (i.e. uncontrolled, as in Fig. 2.1 f) in a significant number of HEs (Ho et al. [2011], Iqbal et al. [2010], Schabowsky et al. [2010], Ren et al. [2009], Kutner et al. [2010], Takahashi et al. [2008], Rosati et al. [2009], Wolbrecht et al. [2011], Fu et al. [2008], Sarakoglou et al. [2004] and Loureiro and Harwin [2007]). In addition under-actuated mechanisms are adopted in Chiri et al. [2009] where the number of actuators is smaller than the DOFs of the mechanisms (as in the schemes of Fig. 2.1(e, i, k)) so that one or more DOFs are indirectly controlled by the dynamic behavior of the mechanical system exploiting the natural stiffness of the human articulations;
- the physical coupling of the four human fingers (excluding the thumb) by means of rigid links is adopted in nine HEs (Kinetec-Maestra-Hand [2011], Mulas et al. [2005], Schabowsky et al. [2010], Ren et al. [2009], Kutner et al. [2010], Takahashi et al. [2008], Rosati et al. [2009], Wu et al. [2010] and Loureiro and Harwin [2007]);
- active control in a single directions (to actively control the flexion or the extension movements, (but not both) is a fairly common option. In many rehabilitation exercises for post-stroke patients the main movement to be recovered is the finger extension, due to the possible presence of a residual contracting force that tends to maintain the hand closed. In this situation, the design of a system with actuators simply devoted to assist patients in opening the hand only is reasonable (whereas the closing phase is supported by springs or left uncontrolled at all): a number of solutions leading to

simple mechanism architectures are available (mostly using cable-driven transmissions);

- among the commercial solutions, three ones have 1 DOF finger mechanism with a very simple architecture ([WaveFlex-Hand \[2011\]](#), [Kinetec-Maestra-Hand \[2011\]](#) and [Kutner et al. \[2010\]](#)) whereas the Exohand by [Festo-Company \[2012\]](#) presents index and thumb finger exoskeletons with 2 DOFs each (abduction/adduction of the first phalanx and the coupled flexion/extension of the three phalanges) and the other three fingers with 1 DOF for the coupled flexion/extension of the phalanges.

The choice of the number of DOFs of a single finger mechanism and the number of fingers to independently control (i.e. the total number of actuators for the HE) seems to strictly depend on the target application of HEs, i.e. the kind of rehabilitation program and training exercises that must be performed. As a general rule, complex tasks require a good versatility of the finger exoskeletons to accomplish different movements, so that several active DOFs are required. The consequence of this option is the weight and the control complexity of the resulting HE, increasing with the number of actuators. Most of the solutions found in the literature seem to reflect the preference for the simplicity of the system, which is consistent with the movement simplicity needed to perform a cylindrical grasp, targeted as the main manipulation task in exercises addressed to post-stroke patients in the acute phase (that is the main population for which the rehabilitation HEs are developed).

The choice of the number of MCs depends on a number of factors. Generally speaking, two or three connections offer a higher accuracy and safety with respect to a single MC, since the interaction forces are distributed among multiple contact areas thus limiting the stresses transmitted to the human hand and averting the possibility to cause pain. Moreover the finger phalanges are constrained to follow properly predetermined trajectories, thus avoiding possible unnatural poses (e.g. hyperextension). Nonetheless, more than one connection per finger causes a higher difficulty during the initial fitting phase, when the HE links are attached to the human hand and fingers. It is worth recalling that post-stroke patients often exhibit a residual spastic force that tend to keep the hand closed:

in such circumstances the fitting operation performed by therapists is obviously much more problematic with respect to healthy users. Furthermore, the choice of many MCs entails the necessity to use many sensors if the interaction forces between the human finger and the mechanism need to be completely measured and/or controlled.

It should be noted that there is a close relation between the two before mentioned classification principles and selecting a certain combination of DOFs and MCs should be carefully based on the design specifications dictated by the specific application of the resulting HE. For instance, if the device is attached to all the three human finger phalanges and is controlled in one or two active DOFs, the force exerted to the human phalanges are not controllable separately. In rehabilitation HEs, the number of MCs is typically equal to or greater than the number of DOFs: it is evident that the safety of the users plays a crucial role (the subjects exhibiting some weakness).

The type synthesis and the design of the exoskeleton mechanisms depend also on the topology chosen. There could be many criteria to distinguish different mechanism topologies: in this work, a high-level classification is adopted to identify the placement of the mechanism with respect to the human fingers and their natural workspace (to take into account interference issues and possible functional limitations). The literature analysis reveals that External Mechanisms are the most widespread ([Brokaw et al. \[2011\]](#), [WaveFlex-Hand \[2011\]](#), [Kinetec-Maestra-Hand \[2011\]](#), [Mulas et al. \[2005\]](#), [Ho et al. \[2011\]](#), [Iqbal et al. \[2010\]](#), [Schabowsky et al. \[2010\]](#), [Rosati et al. \[2009\]](#), [Wolbrecht et al. \[2011\]](#), [Fu et al. \[2008\]](#), [Sarakoglou et al. \[2004\]](#), [Wu et al. \[2010\]](#), [Yamaura et al. \[2009\]](#), [Ito et al. \[2011\]](#), [Wege and Hommel \[2005\]](#), [Li et al. \[2011\]](#), [Wang et al. \[2009\]](#) and [Fu et al. \[2011\]](#)), with ten solutions that are here classified as Integrated and seven ones as Stand-Alone. The Integrated Mechanisms make it possible to use a limited number of artificial links and joints and guarantee a humanlike motion of the finger since the phalanges rotate around their natural relative centers of motion. These features play in favor of the overall mechanism simplicity, which represents the major advantage of this option. The main drawback is that the loads transmitted to the finger parts must be limited to pretty low value in order not to cause pain to the user. Therefore, once that the mechanism is synthesized, the reaction forces

## 2. The Classification

---

must be computed with a kinetostatic analysis and checked. The mechanism is acceptable only if the forces in the human articulations and the contact forces of artificial links with human phalanges are below given thresholds. Stand-Alone Mechanisms do not suffer from this disadvantage (if the mechanism is properly connected to the human finger, the major loads are transmitted among the artificial links) typically at the cost of a more complex architecture (above all if some RCM mechanism is implemented).

Also Lateral Mechanisms represent a quite common solution for rehabilitation HEs, with ten cases found in the literature (Brokaw et al. [2011], Chiri et al. [2009], Ren et al. [2009], Kutner et al. [2010], Takahashi et al. [2008], Ertas et al. [2009], Loureiro and Harwin [2007], Burton et al. [2011], Festo-Company [2012] and ). A superior simplicity characterizes this architecture with respect to the External Mechanisms. Another advantage is that the human articulations are subjected to very low loads (theoretically null) thanks to the presence of the physical links and joints superimposed to the human parts that should absorb the most loads. On the other side two significant drawbacks affect this option. When the HE is formed by more than one finger mechanism (excluding the thumb), the very likely interference of some mechanism links due to the restricted space available between the human fingers would require to maintain the fingers significantly abducted, possibly losing the natural attitude of the user's hand. Secondly, the inherent impossibility to provide the proximal joints of the middle and ring fingers with lateral artificial joints entails the use of some RCM mechanism for these articulations, as in Chiri et al. [2009], Burton et al. [2011] and Festo-Company [2012], thus affecting a little the major advantages mentioned for this solution.

As for the last category, the Internal Mechanisms, the main advantage is the possibility to use cables (or linear actuators) to pull the fingertips and cause motion in a very simple way. The main disadvantages of this solution are that interference occurrence could significantly decrease the range of motion of the fingers and could make the grasping of an object difficult or impossible. The typical applications for this architecture are therefore in virtual reality environment, where the direct contact of the user's hand with real objects is not required (Bouzit et al. [2002]). No rehabilitation HE reported in the literature so far exploits this option, but it is worth mentioning an interesting HE concerned as assistive device that,

## **2. The Classification**

---

thanks to a compliant-mechanism solution and the use of a glove, is not affected by the mentioned drawbacks.

As a conclusion, this classification is helpful to understand both the reason of proposing certain solutions for specific applications and the advantages and drawbacks of the different designs proposed in the literature. Additionally, this classification can provide some useful guidelines for the design of new hand exoskeletons, that was actually the primary motivation of this study.

# Chapter 3

## The Feasibility Study

### 3.1 Introduction

The design of rehabilitation hand exoskeletons revealed significantly different solutions, whose rationale could be hardly understandable without a systematic tool of interpretation. In the last chapter a topological classification that is based on three main key issues which have a major influence on the synthesis of the exoskeleton mechanisms has been reported. The proposed key issues was: the number of actuated degrees of freedom, the number of mechanical connections between a mechanism and the human finger, and the mechanism architecture. This classification can provide some useful guideline for the design of new hand exoskeletons. In addition to the proposed classification, many other design issues such as type of connection between HE and human fingers, safety factors, actuations/motors, control issues, sensor and encoder equipments will be deeply discussed in this chapter. In the next step, the feasibility study of 1 DOF mechanisms for one finger, intended as the basic model of the targeted hand exoskeleton, are outlined. In particular, three kinematic chains having 6, 8 and 12 links respectively will be presented and discussed. Finally, based on the advantages and the drawbacks of each proposed mechanism, one of them (a 12-link mechanism) is selected.

## 3.2 Design Specification

The literature proposes a large number of HEs, which generally present some common characteristics and many special peculiarities concerning their mechanics, electronics (control) and working principle. The best possible device probably does not exist, because the complexity of the overall problem prevents unique design principles to be determined and unambiguous design guidelines to be defined. Depending on the specific application, the designer of a new HE must face a wide range of choices, such as the number of DOFs, the mechanism architecture, the transmission system, the control scheme, etc. A decision on each issue entails some advantages and drawbacks and also it affects other aspects of design. Because several design specifications and objectives are often in contrast, a trade-off must be defined, with weighting factors depending on both the specific application and the designers' sensitivity and experience. The purpose of the next sections is providing a systematic analysis of the design principles involved in the development of a rehabilitation HE, as well as discussing the critical issues.

The most important factor providing technical specifications and guidelines is obviously the intended application of the device. According to various types of hand problems, different rehabilitation protocols can be proposed, with a deep influence on the rehabilitation procedure to be implemented and consequently on the overall structure of the robotic system. Three aspects of the rehabilitation protocols may be pointed out that can lead to completely different solutions:

- global complexity of exercises: one may schematically distinguish between basic movements of the finger joints and the execution of daily-living activities (ADLs). The basic movements of the finger joints consist of simple exercises intended to improve the finger mobility, strengthen muscles and recover basic motion-planning capabilities. Performing manipulation tasks related to ADLs (e.g. grasping a bottle and pouring liquid into a glass) involve cognitive aspects as well and it is intended to restore the ability to autonomously control hand movements;
- complexity of the hand movements: one may schematically distinguish be-

tween gross motion of all fingers (e.g. for a cylindrical shape grasp) and single finger dexterity. Rehabilitation of power grasping (in which all fingers are actuated simultaneously) is one of the main manipulation ability that should be recovered for all patients, whereas the rehabilitation of the finger dexterity is a harder task, requiring the capacity of the brain to move the fingers independently;

- rehabilitation environment: in this respect, one may distinguish between a real setting and virtual reality. When performing exercises for ADLs, manipulation of real objects is closer to what the patient must learn from the rehabilitation procedure. On the other hand, a virtual-reality simulator software can create a wealth of different relevant environments and quickly switch between them with no set-up time. In addition, it can boost patients' motivation to perform exercises because it looks like playing a game.

The overall structure of the robotic system (mechanics and control, hardware and software) strictly depends on these categories, so that the specific rehabilitation protocol must be defined first.

A requirement that is mandatory and independent from the specific application is related to the user's safety (especially for patients who suffer from certain diseases and are more vulnerable than healthy subjects). In particular, the forces transmitted from the machine to the human hand must be limited, in order not to cause pain, and thus fully controllable (which implies the possibility to measure or estimate them, with evident consequences on the sensor apparatus). Moreover, the human like movement of the fingers must be respected, so that the phalanges should not be hyper extended with respect to the natural range of motion. This last limitation provides a significant constraint on the workspace of the HE as well as on the configurations that the mechanism links may assume.

Another mandatory requirement is the HE adaptability to different hand sizes. The system should be designed to be used by a number of different patients. Accordingly, in order to avoid constrained motions that could possibly cause pain if the mechanism were "rigidly" designed for a specific reference hand, the HE should accommodate different hand sizes. This can be obtained by introducing passive joints or compliant connections or by allowing the mechanism geometry

to be slightly modified (i.e. by adjusting some link lengths). Strictly related to this issue is the fitting complexity, that is the easiness of connecting the HE links to the human hand and fingers. On this point it should be noted that post-stroke patients often exhibit residual contraction forces that tend to make their hand be a closed fist. The fitting procedure would require to attach the HE to the patient's fingers while these last are kept extended by a therapist: many connections and rigid-type connection components could make the fitting procedure be very complicated or even impossible if pain is caused to the hand (that is forced to keep an over-constrained configuration).

Depending on the strategies used to control the HE and the interaction between the HE and the environment, high backdrivability features could be required, that would imply low inertia of the mechanism and very low friction forces. An important consequence of this requirement is in the selection of the actuators and the power transmission components, which must be as lightweight and efficient as possible (for instance, in this perspective speed reducers with more than one or two stages are generally unsuitable). In any case a high speed of response of the system is generally requested for both the effectiveness of the rehabilitation procedure implementation and safety reasons.

## 3.3 High level design choices

### 3.3.1 Kinematic architectures

Because of the above factors (requirements of the rehabilitation protocol, safety, fitting on different hand sizes, backdrivability), a number of high-level choices must be determined. The first one concerns the kinematic architecture of the system. Indeed, the designer must choose:

- the number of DOFs of the mechanism that guides the functions of a single finger, namely the number of articulation movements that can be possibly coupled or left free;
- whether controlling all the DOFs of the finger mechanism or designing an

under-actuated solution (i.e. one or more DOFs are controlled by the dynamical behavior of the mechanical system);

- how many finger mechanisms will form the overall HEs, and how many of them must be controlled independently.

Coupling between the joints of a single finger can be done by means of different mechanical solutions such as cables and pulleys or rigid linkages and/or geared systems. Certain mechanisms are stand-alone devices whereas other solutions include human phalanges and articulations in the overall system, as links and joints respectively. The possible coupling among different fingers must be also considered, by assessing the possibility for a single motor to control more than one finger mechanism. The choice about this fundamental feature depends on the trajectories to be followed, the force(s) to be applied (and measured) on the human fingers, the required versatility, and the control strategies to be implemented. Also the simplicity of the overall system (mechanics and control), sometimes constrained by external factors, can play a major role in the definition of the HE kinematics. Active control in a single or in both the directions (to actively control the flexion or the extension movements or both) is another issue. It should be considered in fact that the main movement to be recovered is the extension of fingers for post-stroke patients, due to the possible presence of a residual contracting force that tends to maintain the hand closed. In this situation, the design of a system with actuators simply devoted to assist patients in opening the hand only (whereas the closing phase is supported by springs or left uncontrolled at all) is reasonable: many solutions leading to simple mechanism architectures are available (especially if using cable-driven transmissions). On the other side, the machine cannot completely control the grasping force and this could be not acceptable in some applications.

#### 3.3.2 Connection between HE and human fingers

The HE can be fixed to the fingers in different ways. Usually it is attached by looping a strap or a rigid ring around the finger phalanges or using a cap fixed

to the human fingertip. Alternatively, the user can wear a glove and the HE is connected to the glove. In this respect, the most important decision concerns the number of connections of the HE with each finger, which depends on the number of DOFs of the finger mechanism and the specific application. Generally speaking, more than one connection per finger causes a higher complexity during the fitting phase and the necessity to use many sensors if the interaction forces between the human finger and the mechanism need to be completely measured and/or controlled. Nonetheless, multiple connections offer a higher accuracy and safety, since during the motion the finger phalanges are constrained to follow properly predetermined trajectories, thus avoiding possible unnatural poses (e.g. hyperextension). In rehabilitation HEs, the number of connections is typically equal to or greater than the number of DOFs. Also the stiffness of the connection can be a significant factor in different perspectives. A flexible strap can slightly move with respect to the phalanx, thus determining variable contact areas that can negatively affect the controllability and the accuracy of the system when following certain trajectories. On the other hand, a flexible strap is easier to fix during the initial fitting with respect to a stiffer solution, it is inherently safer (the compliance can play as a mechanical filter of forces) and it lets the HE accommodate different hand sizes due to its intrinsic adaptability.

#### 3.3.3 HE placement relative to the human hand

HEs actuate the movement of fingers by means of a series of links which could be placed above the human fingers, beside the fingers or inside the palm. Each solution contains some advantages and drawbacks according to their placement relative to the human fingers. The most critical problem that must be solved for those devices that are placed above the fingers is the mechanical interference between the mechanism links and the anatomical parts. Indeed, finger phalanges must be guided to rotate about anatomical axes around which no mechanical parts may be placed, for obvious reasons. Some kind of so-called Remote Center of Motion mechanisms must be then adopted to make some links have a remote center of relative motion coinciding with the human joint axes while avoiding mechanical interference. Feasible solutions can be obtained by properly synthe-

sized linkages or epicyclic gearings (Kitada et al. [1997], Fontana et al. [2009] and Nakagawara et al. [2005]) respectively). The exoskeletons that are placed beside the fingers, as well as those in which the anatomical segments are integrating parts of the device, do not need Remote Center of Motion mechanisms. This happens because their centers of rotation can be made easily coincident with the centers of rotation of the human finger. This appears to be a great benefit, but this solution needs room beside the fingers that is not always available. The exoskeletons that are placed inside the palm could make without Remote Center of Motion mechanisms as well (see Bouzit et al. [2002]), and they could be simple and lightweight. The main disadvantage of this solutions is that the exoskeleton placement limits the reachable workspace and it makes impossible the complete grasping of real objects in real settings.

#### 3.3.4 Actuation

Another discriminating characteristic of different HE solutions is the choice of actuators and transmission systems. Rehabilitation HEs typically use pneumatic actuators or electric actuators). HEs that use pneumatic actuators may be more lightweight than those using electric actuators, but they need an external compressor, which is a major drawback. In order to keep the weight of the exoskeletons low, actuator parts can be located far from the device (e.g. fixed to the ground). In this case, power is transmitted to the exoskeleton by means of different transmission systems such as wire-driven mechanisms and/or linkages and/or geared mechanisms. The use of cables (e.g. Bowden cables or cable-and-pulley systems) is quite common, above all in those mechanisms where only one movement is actively controlled (e.g. finger extension), due to the simple, compact and lightweight solution that this way may achieve. However, controlling the preload of cables throughout the device life cycle, as well as the friction losses between the cables and possible sheaths, may represent a problematic issue. Gear trains are also effectively used to transmit power. They may both reduce speed and, if properly arranged, provide Remote-Center-of-Motion mechanisms. However, their efficiency may be too low in applications that require good backdrivability, mainly due to difficulties in maintaining a good lubrication. In this case, linkages

comprising rolling-bearings-equipped joints may be preferred, at the cost of less compact solutions. The use of actuators directly placed above the fingers is non-conventional due to the high specific power that is required (ultrasonic motors could be a promising solution in this perspective (Choi and Choi [1999])).

Active control in a single or both flexion-extension directions is another issue. For post-stroke patients, in fact, the main movement to be recovered is the extension of fingers, due to the possible presence of a residual contracting force that tends to maintain the hand closed. In this situation, the design of a system whose actuators only assist the patient in opening the hand (whereas the closing phase is supported by springs or left uncontrolled) is reasonable. On the other side, the HE cannot completely control the grasping force and this could be unacceptable in some applications.

#### 3.3.5 Control and sensor equipment

The control of a HE is generally in charge of the patient, who must generate proper input signals to control the HE finger functions, e.g. EMG-signals gained from human muscles, or brain signals detected by BCIs, or forces measured on the HE itself. In addition to the input command sensors, exoskeletons need position sensors and force sensors in order to implement proper motion control strategies (typically position control or force control or a combination of both). For position control, the use of incremental encoders integrated in the electric motors is very convenient, in order to calculate joint angles by means of the kinematic scheme of the mechanism. High stiffness and low backlash of the mechanism are required to obtain accurate data. If these qualities are not met, other sensors (e.g. potentiometers, Hall effect sensors, absolute encoders) directly placed on joints can measure the relative angular position of the connected links. Force sensors can also be placed in different parts of the exoskeleton, depending on their characteristics and working principle. The most straightforward way consists in placing them between the HE and the human fingers, in order to directly measure contact forces. However, in this arrangement, sensors do not distinguish between forces exerted by the user and external forces. Thus, during contact with the environment, it becomes impossible to recognize the user's intention. Additional force

sensors located at every possible contact surface in the grasping area could be used to detect external forces, but this would cause losing direct contact between human fingers and the object. Alternatively, strain gages can be placed on some components (e.g. to measure the tension of cables in wire-driven mechanisms) and the grasping force could be calculated based on the retrieved data. Finally, for devices whose kinematic scheme and friction models are accurate enough, the force exerted on the human fingers can be computed and controlled by measuring the current absorbed by the electric motors (whose torque constant must be known). Unfortunately, modeling and/or measuring the force or the power due to friction are very difficult tasks, so that systems using this strategy may generally be not very accurate in force control.

## 3.4 Feasibility study of HEs

In this section the basic steps for the selection of a feasible architecture for the HE of the BRAVO project are outlined, with the aim of illustrating a real application of the design principles provided above.

### 3.4.1 Technical specification

The focus of the BRAVO rehabilitation protocol is on the training of patients in the acute phase, with the aim of recovering the basic functions of manipulation. In this context, two main tasks should be possibly assisted by the HE, namely the finger extension for correctly pre-shaping the patient's hand when approaching the target and the control of motion and force of the fingers when grasping cylindrical objects. A 2 DOFs HE oriented to assist the power grasp was defined as the target solution for the first prototype to be realized. One actuator will be devoted to control the thumb flexion/extension whereas a second actuator will control the flexion/extension of the other four fingers. For a cylindrical shape grasping, a device with 1 DOF only is theoretically sufficient. However, the independent action of the thumb with respect to the four fingers is considered as necessary (or, at least, convenient) to properly control the motion coordination in order to correctly grasp the object. Moreover, in order to let the human finger

### 3. The Feasibility Study

---

in direct contact with the grasped object and not to suffer from strict constraints of room availability to host the exoskeleton links, the location of the mechanism links above the fingers was decided a priori. The two actuator groups will be located in the hand backside.

Difficulties were encountered in finding reliable reference trajectories from literature analysis, since reported data are mutually inconsistent. By considering the task of grasping middle size cylindrical objects, starting from a configuration with fingers being fully extended, the trajectory data reported in [Gülke et al. \[2010\]](#) and relative to the grasping of cylinders with different diameters were considered as a reference. As reported in [Gülke et al. \[2010\]](#), five cylinder grips using 5 cylindrical objects of different diameters are analyzed: grip size (G1) diameter was 12 cm; grip size (G2) diameter was 9 cm; grip size (G3) diameter was 7 cm; grip size (G4) diameter was 5.5 cm and grip size (G5) diameter was 4 cm. Each grip was performed 3 times during each measurement unit. Accordingly, the mean of the 3 measurements for each joint were calculated. The analysis included all 14 joints and all 5 cylinder grips. Maximum flexion/extension of the joints, gauged during the time intermission, displayed constant adaptation to the object size (as shown in [Table 3.1](#)). As expected, the maximum flexion enlarged with decreasing object size. This hypothesis is supported by the fact that the mean values of all measured flexion angles had the tendency to increase from object G1 to object G5. The following angles showed the average angle of all joints and all subjects during grip for all 5 objects (G15). G1:  $17.9^\circ$  ( $16.6^\circ, 19.3^\circ$ ), G2:  $21.9^\circ$  ( $20.4^\circ, 23.4^\circ$ ), G3:  $27.6^\circ$  ( $26.0^\circ, 29.3^\circ$ ), G4:  $32.6^\circ$  ( $30.8^\circ, 34.4^\circ$ ), and G5:  $47.8^\circ$  ( $45.7^\circ, 50.1^\circ$ ). The increase of flexion angle with decreasing object size was more frequently observed at the MCP joint than at the PIP and DIP joints and was considerably noticeable at the index and small fingers ([Table 3.1](#)). From the largest to the smallest object, the flexion angle at the MCP joint of the index finger multiplied by 4.1, of the middle and ring finger by 2.1, and of the small finger by 4 ([Gülke et al. \[2010\]](#)). At the PIP joint, the multiplication measured 2.2 for the index, 2.1 for the middle, 2.1 for the ring, and 2.5 for the small finger. At the DIP joint, it averaged 3.1 for the index, 2.5 for the middle, and 2.4 for the ring and small fingers. At the thumb, the distribution of the total ROM showed significant greater flexion at the IP joint, independent of the size of the object

### 3. The Feasibility Study

Thumb				
	MCP		IP	
	Mean	SD	Mean	SD
G1	9.4	9.3	20.6	15.6
G2	10.7	7.5	30.7	14.3
G3	15.9	11.1	44.7	17.4
G4	21.3	13.0	50.8	19.3
G5	24.8	11.6	49.7	22.3

Table 3.1: Thumb Joint Flexion (degrees) (taken from [Gülke et al. \[2010\]](#))

Index finger						
	MCP		PIP		DIP	
	Mean	SD	Mean	SD	Mean	SD
G1	11.5	11.1	27.8	17.5	9.1	8.7
G2	12.3	14.6	35.7	20.5	12.1	6.8
G3	16.1	11.0	45.1	21.6	17.5	7.8
G4	23.0	15.7	53.3	20.9	22.1	9.9
G5	47.4	22.3	62.3	19.8	28.0	15.0

Table 3.2: Index finger joint Flexion (degrees) (taken from [Gülke et al. \[2010\]](#))

(p.001) (Table 3.1). Looking at G1, the MCP joint was flexed  $9.4^\circ$ , whereas the IP joint was flexed an average of  $20.6^\circ$ . The results for the fingers were different. There, the PIP joint mainly contributed to the total amount of flexion, followed by the MCP and DIP joints (p.001). However, there is no significant difference between the MCP and DIP joints. The motion of the joints of the index finger in G1 underlined this. There, the PIP joint was flexed  $27.8^\circ$ , the MCP joint  $11.5^\circ$ , and the DIP joint  $9.1^\circ$ .

The coupling ratio of the DIP and PIP joints is the ratio of their maximum flexion angles. The greatest ratio was reported for the ring finger. Depending on the size of the object, it measured between 0.88 and 1.03 for the ring finger and between 0.44 and 0.54 for the little finger (Table 3.6). This documents that the coupling ratio varies considerably among the index, middle, ring, and small finger but presents relative consistency for the individual finger independent of the size

### 3. The Feasibility Study

Middle finger						
	MCP		PIP		DIP	
	Mean	SD	Mean	SD	Mean	SD
G1	22.0	14.6	32.8	11.5	18.8	9.2
G2	25.4	15.2	39.8	14.9	22.4	9.6
G3	31.3	12.8	48.6	13.8	30.3	11.8
G4	37.3	14.8	58.2	11.1	38.3	12.4
G5	59.6	14.6	68.9	10.9	46.2	13.9

Table 3.3: Middle finger joint Flexion (degrees) (taken from [Gülke et al. \[2010\]](#))

Ring finger						
	MCP		PIP		DIP	
	Mean	SD	Mean	SD	Mean	SD
G1	18.8	9.7	26.8	10.9	25.5	8.5
G2	22.8	12.0	30.7	10.7	28.9	8.0
G3	27.8	12.4	38.7	10.7	36.3	10.9
G4	31.3	12.7	45.5	13.4	42.1	12.5
G5	50.4	15.1	62.9	11.9	52.8	14.2

Table 3.4: Ring finger joint Flexion (degrees) (taken from [Gülke et al. \[2010\]](#))

Little finger						
	MCP		PIP		DIP	
	Mean	SD	Mean	SD	Mean	SD
G1	13	8.7	23.3	12.6	11.2	6.7
G2	14.3	11.1	27.3	13	12.5	7.7
G3	17.8	12.9	34.0	12.7	14.7	8.1
G4	20.0	17.1	39.3	15.5	16.9	11.3
G5	52.1	25.4	58.1	14.9	23.6	15.3

Table 3.5: Little finger joint Flexion (degrees) (taken from [Gülke et al. \[2010\]](#))

### 3. The Feasibility Study

	Index		Middle		Ring		Little	
	Mean	SD	Mean	SD	Mean	SD	Mean	SD
G1	0.50	0.50	0.63	0.42	1.02	0.36	0.54	0.33
G2	0.69	0.86	0.66	0.47	1.03	0.39	0.53	0.32
G3	0.72	0.86	0.72	0.44	0.99	0.38	0.48	0.30
G4	0.56	0.72	0.70	0.30	1.00	0.38	0.49	0.30
G5	0.59	0.48	0.70	0.25	0.88	0.27	0.44	0.33

Table 3.6: Coupling Ratio of DIP and PIP Joints (taken from [Gülke et al. \[2010\]](#))

of the object. According to this, the only significant variable is the finger itself.

As for the forces, the hardest required task is assisting the finger extension due to some possible residual contracting force. Also in this case the literature does not offer definite reference data. The effect of the residual contraction was thus arbitrarily modeled as an external force of 10 N applied on the fingertip of each finger, orthogonal to the third phalanx middle line for every configurations along the finger trajectory. For the opposite movement (i.e. the flexion one), the maximum grasping force was set at 30 N, which was considered enough to securely hold small to medium size objects (e.g. a glass full of water). It should be noted that 30 N is the force acting on the thumb on one side and on the group of four fingers on the other. These data, defined on the basis of common sense and practitioners' advice, prove consistent with the experience retrieved from the clinical practice. They will provide the reference values in the static and kinetostatic analyses that shall be performed to select appropriate commercial components (e.g. the actuators) and properly design the mechanism links. As far as the human hand geometry is concerned, average data were taken as reference by combining the anthropometrical proportions retrieved from [Buchholz and Armstrong \[1992\]](#) and [Drillis et al. \[1964\]](#).

#### 3.4.2 Feasibility study of different architecture

The basic module of the pursued HE is a mechanism attached to one human finger, that must couple the flexion/extension movements of the three anatomical phalanges (the abduction/adduction of the first phalanx is inhibited). The feasibility study of a planar mechanism with 1 DOF, whose topology is conceived as suitable for all the fingers (though with different geometries due to the diverse lengths of the five human fingers), is the target of this first design step. The driving link of the thumb mechanism must be controlled by one actuator, whereas the driving links of the four mechanisms attached to the opposite fingers will be connected to the axis of a second actuator.

Some basic considerations for the synthesis of the targeted 1 DOF planar mechanism can be done, starting from the well known Grubler's formula for the planar mechanisms:

$$l = 3n - 3 - 2c_1 - c_2 \quad (3.1)$$

where  $l$  is the number of DOFs of the mechanism,  $n$  is the number of its links,  $c_1$  and  $c_2$  are the number of lower pairs (revolute and prismatic joints) and higher pairs (cam-follower type joints) respectively. Higher pairs are generally not considered as suitable for HE mechanisms due to a number of reasons (e.g. design complexity for obtaining a bilateral constraint, friction forces possibly unacceptable, etc) so that the following straightforward relation between the number of links and the number of lower pairs holds (being  $l=1$  and  $c_2=0$ ):

$$c_1 = 3/2n - 2 \quad (3.2)$$

that leads to the results for  $c_1$  and  $n$  reported in Table 3.7.

The synthesis problem to solve was to determine the 1 DOF planar mechanism that, placed above the human finger and connected to it, makes the finger follow - though approximately - the trajectory retrieved from [Gülke et al. \[2010\]](#).

Table 3.7: Topology elements for 1 DOF planar mechanisms.

n	4	6	8	10	12	...
c	4	7	10	13	16	...

The main concern is finding out a mechanism with a suitable architecture (as simple as possible and with reasonable dimensions) that guarantees the interference avoidance between links and phalanges (and between links themselves). To this aim a number of solutions corresponding to possible combinations retrievable from table 3.7 were synthesized for the index finger, taken as reference in this first step, and then critically analyzed. In this context only three of them will be outlined and discussed, due to their significant differences that can be a stimulus for the reader.

#### 3.4.2.1 6-linkage mechanism

By excluding a priori the possibility that a 4-link mechanism could target the design goals (a designer easily understands that the interference avoidance through the whole workspace with reasonable link lengths is impossible), the simplest architecture to study (and to design and manufacture) is the 6-link linkage with all revolute joints. Very good qualities were expected from this simple architecture due to the low number of links and joints, the presence of all revolute joints (easier to accurately manufacture than the prismatic joints and suffering from less problems from a functional viewpoint) that would leave the possibility to realize a compliant mechanism with all the known advantages. The synthesis of the linkage can be performed in different methods. The synthesis method that is performed here is the Burmester-theory-based procedure proposed by McCarthy (Soh and McCarthy [2008]). Accordingly, in order to keep this work self-contained, the method is extensively explained in the appendix.

The philosophy of the synthesis method can be briefly explained as follows (McCarthy [2000]): the mechanical constraints is introduced to a planar 3R serial chain to guide the movement of its end effector through a set of five specified task positions to obtain a six-bar linkage, as illustrated in Fig. 3.1.

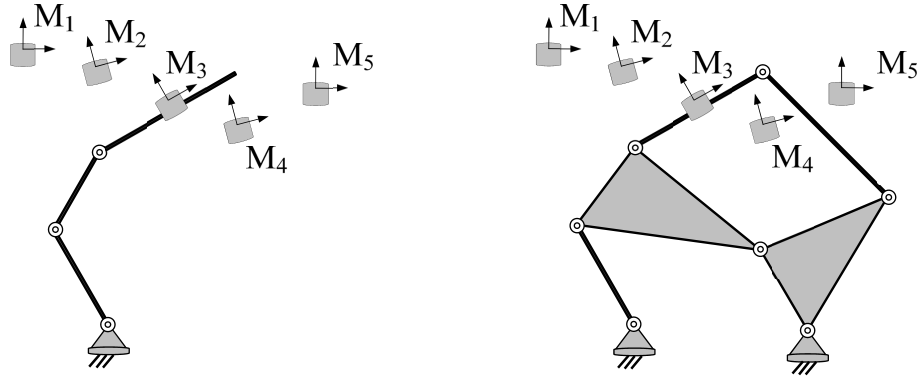


Figure 3.1: A planar 3R serial chain is constrained by two RR chains to define a six-bar linkage.

Based on this method, the Watt Ia six-bar was deeply analyzed. The mechanism is attached to human finger phalanges as presented in Fig. 3.2. The result is the mechanism where link 7 is the driver and link 4, fixed to the third phalange, is the follower.

Thus the exoskeleton should be able to correctly guide the fingertip through a number of poses (position and orientation) that entail a natural motion of the whole finger along the grasping trajectory. As mentioned before, the configurations obtained from [Gülke et al. \[2010\]](#) were considered as reference configurations (presented in Fig. 3.3). So, the synthesis problem is to find a suitable 6-link mechanism in which the link 4 (that is fixed to the third phalange) pass through desired poses(positions and orientations).

As for the first step of the synthesis, the dimension of the 3R:  $a_1$ ,  $a_2$  and  $a_3$ , and the location of the base and moving pivots of the 3R chain: [G] and [H] are chosen. We use this data to formulate the inverse kinematic equations of the 3R chain and solve for the 5 configuration angles  $q_j = (\theta_1, \theta_2, \theta_3)$ ,  $j=1, \dots, 5$ , that reach the specified task configurations  $[T_j]$ ,  $j=1, \dots, 5$  as shown in Fig. 3.4 and Fig. 3.3.

Notice that for one configuration, the inverse kinematic equations yield two sets of configuration angles corresponding to a 3R chain with its elbow up and elbow down. In our synthesis, we choose the elbow up configuration, preventing

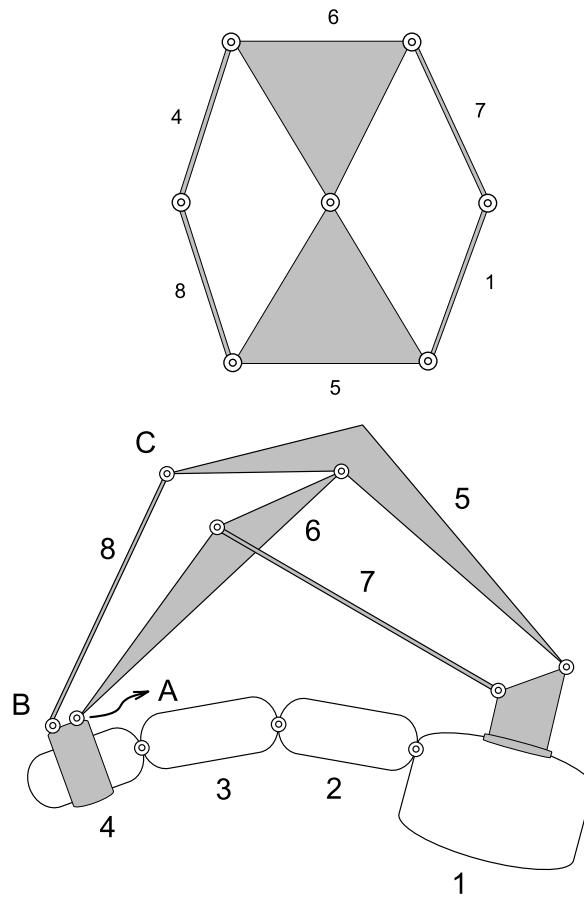


Figure 3.2: Watt kinematic chain and schematic of the watt-chain-based mechanism.

### 3. The Feasibility Study

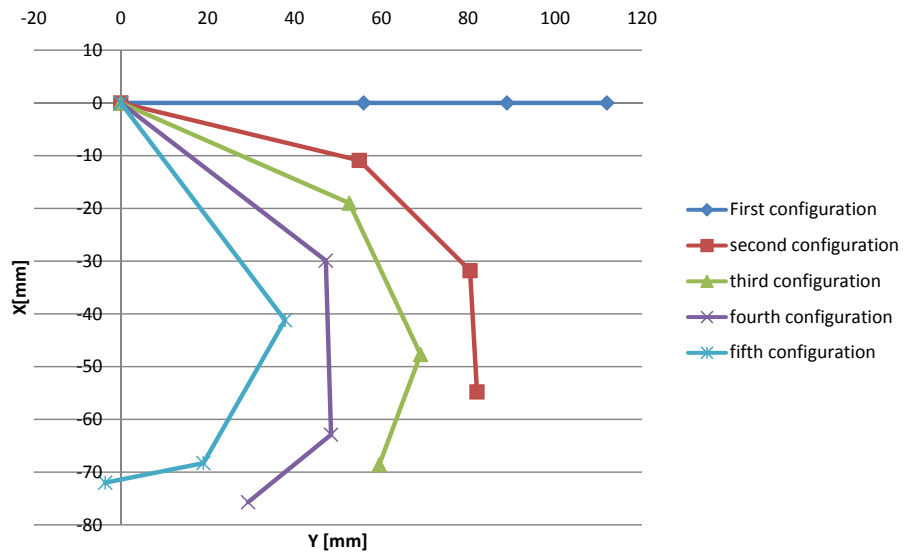


Figure 3.3: 5 configurations considered as reference for synthesis of 6-link mechanism.

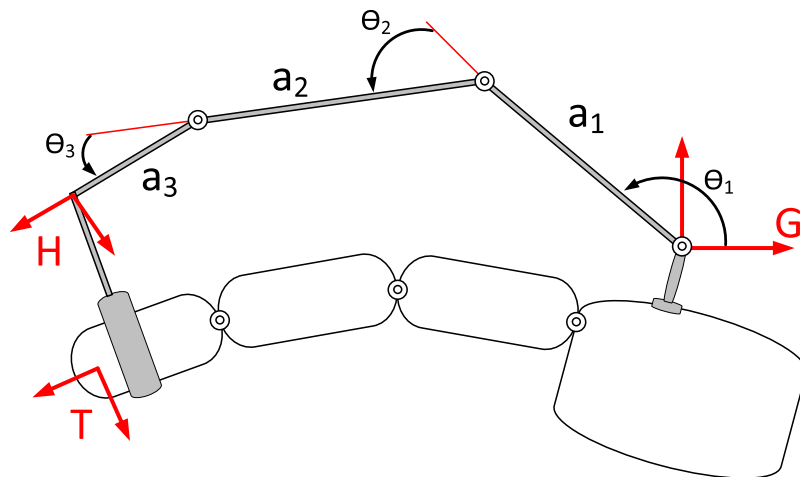


Figure 3.4: A 3R chain connected to the human finger phalanges.

### 3. The Feasibility Study

the possible interference between human phalanges and the mechanism. The five configurations of the 3R chain provide the pose for each link relative to the ground frame. These thirty coordinates(x and y coordinates of 15 points) form the tasks requirements that can be used to synthesize the planar RR constraints. At the next step, we will add two RR constraints (first link is  $G_1W_1$  and the second link is  $G_2W_2$ ) to the 3R chain to obtain the Watt chain as shown in Fig. 3.5.

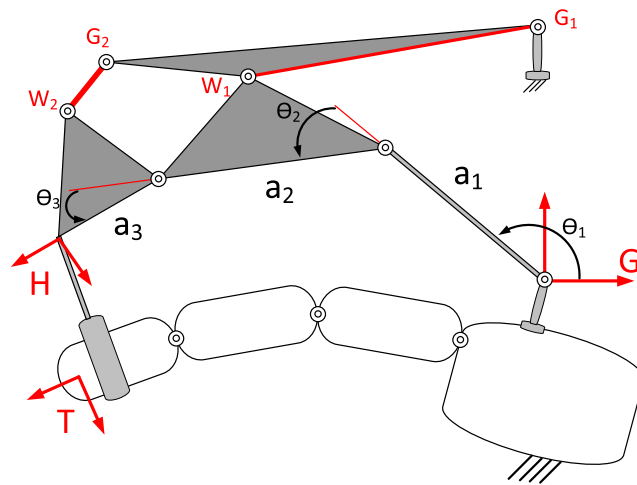


Figure 3.5: A 3R chain connected to the human finger phalanges.

The synthesis procedure was formulated in a Matlab code to reach the desired trajectory while the 6-link mechanism does not interfere the human finger phalanges. The inputs of the program are the three lengths of the 3R chain ( $a_1, a_2, a_3$ ) and the base pivot ( $G$ ) of the 3R chain, then the output is a proper 6-link mechanism that satisfies all the given poses. By a trial-and-error procedure, we ran the code many times (hundreds) to reach the desired results. The main difficulties was keeping the mechanism above the human finger phalanges not interfering the fingers in the whole range of finger motion. Finally, we found a proper mechanism which does not interfere with the human hand (as shown in Fig. 3.6).

Unfortunately, the kinematic analysis performed to simulate a continuous tra-

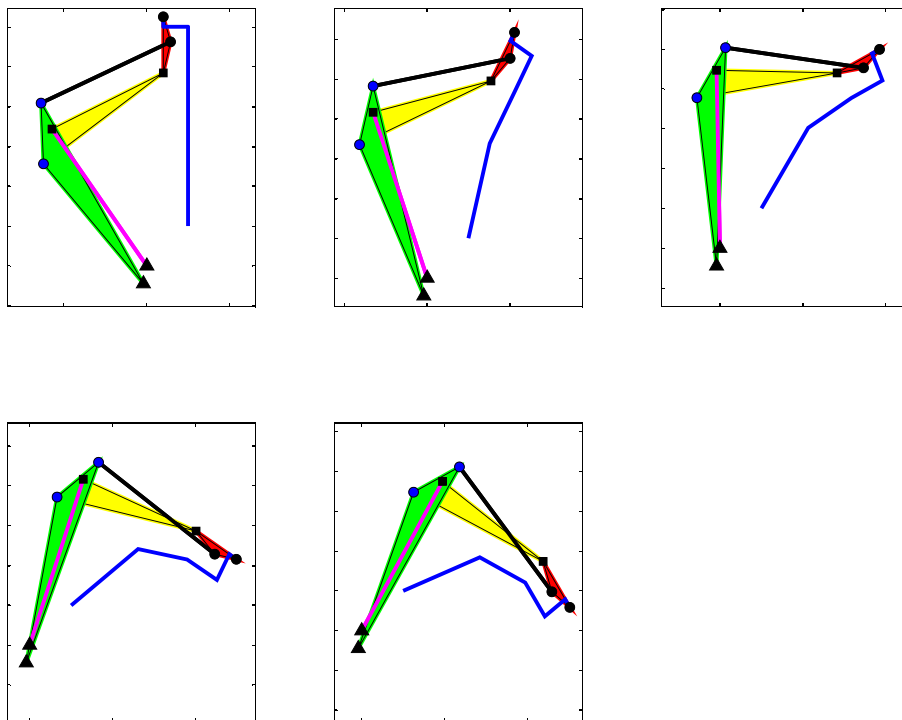


Figure 3.6: A synthesized 6-link mechanism; where the blue lines represent the human finger phalanges, the purple line represents the link with length of  $a_1$ , the yellow link represents  $a_2$  and the red link represents  $a_3$

jectory extending from full extension to the configuration suitable for grasping the smallest cylinder (55 mm diameter) revealed that, due to the large link rotations required to cover the workspace, the linkage would suffer from kinematic singularities (occurring when the centers of joints A, B, C (see Fig. 3.2) are aligned). The problem could be solved by adding some auxiliary mechanism enabling the 6-link mechanism to move out from the singularity configuration into the desired one. Some functional solutions were studied but, due to the high forces exchanged close to the singular configuration and to the increased complexity of the mechanism architecture, the resulting system lost most of the good qualities initially expected. Therefore, this solution was not proposed any longer.

#### 3.4.2.2 8-linkage mechanism

Another mechanism, with a higher number of links was considered as a feasible solution (the chain with  $n=8$  link arranged as in Fig. 3.7(a). The motivation was that a slight complication of the architecture (only two more links and three more joints) could lead to a singularity-free mechanism (in the considered workspace) able to respect the given design goals. Indeed, the higher freedom in the synthesis procedure made it possible to choose some design parameters that let the linkage guide the finger along the reference trajectory while avoiding interference with the human phalanges. Among the numerous possible combinations, the solution shown in Fig. 3.7(b) seemed particularly interesting. Four revolute pairs were replaced by prismatic pairs. The final kinematic chain can be thought of as composed by three 4-link loops, each one formed by four links, two revolute and two prismatic joints, connected in series at the level of intermediate links. The anatomical segments and articulations are considered as integrated parts of the mechanism, so that all the three phalanges are attached to the exoskeleton. Link 5, provided with a linear motion with respect to link 1, is the driving link whereas the phalanges (links 2, 3, and 4) are the three followers that are forced to assume the poses defined by the reference trajectory (and this could be good for the patient's safety, in spite of a possibly limited feedback perception during grasping). The mechanism synthesis was performed, in this case, by following a trial-and-error procedure, in order to realize the desired trajectory. Based on

### 3. The Feasibility Study

Gülke et al. [2010], the relative angles among the human segments (links 1, 2, 3, and 4) in five different configurations from full extension to the configuration grasping the smallest cylinder were considered as the reference trajectory.

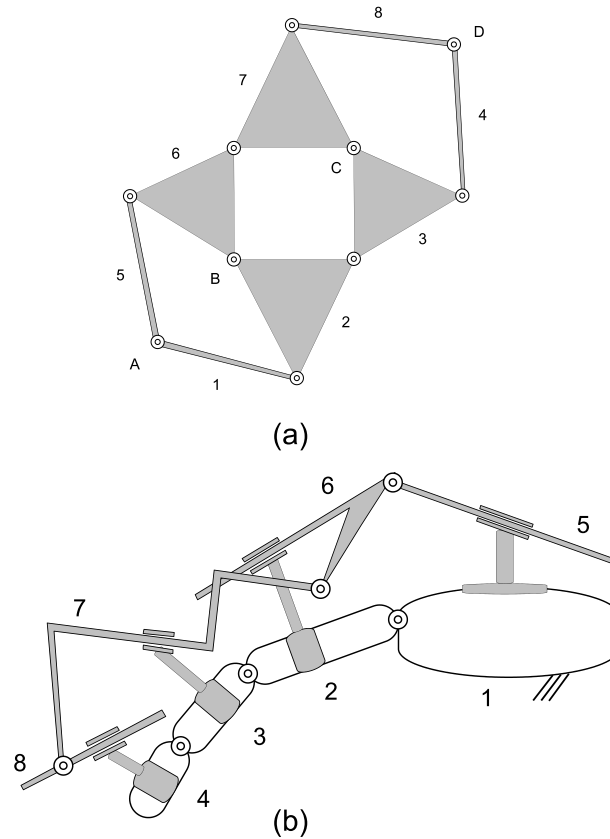


Figure 3.7: (a) 8-link kinematic chain taken as reference for the synthesis of a finger mechanism; (b) schematic of the synthesized 8-link mechanism with revolute and prismatic pairs.

Three loops of links (links 1-2-5-6, 2-3-6-7, and 3-4-7-8 respectively) were sequentially synthesized. After determining the mechanism geometry, the continuous trajectory was analyzed to check the presence of non-natural movements of the phalanges, the occurrence of singularities, possible interferences among links and abnormal behaviors of the mechanism (figures 3.8, 3.9 and 3.10). The introduction of the prismatic joints provides a quite simple solution to the problem of interference avoidance (and it was similarly used in the 4-DOFs finger exoskeleton

proposed in Kitada et al. [1997]). On the other side, the stroke required to the sliders is considerable, so that this architecture is less compact than the previous one. Moreover, preliminary simulations showed the occurrence of high forces in some joints for the given grasping force required. From the static point of view, special care must be paid in order to avoid self-locking configurations.

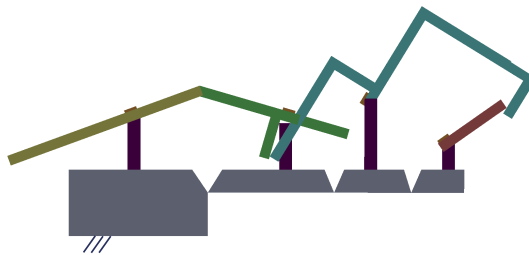


Figure 3.8: Schematic of a configuration of the synthesized 8-link mechanism.

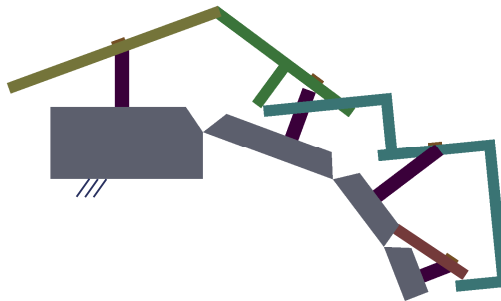


Figure 3.9: Schematic of a configuration of the synthesized 8-link mechanism.

#### 3.4.2.3 12-linkage mechanism

Another mechanism, with a higher number of links was considered as a feasible solution. It comprises 12 links, also including the three phalanges, interconnected by 16 revolute joints, thus resulting in a 1-DOF mechanism. It is worth noting that natural connection between adjacent phalanges is considered as a revolute joint. The mechanism topology and its geometry are reported in Fig. 3.11(a)



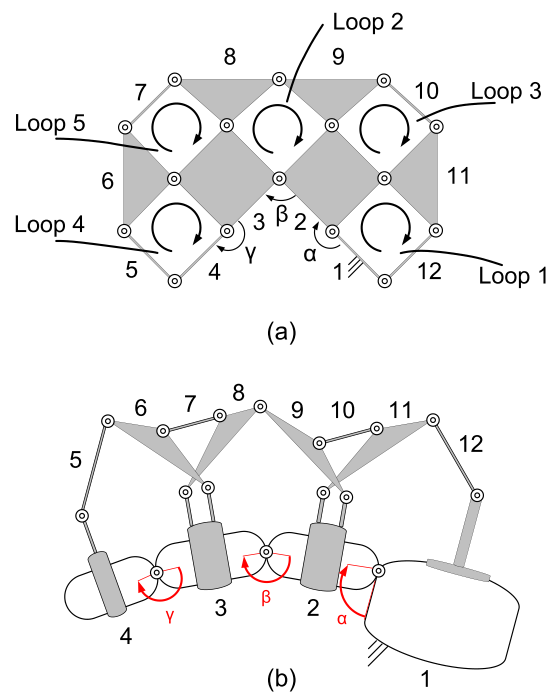


Figure 3.11: (a) 12-link mechanism topology; (b) Schematic of the 12-link mechanism.

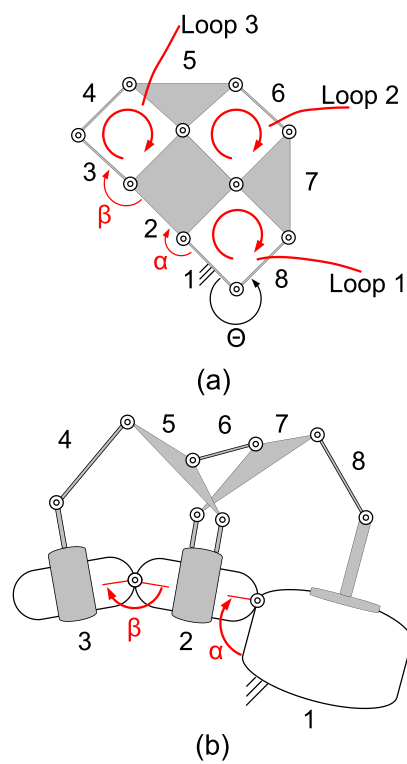


Figure 3.12: (a) 8-link mechanism topology; (b) Schematic of the 8-link mechanism for the thumb.

### 3. The Feasibility Study

---

extremely simple and it leaves the human finger free to directly come in contact in a wide area with the grasped object, but it suffers from a serious singularity configuration within the workspace. The problem could be solved by complicating the architecture and introducing auxiliary links and joints to form an internal sub-mechanism, however it was not presented. The second linkage is free from singularities in the considered workspace and its architecture is still not very complicated, so that it could be a good candidate solution. However, further studies show that for the given grasping force these could raise to unacceptable forces both in the prismatic joints and, above all, in the connections between the links and the human phalanges. The third linkage (12-link mechanism) contains a higher number of links: 12 (in comparison with 6 and 8 of the other two mechanisms) but it contains a number of advantages such as: reaching of the desired trajectory without interfere with the phalanges; high range of motion; maintaining the forces within an acceptable range. Based on the advantages and the drawbacks of the three above-mentioned mechanisms, the 12-link mechanism was selected as the basic model of the targeted HE.

# Chapter 4

## Synthesis, Analysis and Design of 12-Link mechanism

### 4.1 Introduction

As for the design phase, the decision was made through a number of high level design specifications. The hand orthosis features five planar 12-link mechanisms, one per finger (8-link for the thumb), globally actuated by two motors equipped with incremental encoders for implementing position/velocity control schemes. Indeed, the thumb flexion/extension movement along a selected plane is controlled by one actuator (motor and speed reducer), whereas a second actuator is devoted to the control of the flexion/extension of the other four fingers (being the four corresponding mechanisms connected to the same driving shaft). In order to satisfy the desired constraints, the dimensional synthesis should be done for 5 fingers so that all fingers pass through desired configurations. Another important factor in dimensional synthesis is the finger synchronization issue. Since the same topology is used for the group of 4 fingers and all four fingers are actuated by one motor, the synchronization issues should be also taken into account to guarantee the correct grasping. The kinematic and static analyses should be also done in order to verify the kinematic constraints.

### 4.2 Synthesis and Synchronization

After selecting the mechanism topology, the dimensional synthesis was done in order to satisfy the desired configurations (trajectories). In particular, the finger has to pass through some (five) given configurations. By a trial and error procedure, a first acceptable solution was obtained, therefore leaving the adoption of more advanced (sophisticated) techniques (Erdman [1981], Konak et al. [2006] and Datta and Deb [2011]) to a further design. In order to reach the desired trajectory, based on Gülke et al. [2010] the angles  $\alpha$ ,  $\beta$  and  $\gamma$  (Fig. 3.11) in five different configurations from full extension to the minimum grasped cylinder was taken as reference trajectory. Therefore, for each finger mechanism, the synthesis was performed to reach these sets of angles in five configurations. The synthesis was done by considering different groups of the mechanism loops in sequence. Namely (see Fig. 3.11): the first group contains loop 1 (links 1, 2, 11, 12); the second group contains loops 2 (links 2, 3, 8, 9) and 3 (links 2, 9, 10, 11); and the third group contains loops 4 (links 5, 6, 3, 4) and 5 (links 6, 7, 8, 3). The synthesis started by focusing on the first group (loop 1). The input of loop 1 (four-bar mechanism) is the orientation of link 12 with respect to link 1 (ground) and the outputs are the position and orientation of link 2 (proximal phalange) and link 11. The dimensional synthesis was done sequentially for each group in order to reach five desired output angles ( $\alpha$ ) in five configurations. These configurations started from full extension of the finger and continued to flexion that pass through 4 decreasing diameters of a cylindrical object.

The next step is to design the second group which contains two coupled four bar linkages (loops 2 and 3). The inputs of the second group are the positions and the orientations of links 2 and 11, and the outputs are the positions and orientations of link 3 (middle phalange) and 8. The synthesis of the second part (two coupled 4-bar chains) has been done by inspection to reach five desired values for the angle  $\beta$  (the proper angle to grasp the desired cylindrical object). It is worth mentioning that the length of the binary link number 7 plays an important role in controlling the orientation of link 3 (angle  $\beta$ ). Finally, the same procedure was done to synthesize the third group (loop 4 and 5) which contains the distal phalange.

#### 4. Synthesis, Analysis and Design of 12-Link mechanism

---

The allowed range of motion for the flexion/extension angle of the metacarpophalangeal (MCP) ( $\alpha$ ), the proximal interphalangeal (PIP) ( $\beta$ ) and the distal interphalangeal (DIP) ( $\gamma$ ) joints are kept in a proper range: ( $5\div 80$ ), ( $0\div 90$ ) and ( $0\div 20$ ) respectively. Additionally, the link size (mainly the distances between two adjacent joints in one link) are kept in a proper range ( $10\div 52$  mm).

The same dimensional synthesis was done for the other finger mechanism. The synthesis was done based on the lengths of each phalanges of the selected fingers and the proper grasping angles of each joint. It is worth deepening both the "adaptability" of the mechanism and the "sensitivity" of the human hand configuration with respect to different hand sizes. With reference to each one of the four-finger mechanisms, three artificial links are connected to the three phalanges by means of 5 mm wide Velcro strips (the thumb has only two connections for the two moving phalanges). The intrinsic compliance of these couplings and the possibility to tight the strip in variable positions along the phalanges allow the finger exoskeleton to adapt to human hands with different sizes. As mentioned before, the average configuration data reported in [Gülke et al. \[2010\]](#) were assumed as the finger configurations considered as reference for the mechanism design. The data (mean value and standard deviation) are expressed in terms of joint angles ( $\alpha$ ,  $\beta$  and  $\gamma$  in Fig. 3.11) experimentally retrieved from subjects grasping cylinders with diameters of 55, 70, 90 and 120 mm. Being the human segment and joints integrating parts of the mechanism, the different geometry of the resulting four 1-DOF mechanisms entails a variation in the actual configurations, in terms of relationships among the joint rotations as shown in Fig. 4.1. By calculating the variations of  $\alpha, \beta$  and  $\gamma$  for grasping the cylindrical object among the different hand sizes (Figures 4.2, 4.3 and 4.4), the results show small and acceptable variations with respect to the standard deviation reported in [Gülke et al. \[2010\]](#). In other word, the mechanisms' configuration has not shown a great sensitivity to different hand sizes.

Apart from the configurations of each single finger, the motion of all fingers should be synchronous. It means that when grasping a cylindrical object, phalanges should have a trajectory consistent with the requirement to have all phalanges that come into contact with the cylindrical object to be grasped at the same time (this would avoid to change the pose of the cylinder once it has been

#### 4. Synthesis, Analysis and Design of 12-Link mechanism

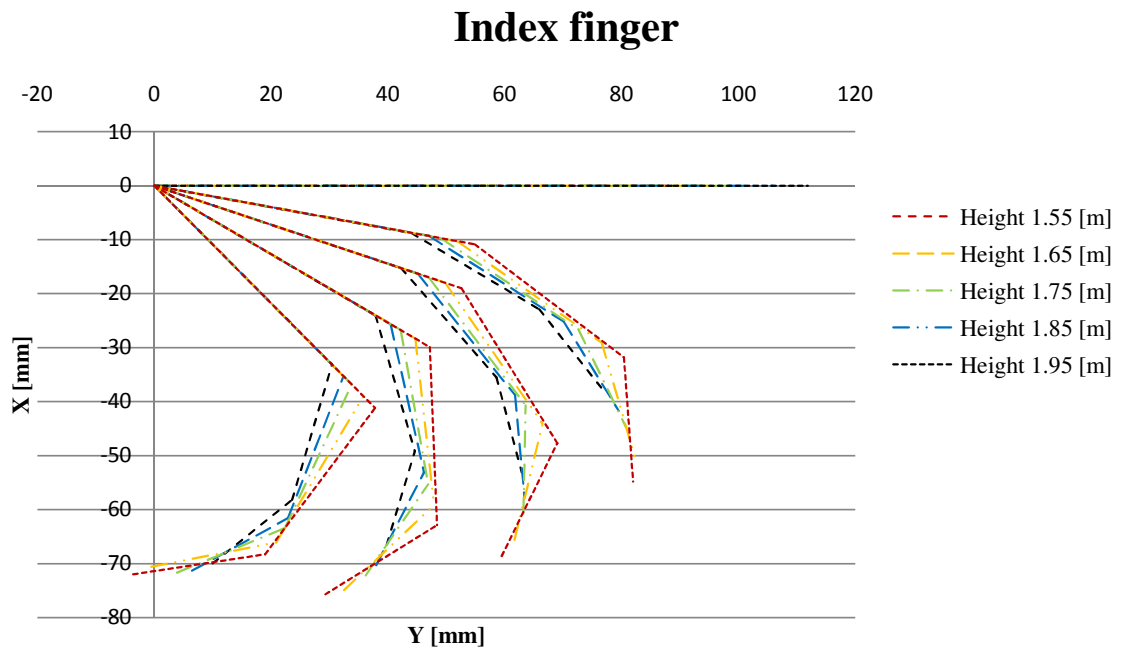


Figure 4.1: Index finger Configuration for different size hands (with respect to the height of the person) when grasping cylindrical objects of diameter 55, 70, 90 and 120 [mm] respectively

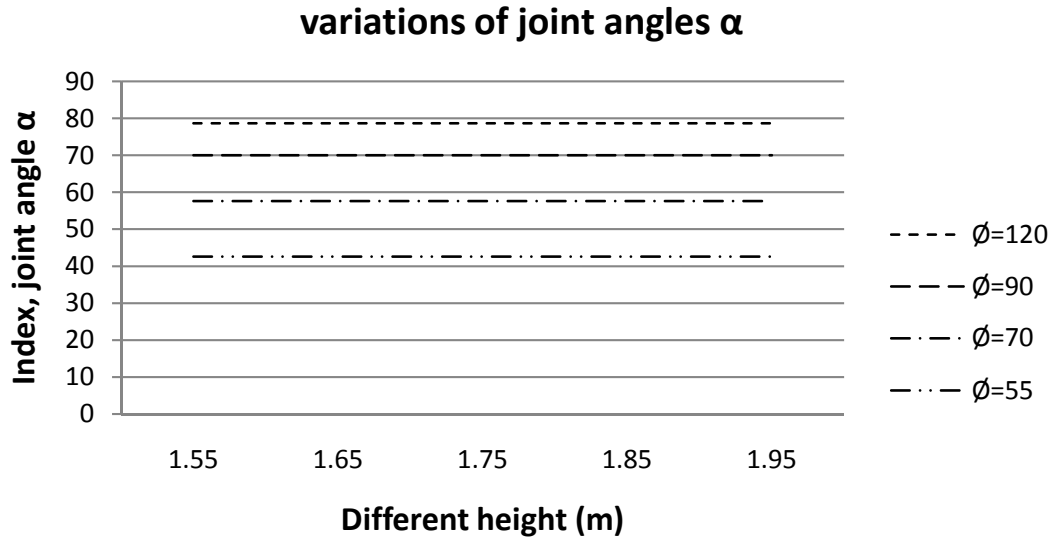


Figure 4.2: Joint angle  $\alpha$  in different size hands when grasping cylindrical objects of diameter 55, 70, 90 and 120 [mm] respectively.

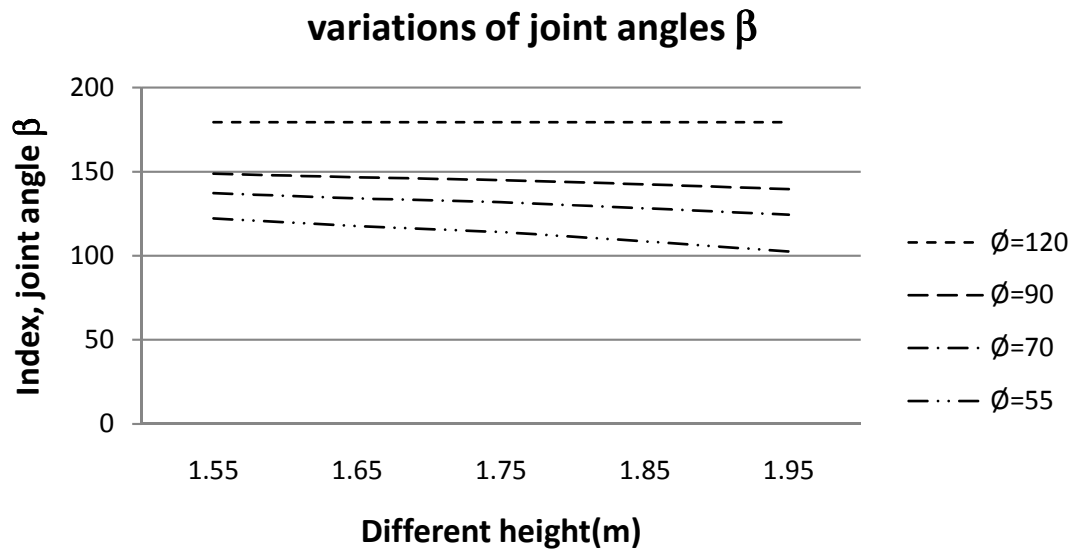


Figure 4.3: Joint angle  $\beta$  in different size hands when grasping cylindrical objects of diameter 55, 70, 90 and 120 [mm] respectively.

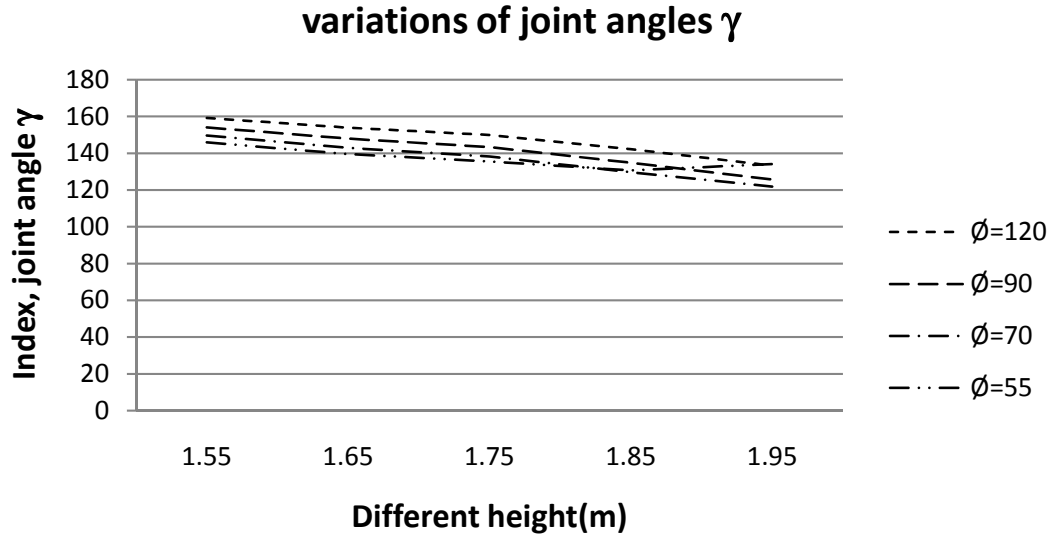


Figure 4.4: Joint angle  $\gamma$  in different size hands when grasping cylindrical objects of diameter 55, 70, 90 and 120 [mm] respectively.

grasped). The problem of finger synchronization was satisfactorily achieved by minimizing the errors when the group of four fingers grasp a cylindrical object of diameter 60 mm, taken as a reference diameter for the selected range (50÷70 [mm]).

Another constraint to be taken into account is the placement of the links and joints with respect to finger phalanges. In the whole range of motion, the links and joints of the mechanism should be kept above the human finger phalanges (above the links 1, 2, 3, 4) not to disturb the movement of the fingers. Of course interference among the links of the mechanism and the phalanges must be avoided in all configurations. Moreover, if two links or joints interfere in their workspace, they have to be manufactured in order to operate in two different planes. The total number of planes for each finger should be as lower as possible.

### 4.3 Kinematic Analysis

Once the mechanism geometry was defined, the static analysis was performed to both calculate the forces exerted by the mechanism links at the interface with the phalanges and the required driving torque for grasping an object or to balance the possible residual contracting forces.

In order to reach this purpose, the static analysis was done to find out the amplitude and the direction of the forces exerted at each joint. These forces were computed as a resultant of a residual contraction modeled as an external force of 10 N applied at the fingertip. The maximum force exerted at joints is about 150 N which occurs in the full extension mode in the joints of the binary link 7 (see Fig 3.11b). Other forces that should be taken into account are the forces exerted at each connection between the mechanism links and the human phalanges. In order to calculate these forces, the internal forces in the links 2, 3 and 4 of each fingers are calculated. Figure 4.5 shows the names assigned to each revolute joint and figures 4.6 and 4.7 show the forces between the mechanisms' links at these joints. The diagrams of Figures 4.6 and 4.7 show the modules of the force [N] in the revolute joints with respect to input link angle  $\alpha$  [Degree] (see Fig. 3.11b). The last diagram in Fig. 4.7 shows the modulus of the required torque [N.mm] for grasping an object with respect to input link angle  $\alpha$  [Degree] (see Fig. 3.11b). Further, the first diagram of each row in Fig. 4.8 and 4.9 show the modules of the force [N] with respect to input link angle  $\alpha$  [Degree] in joints Q, M, K and G, while the next two diagrams in each row present the modulus of each force [N] in the "X" and "Y" directions with respect to input link angle  $\alpha$  [Degree] (the "X" and "Y" components allow defining the direction and modulus of each force in reference system). Figure 4.10 shows the forces exerted at the mechanism link-finger phalange interface. The maximum force exerted at the finger is about 150 [N]. It is possible to find the required amount of torque to actuate link (link 5) to balance the force of 10 N in the fingertip. The required torque from full extension to full flexion is increasing from 0.750 Nm to 2 Nm, so the global maximum torque required for the group of four fingers would be approximately about 8 Nm (as shown in figures 4.7). The same static analysis was done for the thumb. In comparison with the other four fingers, the maximum required torque takes

## 4. Synthesis, Analysis and Design of 12-Link mechanism

---

place in a flexed mode (when grasping an object with a force of 30N) as shown in Fig. 4.6. The maximum calculated torque was about 3.5 Nm (Fig. 4.7). The velocity and acceleration analysis were done as well. Figures 4.11 and 4.12 show the velocities [m/s] of each joint and figures 4.13 and 4.14 show the accelerations [m/s<sup>2</sup>] of each joint with respect to input link angle  $\alpha$  [Degree]. So, the results of the kinematic and static analysis confirmed the validity of the design.

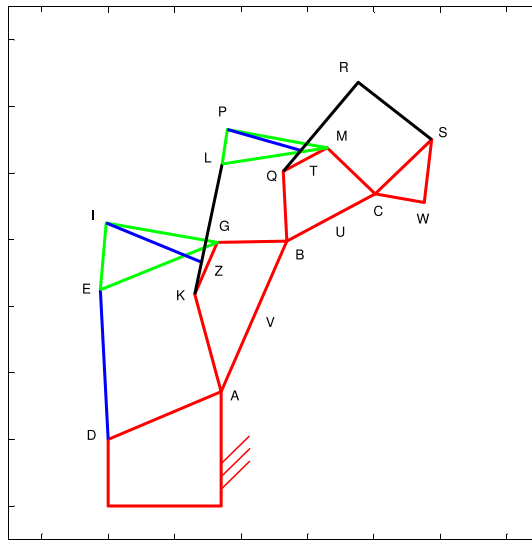


Figure 4.5: The names assigned to each revolute joint, where the joints A, B and C are human MCP, PIP and DIP joints respectively.

### 4.4 Mechanical Design

The hand orthosis is formed by five planar 12-link mechanisms, one per finger, globally actuated by two motors equipped with incremental encoders for implementing position/velocity control schemes. Indeed, as shown in figures 4.15, 4.16 and 4.17, the thumb flexion/extension movement along a certain plane is controlled by one actuator (motor and speed reducer), whereas a second actuator is devoted to the control of the flexion/extension of the other four fingers (being the four corresponding mechanisms connected to the same driving shaft). The

#### 4. Synthesis, Analysis and Design of 12-Link mechanism

---

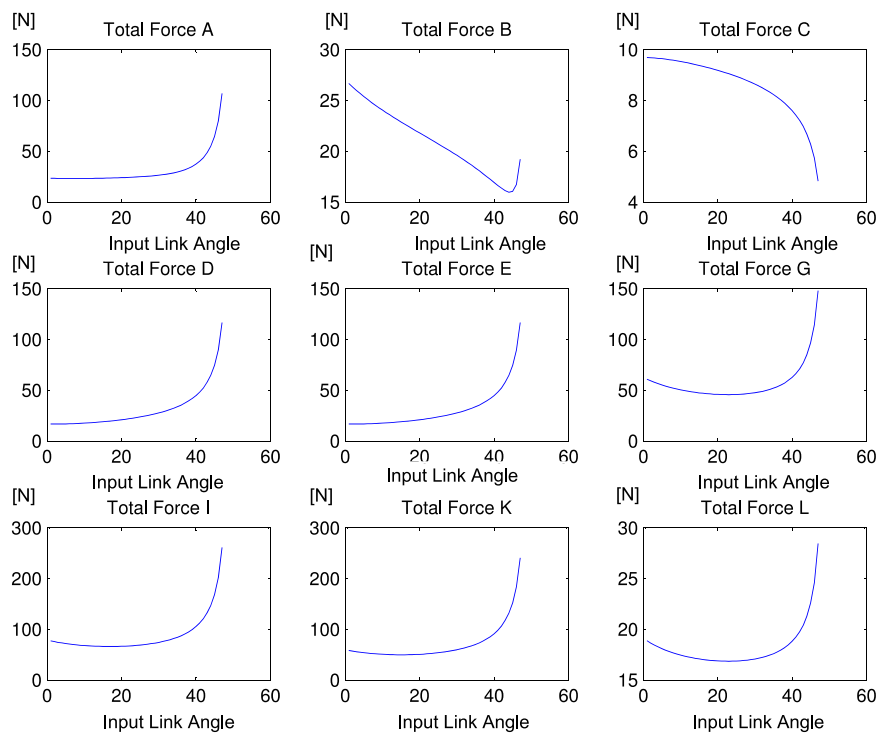


Figure 4.6: The forces between the mechanisms' links at different kinematic pairs. The diagrams show the modules of the force [N] in the revolute joints with respect to input link angle  $\alpha$  [Degree].

#### 4. Synthesis, Analysis and Design of 12-Link mechanism

---

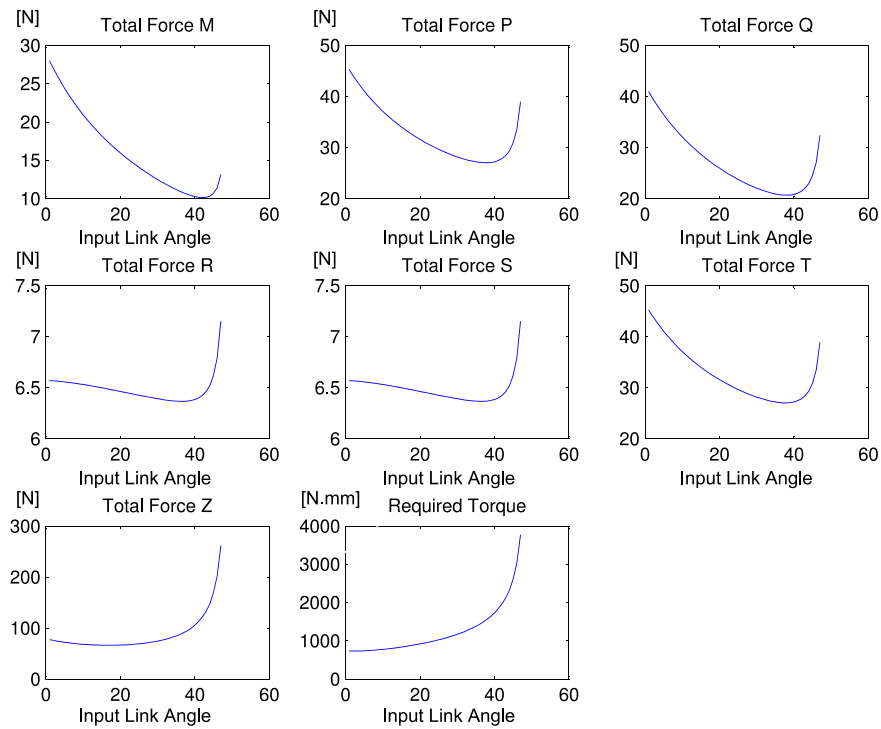


Figure 4.7: The forces between the mechanisms' links at different kinematic pairs. The diagrams show the modules of the force [N] in the revolute joints with respect to input link angle  $\alpha$  [Degree]. The last diagram presents the modulus of the required torque [N.mm] for grasping an object with respect to input angle  $\alpha$  [Degree].

#### 4. Synthesis, Analysis and Design of 12-Link mechanism

---

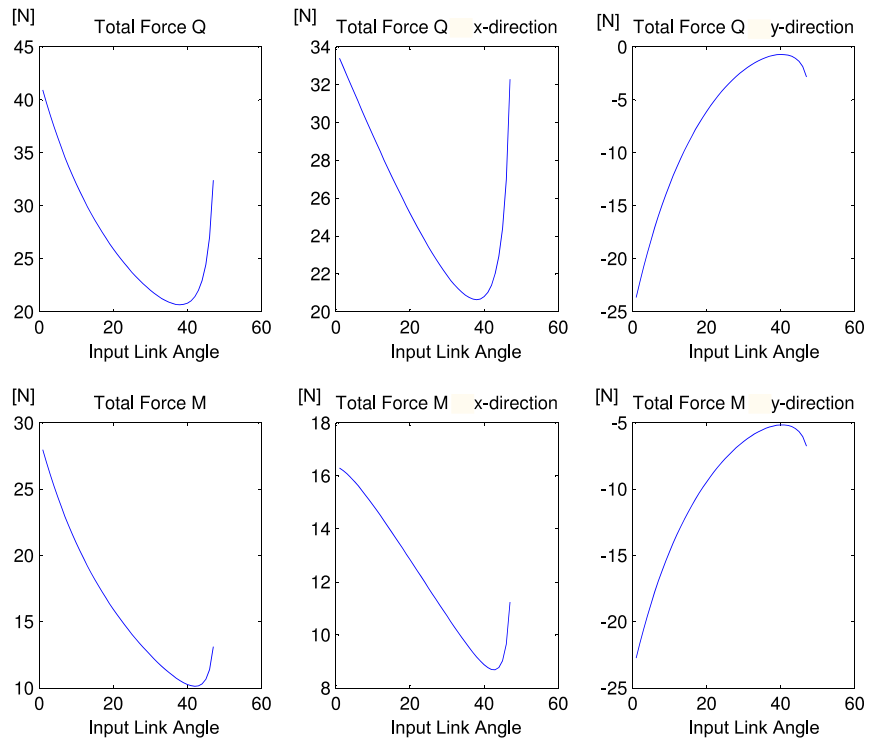


Figure 4.8: The modules and x,y components of the force in the joints Q and M. The first diagram of each row show the modules of the force [N] with respect to input angle  $\alpha$  [Degree] in joints Q and M, while the next two diagrams in each row present the modules of each force[N] in the "X" and "Y" directions with respect to input link angle  $\alpha$  [Degree].

#### 4. Synthesis, Analysis and Design of 12-Link mechanism

---

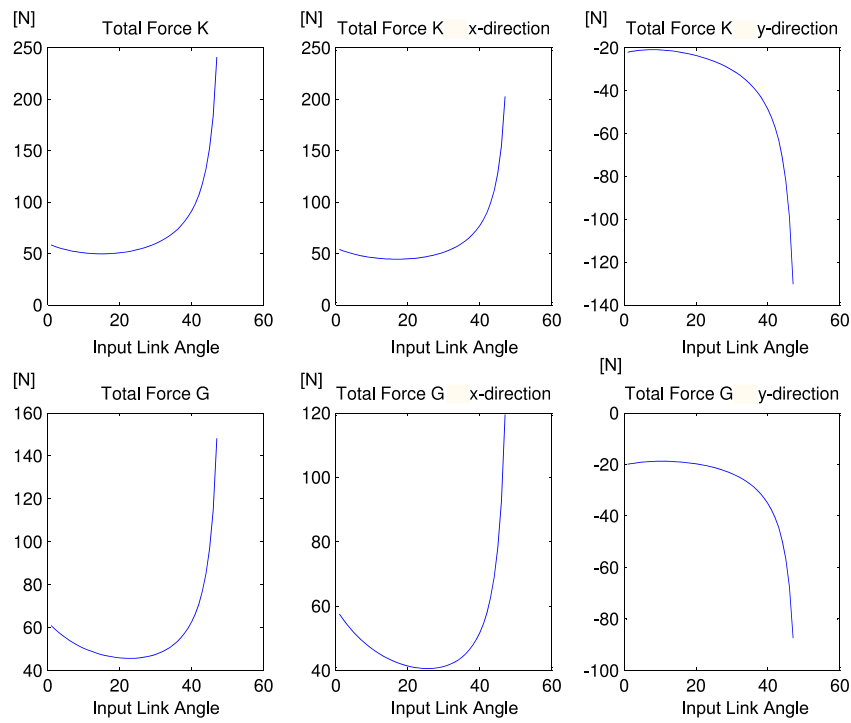


Figure 4.9: The modules and x,y components of the force in the joints K and G. The first diagram of each row show the modules of the force [N] with respect to input angle  $\alpha$  [Degree] in joints Q and M, while the next two diagrams in each row present the modules of each force[N] in the "X" and "Y" directions with respect to input link angle  $\alpha$  [Degree].

## 4. Synthesis, Analysis and Design of 12-Link mechanism

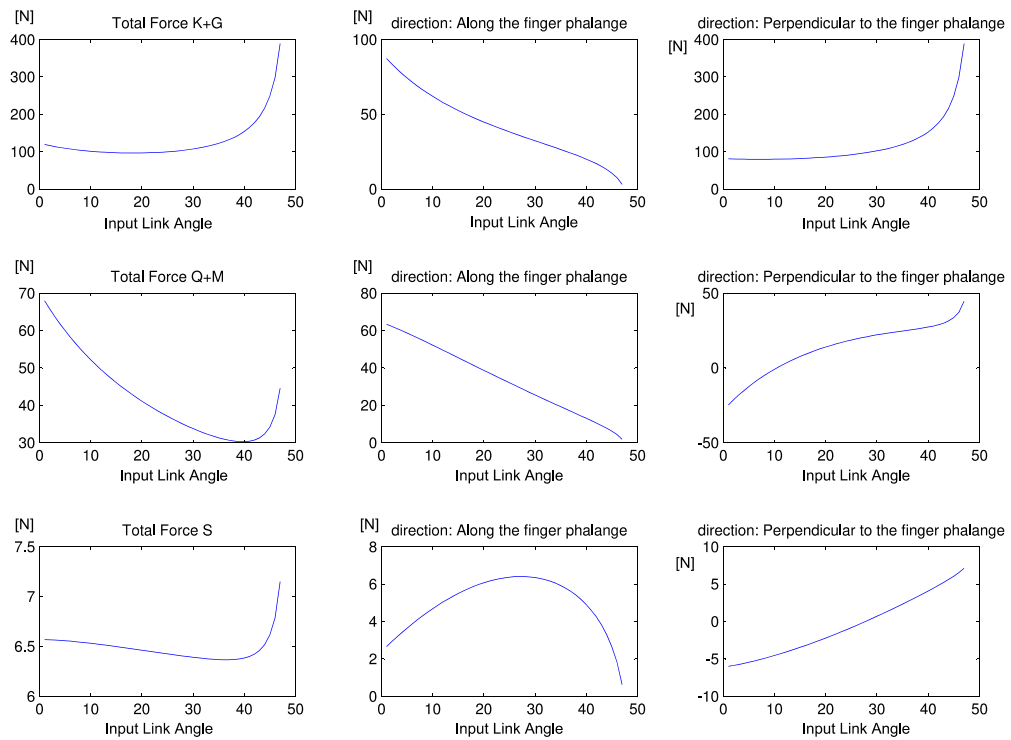


Figure 4.10: The forces exerted to the human finger phalanges with respect to input link angle  $\alpha$  [Degree]..

#### 4. Synthesis, Analysis and Design of 12-Link mechanism

---

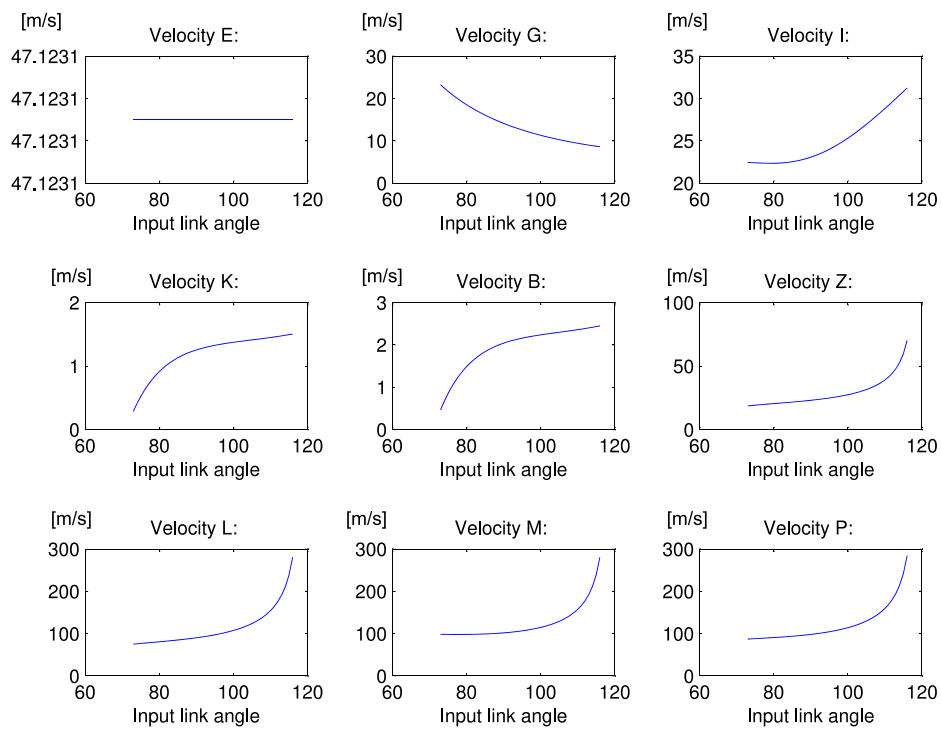


Figure 4.11: The velocities [m/s] of each joint with respect to input link angle  $\alpha$  [Degree].

#### 4. Synthesis, Analysis and Design of 12-Link mechanism

---

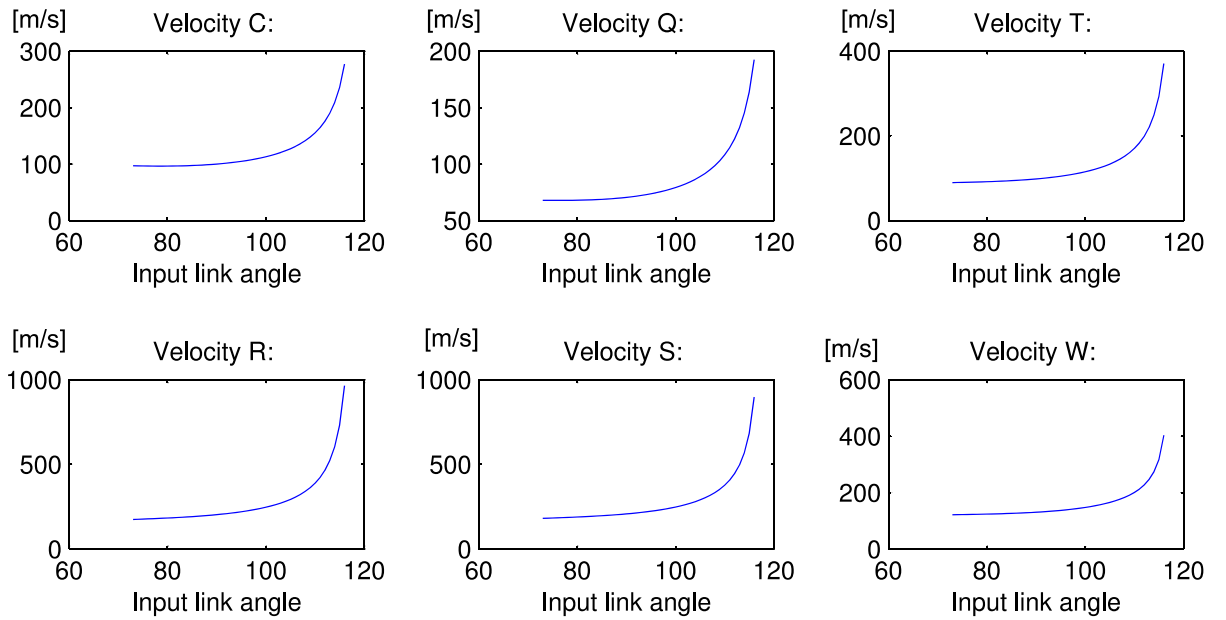


Figure 4.12: The velocities [m/s] of each joint of the mechanism with respect to input link angle  $\alpha$  [Degree].

#### 4. Synthesis, Analysis and Design of 12-Link mechanism

---

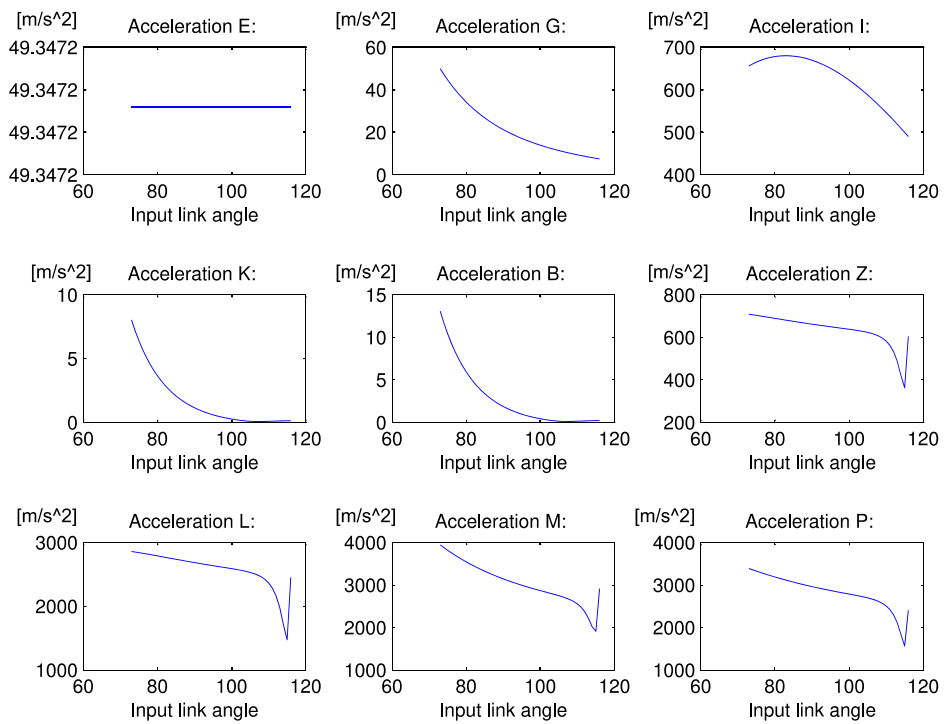


Figure 4.13: The accelerations  $[\text{m/s}^2]$  of each joint of the mechanism with respect to input link angle  $\alpha$  [Degree].

#### 4. Synthesis, Analysis and Design of 12-Link mechanism

---

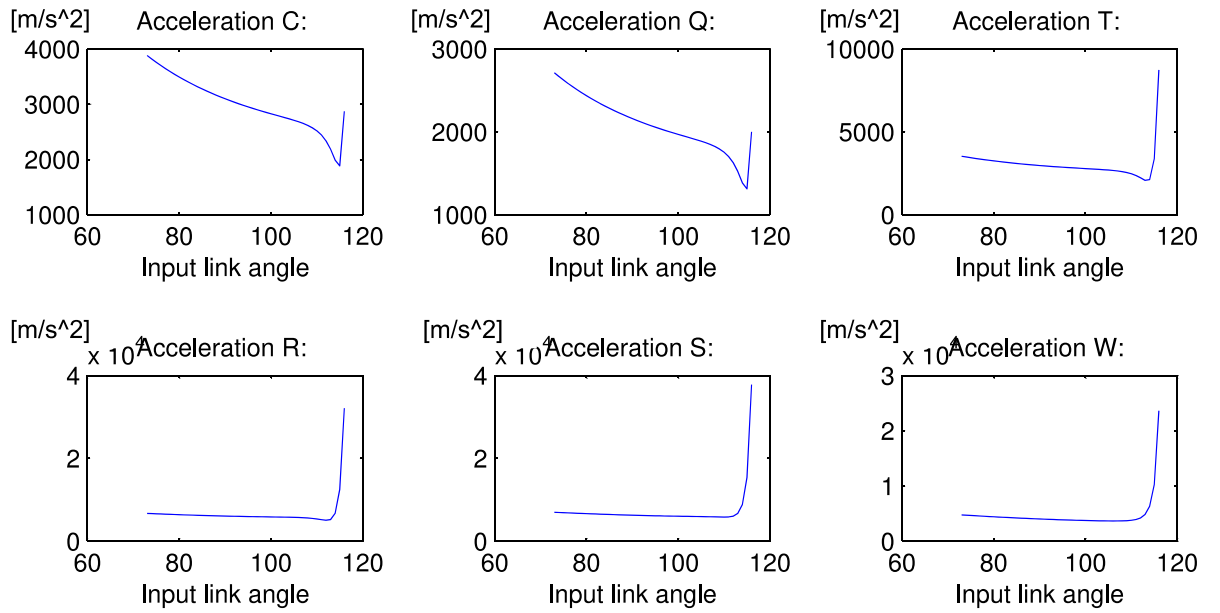


Figure 4.14: The accelerations  $[\text{m/s}^2]$  of each joint of the mechanism with respect to input link angle  $\alpha$  [Degree].

#### 4. Synthesis, Analysis and Design of 12-Link mechanism

---

abduction/adduction of the first phalanx of all the fingers is thus inhibited. For a cylindrical grasp, a device with one degree of freedom (DOF) only would be theoretically sufficient. However, the independent action of the thumb with respect to the four fingers was preferred to properly control the motion coordination in order to correctly grasp the object. All links of the mechanisms are located above the fingers not to disturb the finger movements and the grasping of objects, whereas the two actuators are placed on a frame fixed to the hand backside (see Fig. 4.15). The frame and the mechanisms are respectively connected to the hand and fingers by means of Velcro strips. The same topology is kept for the index, middle, ring, and little finger mechanisms(see Fig. 3.11), being the geometry resized to fit the specific finger size it is coupled with and to perform the corresponding trajectories. As already mentioned, the driving links of the four mechanisms are connected to the same driving shaft that receives power from one single actuator, so that the resulting group of fingers has 1-DOF. The same approach was considered for the design of the thumb mechanism. However, although the human thumb has the same number of phalanges, joints, and DOFs of the other four fingers, it was decided to keep the first phalanx fixed at a given pose, being this assumption based on the data taken from [Gülke et al. \[2010\]](#). The fixed pose of the first thumb phalanx with respect to the mechanism frame can be adjusted (by means of an internal 6 DOFs mechanism whose configuration can be passively regulated and fixed during the orthosis fitting) in order to select a proper plane of the thumb flexion/extension (being the optimal plane of motion variable from patient to patient). The thumb motor axis is generally skew with respect to the plane of motion: a spatial four-bar linkage (made of four links, two revolute joints and two spherical joints) is used as the transmission chain that connects the actuator axis to the axis of the mechanism driving link (see Fig. 4.15). The connecting rod between two spherical joints of the mentioned RSSR mechanism is adjustable, that can provide us the optimal force transmissibility for different patient hands.

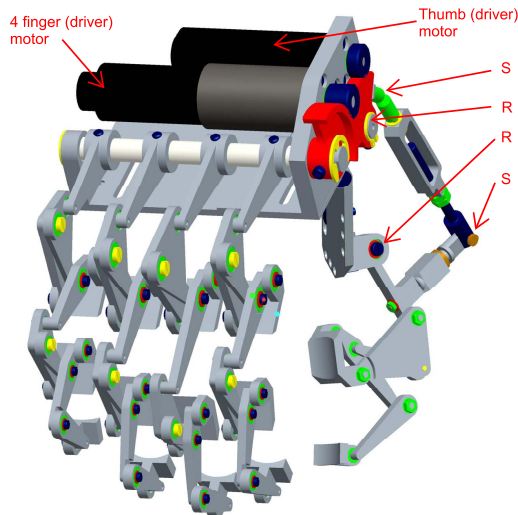


Figure 4.15: Schematic CAD model of the B.H.O. hand exoskeleton

### 4.5 B.H.O. Prototype

After designing the CAD model, the prototype was manufactured at Bologna University (see figures 4.18, 4.19 and 4.20). All machining process of each single part such as drilling and cutting (which is done by a CNC metalworking lathe) were done at the workshop of Bologna University. The Assembly process was also done in the same laboratory.

As a conclusion, an original solution for a hand exoskeleton conceived to support post-stroke patients in cylindrical shape grasping tasks with the aim of recovering the basic functions of manipulation was proposed. The device is formed by five planar mechanisms, one per finger, globally actuated by two electric motors. Indeed, the thumb flexion/extension movement along a certain plane is controlled by one actuator whereas a second actuator is devoted to the control of the flexion/extension of the other four fingers (being the four corresponding mechanisms connected to the same driving shaft). All links of the mechanisms are located above the fingers not to disturb the finger movements and the grasp-

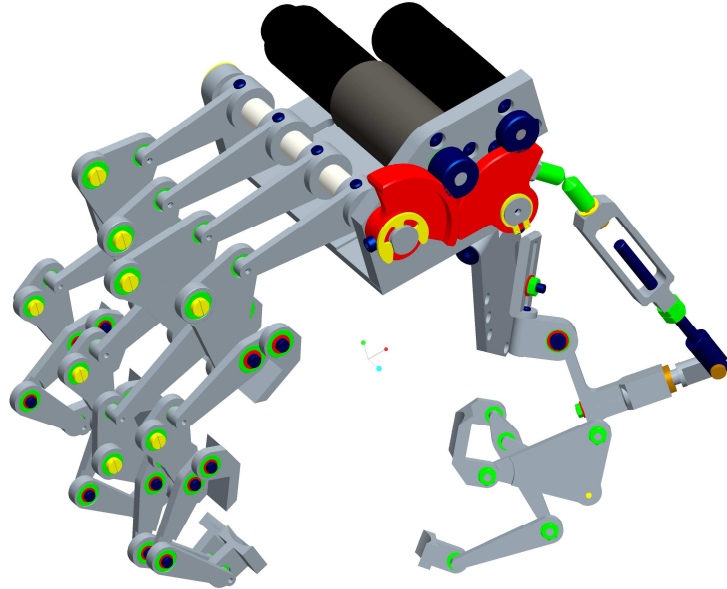


Figure 4.16: Schematic CAD model of the B.H.O. hand exoskeleton

ing of objects, whereas the two actuators are placed on a frame fixed to the hand backside. The mechanisms are connected to the fingers at the level of all the three phalanges by means of Velcro straps. All the finger mechanisms are based on the same kinematic architecture: with reference to Fig. 3.11, the mechanism comprises 12 links, also including the three phalanges that are fixed to three artificial moving links, interconnected by 16 revolute joints (three of which are provided by the anatomical articulations). The same approach was considered for the design of the thumb mechanism. However, although the human thumb has the same number of phalanges, joints, and DOFs of the other four fingers, it was decided to keep the first phalanx fixed at a given pose. The fixed pose of the first thumb phalanx with respect to the mechanism frame can be adjusted as mentioned in the last part (by means of an internal 6 DOFs mechanism whose configuration can be passively regulated and fixed during the orthosis fitting) in order to select a proper plane of the thumb flexion/extension (being the optimal plane of motion variable from patient to patient).

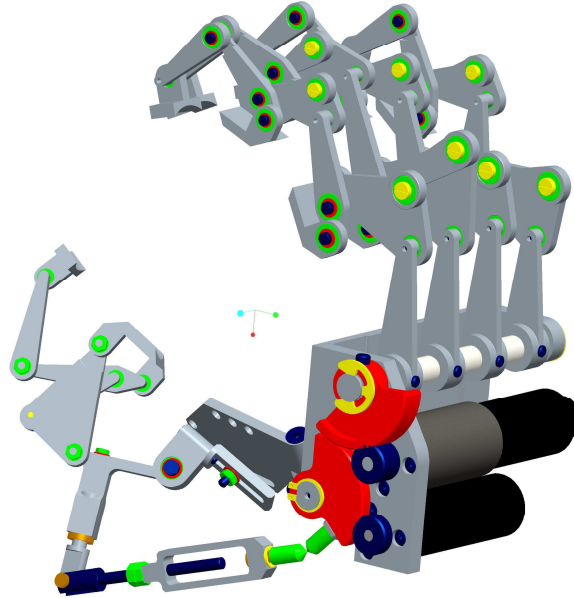


Figure 4.17: Schematic CAD model of the B.H.O. hand exoskeleton

In order to satisfy the desired constraints, the dimensional synthesis was done for 5 fingers so that the fingers pass through desired configurations. Another factor that was taken into account in dimensional synthesis was the synchronization problem. As already mentioned, the driving links of the four finger mechanisms are connected to the same driving shaft that receives power from one single actuator. Because of this single actuator, the motion of all fingers should be synchronous, so that when grasping a cylindrical object, phalanges should have a trajectory consistent with the requirement to have all phalanges that come into contact with the cylindrical object to be grasped at the same time (this would avoid to change the pose of the cylinder where it is grasped). The problem of finger synchronization was satisfactorily achieved by minimizing the errors when the group of four fingers grasps a cylindrical object of diameter 60 [mm], taken as a reference diameter for the selected range ( $50 \div 70$  [mm]).

After the dimensional synthesis, as already reported in previous sections, the static analysis was performed to both calculate the forces exerted by the mech-

#### 4. Synthesis, Analysis and Design of 12-Link mechanism

---

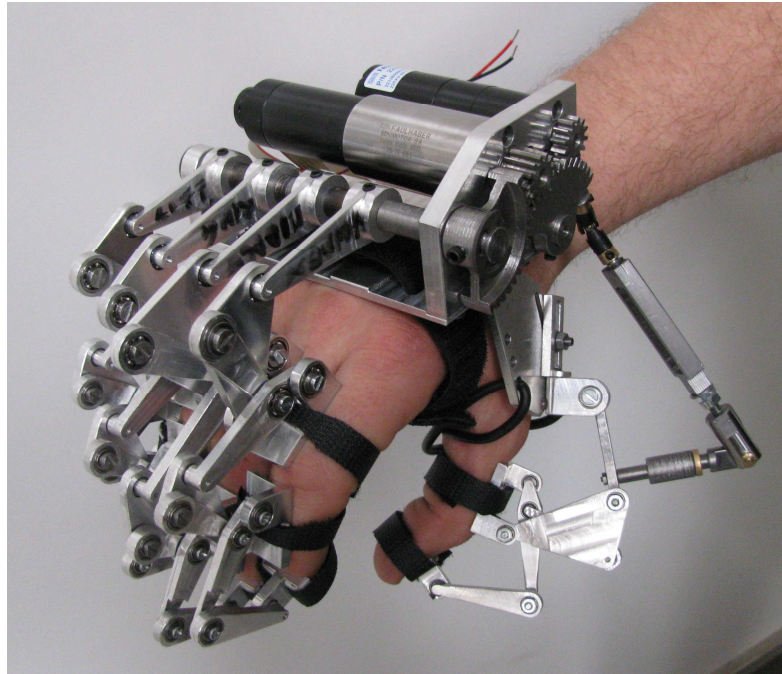


Figure 4.18: The manufactured prototype of the B.H.O. hand exoskeleton

anism links at the interface with the phalanges and the required driving torque for grasping an object or to balance the possible residual contracting forces. After designing the CAD model, the prototype was manufactured at the workshop of the department of Industrial Engineering (DIN) of Bologna University.

#### 4. Synthesis, Analysis and Design of 12-Link mechanism

---

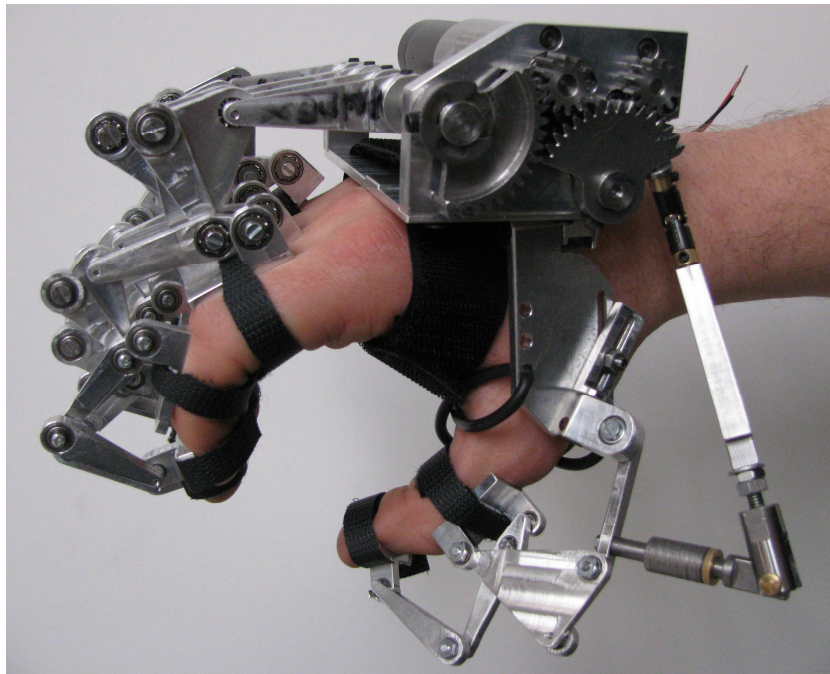


Figure 4.19: The manufactured prototype of the B.H.O. hand exoskeleton

#### 4. Synthesis, Analysis and Design of 12-Link mechanism

---

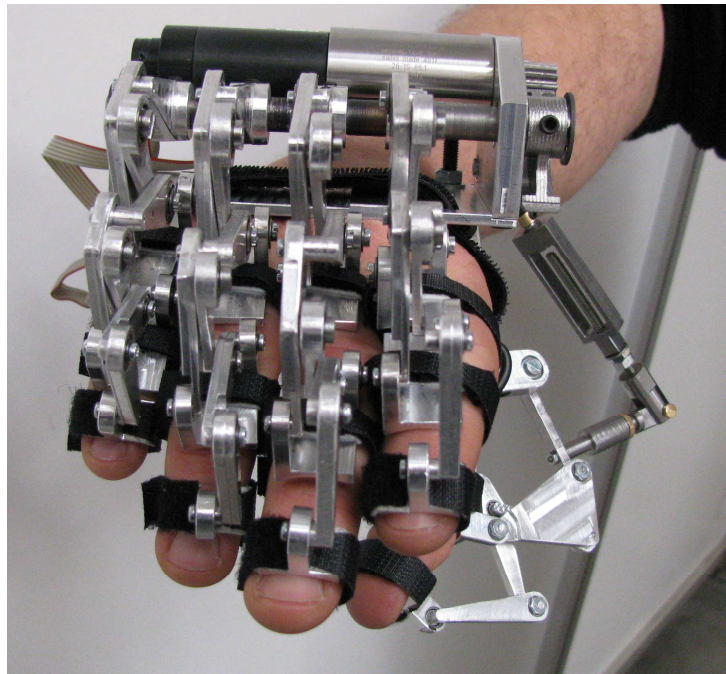


Figure 4.20: The manufactured prototype of the B.H.O. hand exoskeleton

# Chapter 5

## The Experimental tests

### 5.1 Introduction

After designing and manufacturing the HE, the prototype was delivered to PER-CRO laboratory of the Scuola Superiore Sant'Anna in Pisa (Italy) for some experimental tests. Two tests are reported here: the first one is testing the application of HE by using the Electromyography (EMG) signals for bilateral active training of grasp motion in stroke patients, and the second test is testing the application of HE connecting to the arm exoskeleton for motor rehabilitation of reaching and hand grasping motion in stroke patients.

### 5.2 An EMG-based robotic hand exoskeleton for bilateral training of grasp

This section presents the development and the preliminary experimental assessment of a novel EMG-driven robotic hand exoskeleton (B.H.O.) for bilateral active training of grasp motion in stroke. The system allows to control the grasping force required to lift a real object with an impaired hand, through the active guidance provided by a hand active exoskeleton, whose force is modulated by the EMG readings acquired on the opposite unimpaired arm. To estimate the grasping force, the system makes use of surface EMG recordings during grasping, developed on the opposite unimpaired arm. The design, integration and experi-

mental characterization of the system during the grasp of two cylindrical objects is presented. The experimental results show that the B.H.O. prototype can reach the desired configurations for grasping an objects while an optimal force tracking of the interaction force with the object can be achieved.

### 5.2.1 System Description

The proposed system allows users to bilaterally train the impaired hand movements for grasping purposes. The system, shown in Fig. 5.1, is composed of an EMG processing subsystem, that allow measuring the electromyographic muscle activity, combined with the B.H.O. Hand exoskeleton system, that assists the hand during grasping movements. Moreover in order to perform the tuning and performance evaluation of the system, it has been completed with two Force Sensing Resistors (FSR) sensorized objects, used to measure the interaction forces between the hands and the grasped objects.

#### 5.2.1.1 A graspable force sensorized object for rehabilitation applications

In order to measure the interaction forces between the hands and the cylindrical grasped objects, each object (an aluminum can) was equipped with four FSR sensors, as shown in Fig. 5.2. Given the limited number of four sensors per object, we identified the most suitable positions on the objects to estimate the grasping force, locating the FSRs in various positions corresponding to the contact points of the phalanxes and palm. The more efficient positions on the cans, for a grasping diameter of 65 mm, were chosen as the contact points of the proximal interphalangeal joint of the thumb and the intermediate phalanxes of the index, medium and ring fingers.

#### 5.2.1.2 EMG processing subsystem for grasp control

Surface EMG signals can be correlated with the force produced by muscles and the resulting torque at the joint level. It follows that they can be used to provide command in human machine interaction (De [1997], Buchanan et al. [2004], Muzumdar [2004]). In this study, in order to measure the electromyographic activity during

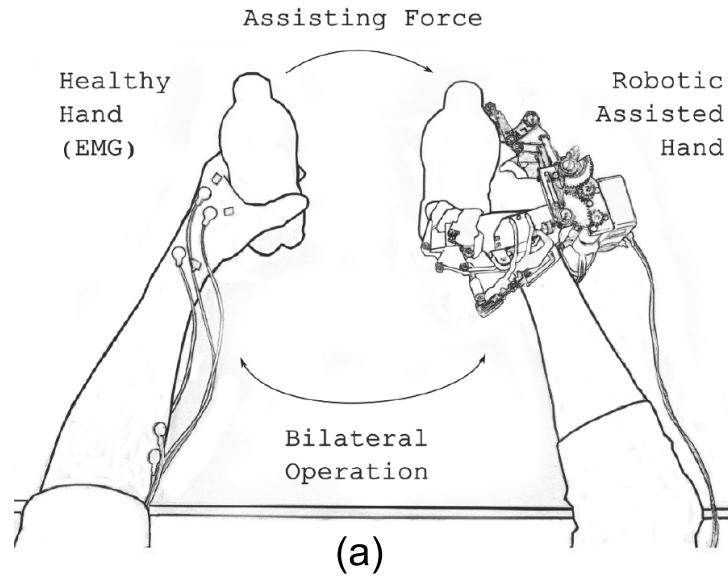


Figure 5.1: Conceptual scheme of the proposed system, (a) schematic overview (b) the captured picture.

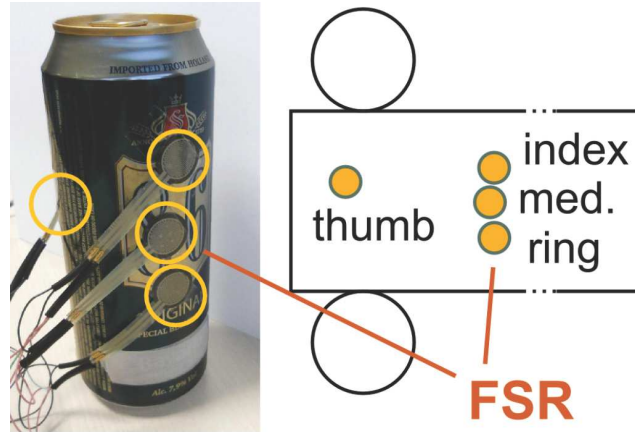


Figure 5.2: The sensorized cylindrical object (left) showing the correspondance between each FSR and the fingers (right).

grasping tasks, three pairs of electrodes were placed on three main forearm muscles, the extensor digitorum longus (EDL), the flexor digitorum longus (FDL) and the adductor pollicis brevis (APB). The EDL and the FDL are relative long muscles positioned respectively on the posterior and anterior forearm, whereas the APB is a superficial muscle located on the posterior side of the hand. The map of the EMG sensor locations is shown in Fig. 5.3.

### 5.2.2 The EMG-based robotic-assisted bilateral training

The setup of the proposed bilateral control architecture is shown in Fig. 5.4. The control architecture diagram with indication of information flow and processing among all different module is shown in Fig. 5.5. More in detail, the output signal of the sensorized object in the Hand (first block) is used to estimate the grasping force from EMG recordings. During the validation phase, outputs of the sensorized objects were used to calculate the interaction force error exerted by the hand wearing the hand orthosis with respect to the one exerted by the dominant/healthy hand.

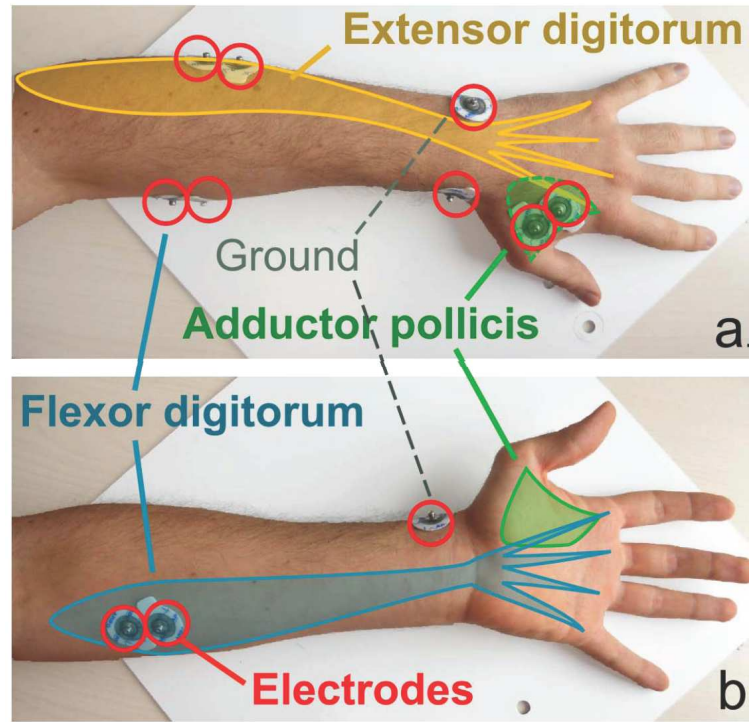


Figure 5.3: The sensor location of the EMG electrodes on the arm. Anterior surface (a.) and posterior surface (b.) of the left arm.

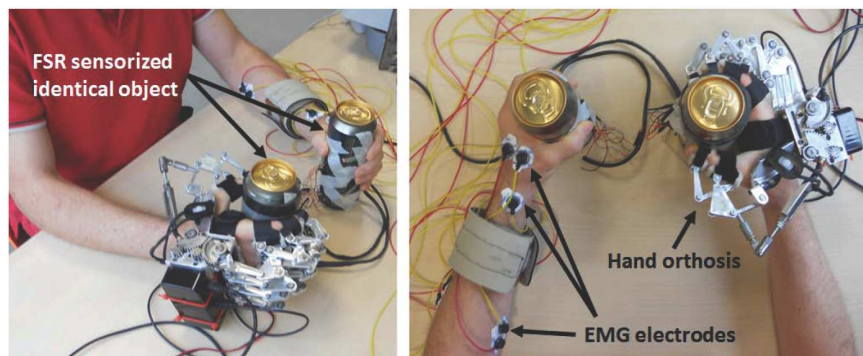


Figure 5.4: The setup for the experimental evaluation of the proposed system: side view (left) and top view (right).

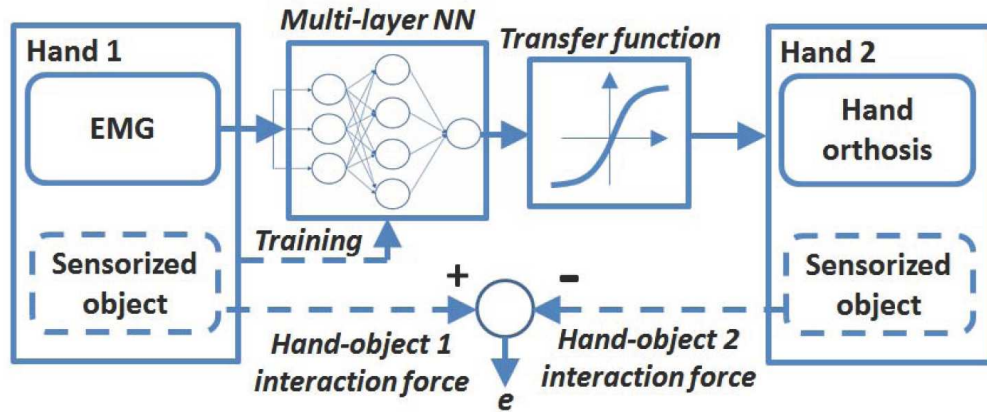


Figure 5.5: Global data flow of the system. Dotted lines indicate either training or evaluation information.

### 5.2.2.1 Experiment description

The two sensorized objects are used to measure the grasping force exerted by the hands with respect to time. From the difference between the grasping force exerted by the dominant/healthy hand and that exerted by the hand wearing the hand orthosis, it is possible to easily calculate the bilateral error. The conducted experiment consisted in five repetitions of the grasping task by a healthy subject (male, 25 yrs old). It was conventionally decided to use the left hand as dominant/healthy and the right one as the impaired one. To simulate this condition, we asked the subject to keep his own right hand completely passive.

### 5.2.2.2 Experimental results

Figure 5.6 reports the results of the quantitative experimental evaluation. More in detail, the plots of the grasping forces acquired by the sensorized objects are reported (left hand is the dominant/healthy hand). As it is possible to see, the user is able to control the grasping force achieving an optimal tracking of the force reference. The subject was able to grasp and lift up the object in his hand with a good grasp control.

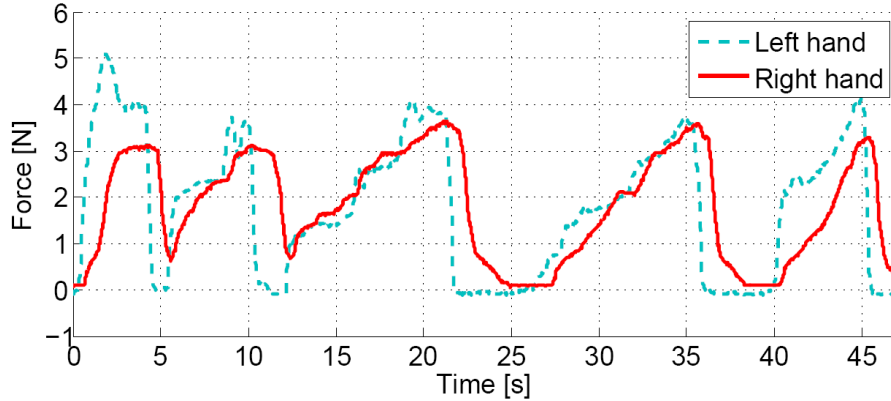


Figure 5.6: Grasping forces acquired by the sensorized objects during the experiment exerted by the left (dominant/healthy) and right (wearing the hand orthosis) hands.

As a conclusion, the results provided by both analysis of the conducted experiment are promising and demonstrate the usability of the proposed EMG-based robotic-assisted system for the bilateral hand training of grasping. This myoelectrically controlled robotic hand exoskeleton system is promising and appears particularly indicated for the rehabilitation of hand function for people with hemiparesis (i.e. after stroke).

### 5.3 A Motor Imagery BCI approach to robotic-assisted neuro-motor rehabilitation of reaching and hand grasping in stroke

This part proposes a novel approach to motor rehabilitation of reaching and hand grasping in stroke affected patients. Patients are allowed to perform goal directed manipulation activities with the intentional control of an upper limb exoskeleton triggered by mental activity through a self-paced asynchronous BCI. Patients are instructed to plan only mentally movement execution, and only when sufficient Event-Related-Desynchronization (ERD) activity is detected at contralateral mo-

tor areas, motion is triggered with the assistance of the combined action of an arm and hand exoskeleton. The assistance to both reaching and grasping movements, taking into account pre-shaping of hand for object affordability, combines uniquely rehabilitation training to grasping of both distal and proximal upper extremity segments. In this preliminary study, we show how this approach can be successfully used in chronic stroke, by analyzing the performance of four chronic stroke patients specifically enrolled to this aim. Results show how BCI control can be successfully used, and how patients are able to perform assisted reaching and grasping tasks of simple objects.

### 5.3.1 System Description

#### 5.3.1.1 The BRAVO Exoskeleton

The BRAVO exoskeleton was explicitly conceived to provide assistance to patients in the execution of functional tasks of reaching and grasping with the impaired arm, see Fig. 5.7. To this purpose the L-Exos, an active robotic exoskeleton with four degrees of freedom (Frisoli et al. [2009]) supporting elbow and shoulder movements, was integrated with an active wrist with two degrees of freedom, and one hand exoskeleton(B.H.O)(Mozaffari-Foumashi et al. [2013] and Loconsole et al. [2013a]) for thumb and fingers (two dofs).

#### 5.3.1.2 The integrated BCI system

The motor imagery Brain Computer Interface system is based on the analysis of the patients  $\mu$  (8-12Hz) and  $\beta$  (12-24Hz) EEG rhythms recorded through a pattern of 13 electrodes placed over the motor-cortex (here  $\beta$  in italic has not to be confused with the angle of PIP joint in Fig. 3.11).

#### 5.3.1.3 Control

L-Exos control was based on bounded-jerk trajectory planning described in Frisoli et al. [2012]: the shoulder, the forearm, and the wrist (handpalm) were involved in the exoskeleton trajectory planning to allow on-line generation of motion primitives mimicking human movements in reaching tasks. The Hand-Exos (B.H.O.),

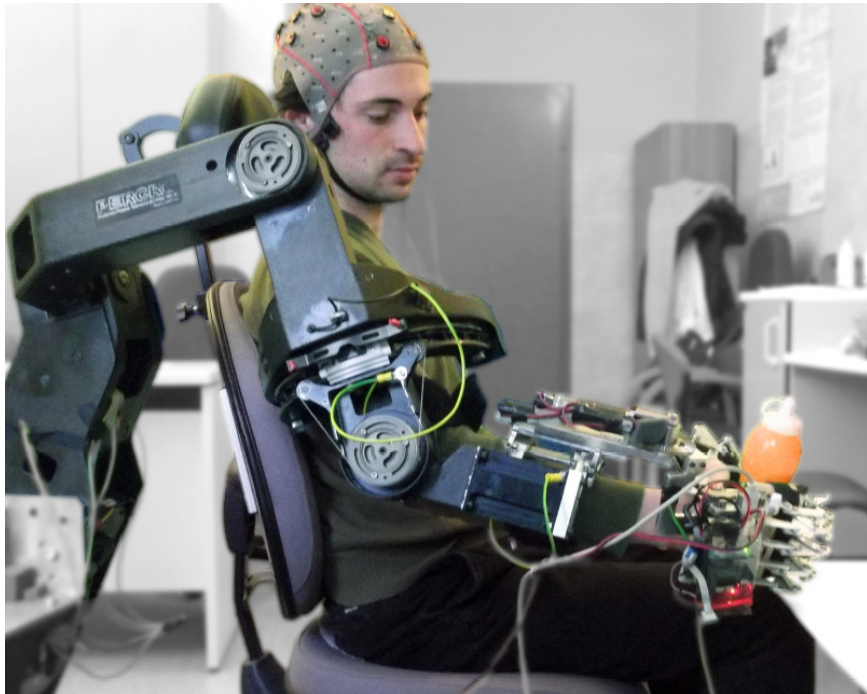


Figure 5.7: The BRAVO hand exoskeleton

instead, was controlled through a torque reference as described in [Loconsole et al. \[2013b\]](#), in order to control opening and closure hand movements. Due to the almost isometric nature of the task, requiring small velocities of fingers in the grasping phase, the voltage applied to the actuators was estimated in feedforward from the electrical parameters of the motor, according to the supply voltage provided to each actuator.

### 5.3.2 Experimental Evaluation

#### 5.3.2.1 Participants

Four chronic stroke survivors (age  $58 \pm 9$ , 2 males/2 females) with right arm hemiparesis were enrolled in the study. They were instructed about the study finality and given their written consensus. A clinical assessment was performed to evaluate the baseline at the enrollment with upper extremity scales. Furthermore a preliminary test session to ensure their ability of usage of the BCI was performed.

#### 5.3.2.2 Procedure and methods

The rehabilitation session consisted of two phases: a first training phase lasting 10 minutes and a second robot-aided therapy phase lasting 30 minutes. The training session was executed in order to train the BCI parameters, and to let the subject become familiar with the execution of the rest and mental activity. The training session was composed of a sequence of 40 tasks randomly sorted between rest and mental activity classes, each one lasting 5 seconds and spaced with a random relaxation period of 4 s. During each task, the subject was asked through visual cues either to perform mental activity involving the impaired limb, or to hold a mental rest state. The rehabilitation phase consisted in a reaching and grasping scenario composed of three main tasks, as illustrated in [Fig. 5.8](#).

- from home position (H), move to target A (or B), grasp the target object, then move to H and release grasp;
- from H, move to target A, grasp the target object, then move to B position, release grasp, then go to H.

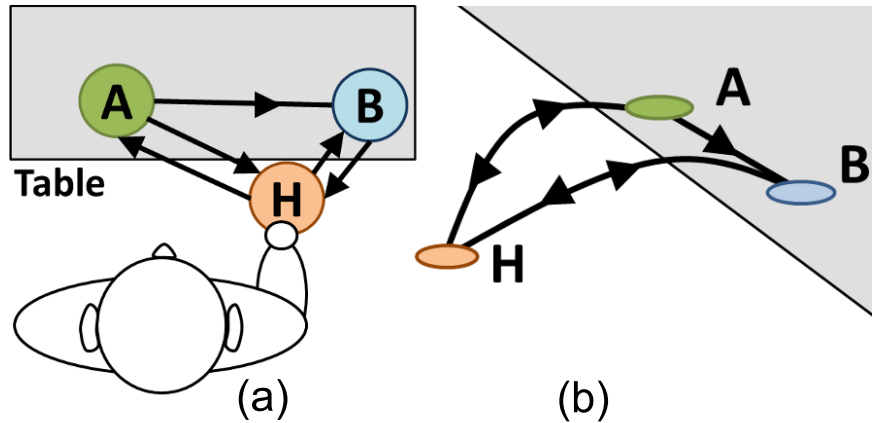


Figure 5.8: Conceptual scenario for the reaching and grasping tasks proposed to the patients; from home position (H), move to target A (or B), grasp the target object, then move to H and release grasp; from H, move to target A, grasp the target object, then move to B position, release grasp, then go to H.

The tasks were designed with the intent of replicating typical daily tasks of object manipulation on a desktop. Common objects with shape well suited for hand affordability were employed, such as fruits (apples, pears) or daily object, such as glasses and cans. Each grasping task was composed of four subsequent phases: Preparation of movement, Reaching, Grasping, Bringing back and Releasing. Figure 5.9 illustrates the general procedure, with the indication of preshaping, grasp and release movements, and BCI feedback monitoring. During the Preparation of movement phase, the patient was asked to perform mental activity involving the reaching and grasping of the target object with the impaired limb. The patients mental state was monitored through the BCI, and as soon as a cumulative period of 2 s of mental activity was collected, the system was triggered for the next Reaching phase (yellow background color in Fig. 5.9). A timeout of 9 s was implemented for triggering the next phase independently of the patient brain activity.

In the following Reaching, Grasping and Bringing back phases the patient motion was assisted and guided by the BRAVO Exoskeleton. In the Reaching phase, the exoskeleton approached the target object through a task-oriented pre-

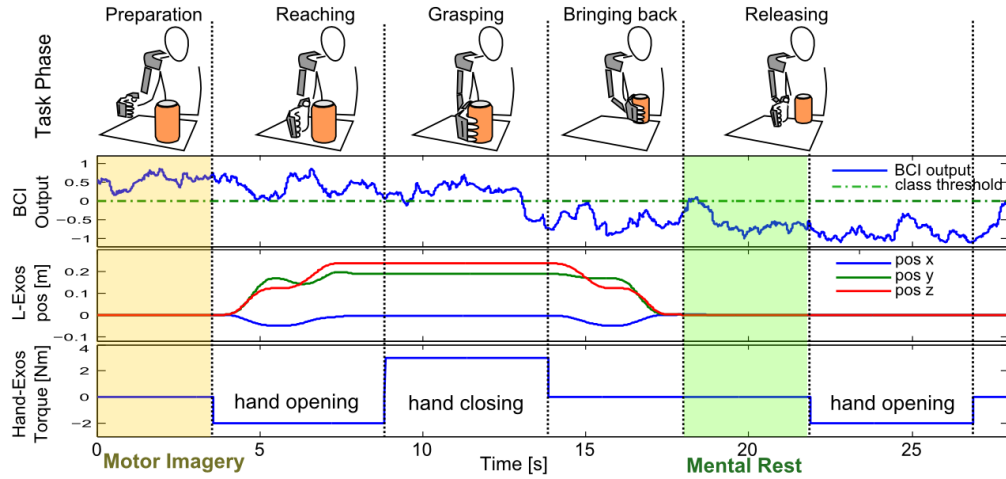


Figure 5.9: The grasping sequence.

computed trajectory, and applied a reference opening force to fingers for executing the hand pre-shaping. The Grasping phase lasted 5 s, during which the exoskeleton applied a constant force to fingers in order to grasp the target object. In the following Bringing back phase, the exoskeleton brought the patients arm to the home position, holding fingers closed onto the grasped object. During the last phase (Releasing), the patient was asked to recover a rest mental state in order to release the object. Similarly to the Preparation of movement phase, a cumulative period of 2 s of Rest mental state had to be collected, with a timeout of 9 s, in order to trigger the opening of the Hand Exos (green background color in Fig. 5.9). The global time required for completing one grasping sequence was 30 s for the best performance, while 44 s were required for the worst case (in case the processed mental activity never matched the requested mental state). Patient 4 performed the rehabilitation phase with a timeout of 2 s for the Releasing phase.

### 5.3.3 Preliminary Results

Figure 5.10 shows the actual trajectory performed by one of the patients during the reaching task, corresponding to a task such as the one shown in Fig. 5.11. Performance evaluation of the rehabilitation session was based on the time

required for accomplishing each reaching-grasping task and on the correct classification rate of the BCI output. Table 5.1 reports the following parameters: in the first column the BCI classification performance (correct rate), expressed as the percentage of time during which mental activity was correctly classified (mental activity for the Preparation phase and Rest for the Releasing phase), in the second and third columns respectively the elapsed time for accomplishing each of the Preparation and Releasing phases expressed in second and in time percentage, normalized between the minimum (0%, 2 sec) and maximum (100%, 9 sec) required time.

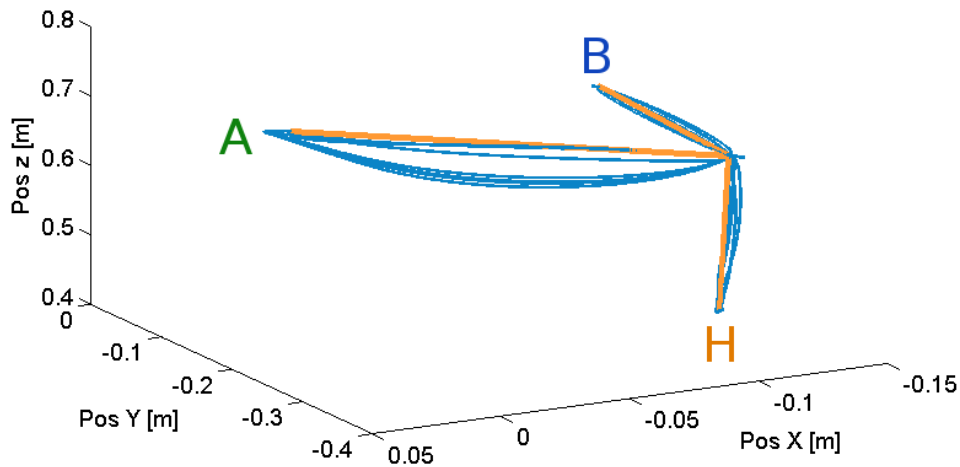


Figure 5.10: Trajectories executed during the rehabilitation session for one patient

As a conclusion, a novel approach for rehabilitation of both reaching and hand grasping in stroke was proposed. Robotic assistance triggered by a motor imagery BCI system was integrated into a more ecologic rehabilitation scenario involving the whole sequence of phases (preparation of movement, reaching, grasping, bringing back and releasing) occurring during natural execution of a reaching-grasping task. The BRAVO exoskeleton, featuring shoulder and elbow assistance and adaptive kinematics for the hand, allowed patients to accomplish goal di-

## 5. The Experimental tests

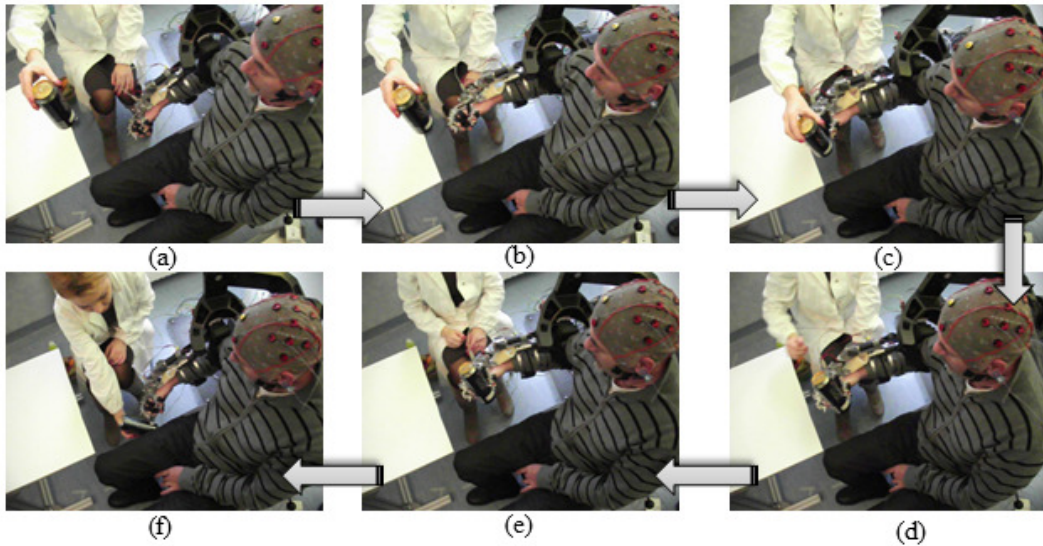


Figure 5.11: Sequence of movements performed by one patient under BCI control: a→b reaching, c→d grasping, e return movement, f release

	Mental Activity					
	Feedback[%]		Time[S]		Time[S]	
	Mean	SD	Mean	SD	Mean	SD
Subject 1	59.5	24.04	4.18	2.30	31.10	32.82
Subject 2	66.62	29.22	3.83	2.02	26.04	28.81
Subject 3	88.60	15.16	2.35	0.49	4.98	7.00
Subject 4	70.76	38.58				
	Rest					
Subject 1	65.00	17.07	3.35	1.06	19.27	15.15
Subject 2	83.29	20.60	2.60	0.77	8.56	10.99
Subject 3	51.31	28.53	4.77	2.20	39.52	31.44
Subject 4	82.86	25.56				
Average	70.94	27.39	3.52	1.82	21.58	25.95

Table 5.1: Results of the rehabilitation session

rected activities of manipulation. The BCI system, triggering the task execution through mental activity, represents a key-factor of the rehabilitation paradigm for closing the feedback loop between the patients mental activity and the proprioception of the robotic-assisted task execution. Moreover, the proposed paradigm introduced the rest mental state as a required activity for the task accomplishment, thus balancing the mental effort of the patient, and focusing his attention also onto hand relaxation controlled through brain activity. The feasibility of the proposed rehabilitation scenario was assessed by performance results shown in table 5.1. All subjects were able to successfully complete the rehabilitation session, reporting an average correct classification rate of the mental activity vs rest brain activity of 70.9%, and with an averaged time of 3.52 s for accomplishing each of the BCI triggered phases (Preparation of movement and Releasing). It was shown that motor imagery BCI can be profitably implemented for triggering robotic assistance, allowing patient to conduct the whole rehabilitation session with reasonable mental effort. Results are thus promising for assessing the efficacy of the proposed approach in a larger clinical study.

# Chapter 6

## Conclusions

The synthesis of hand exoskeleton for the rehabilitation of post-stroke patients was presented in this dissertation. As for the first step, the analysis of state-of-the-art was reported. Based on this, a topological classification focused on three main key issues that have a major influence on the synthesis of the exoskeleton mechanisms was proposed, namely on the number of actuated degrees of freedom, on the number of mechanical connections between the mechanism and the human finger, and on the mechanism architecture. There is a close relation among the different key factors, and selecting a given specific solution can solve a group of problems related to one aspect of the design, but it could trigger other kinds of problems or limitations in other aspects. Based on these three principles, the rehabilitation hand exoskeletons were systematically analyzed and classified. This classification is helpful to understand both the reason of proposing certain solutions for specific applications and the advantages and drawbacks of the different designs proposed in the literature. Additionally, this classification can provide some useful guidelines for the design of new hand exoskeletons, that was actually the primary motivation of this study.

In addition to the proposed classification, many other general design issues emerged from the literature analysis such as type of connection between the exoskeleton and the human fingers, safety factors, actuations/motors, control issues, sensor and encoder equipments were deeply discussed and some common principles were offered to researchers who are approaching this design problem. After that, the feasibility study of three different 1-DOF mechanisms for a single finger, intended

as the basic model of the targeted hand exoskeleton, were also presented: one is a 6-link mechanism based on the Watt chain connected to the human finger only at his tip; another one is an 8-link mechanism with four prismatic and nine revolute joints, where phalanges and articulations are part of the kinematic chain (with three connection points between the exoskeleton and the human finger being necessary to close the chain), and the third one is a 12-link mechanism with all revolute joints where still the human phalanges and articulations are part of the kinematic chain. The Watt-chain-based linkage is extremely simple and it leaves the human finger free to directly get in contact in a wide area with the grasped object, but it suffers from a serious singularity configuration within the workspace. The problem can be solved by complicating the architecture and introducing auxiliary links and joints to form an internal sub-mechanism. The second linkage is free from singularities in the considered workspace and its architecture is yet not very complicated, so that it could be a good candidate solution. However further studies, show that these could raise to unacceptable high forces both in the prismatic joints and, above all, in the connections between the links and the human phalanges. The third linkage contains higher number of links but it contains many good advantages such as: reaching the desired trajectory without interference with the human phalanges, high range of motion, maintaining the forces in acceptable range. Based on the advantages and drawbacks of the proposed three planar mechanisms, the 12-link mechanism was selected as a suitable candidate for the single finger exoskeleton. After selecting the mechanism, the dimensional synthesis, kinematic and static analyses were done for all fingers separately in order to satisfy the desired constraints. The proposed solution successfully provides the desired trajectory for the specified grasping motion, while the forces exerted on human phalanges at the interface with the mechanism links are in a proper range.

As for the primary motivation of this study, a novel hand exoskeleton device was designed for the rehabilitation of the hand of post-stroke patients to enable the cylindrical shape grasping tasks with the aim of recovering the basic functions of manipulation. The proposed device features five proposed planar 12-link mechanisms, one per finger, globally actuated by two electric motors. In particular, the thumb flexion/extension movement, in a plane, ... selected within a certain range,

is controlled by one actuator, whereas a second actuator is devoted to the control of the flexion/extension of the other four fingers (being the four corresponding mechanisms connected to the same driving shaft). As the same topology is used for the group of four fingers and all four fingers are actuated by one unique motor, the synchronization issue is taken into account in the final synthesis procedure in order to guarantee a correct grasping. The problem of finger synchronization was satisfactorily achieved by minimizing the errors when the group of the four fingers grasp a cylindrical object of diameter 60 [mm].

After manufacturing the device at the DIN workshop of the University of Bologna, the prototype was delivered to "PERCRO laboratory" of the Scuola Superiore Sant'Anna in Pisa (Italy) for experimental tests. Two experimental tests were done: the first one is testing the application of the hand exoskeleton by using the EMG signals for bilateral active training of grasp motion in stroke patients, and the second one is testing the application of hand exoskeleton integrated to the arm exoskeleton for motor rehabilitation of reaching and grasping tasks in stroke patients. The results obtained by both experiments are promising and demonstrate the usability of the proposed robotic-assisted system for the hand training in grasping tasks.

# Appdx A

The synthesis method that was applied in this dissertation was the Burmester-theory-based procedure proposed by McCarthy (Soh and McCarthy [2008]). The philosophy of the synthesis method can be briefly explained as follows (McCarthy [2000]): the mechanical constraints is introduced to a planar 3R serial chain to guide the movement of its end effector through a set of five specified task positions to obtain a six-bar linkage, as illustrated in Fig. 1.

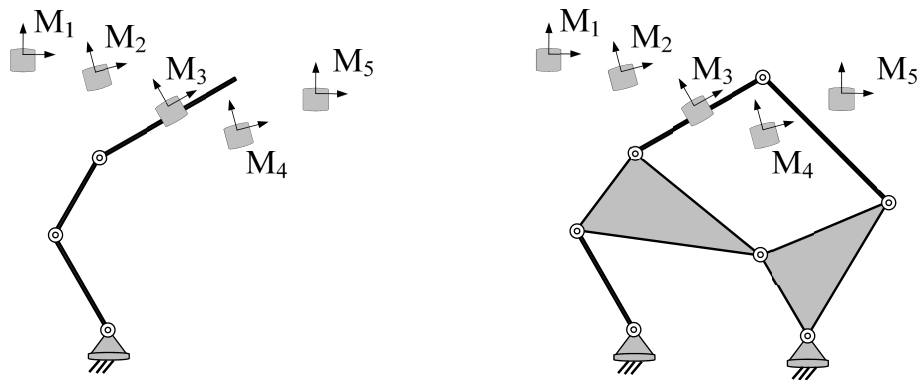


Figure 1: A planar 3R serial chain is constrained by two RR chains to define a six-bar linkage.

A planar 3R chain includes four links and three revolute joints  $C_i$ ,  $i = 1, 2, 3$  as shown in Fig. 2. We assume that this chain has full mobility in the plane with its configuration defined joint angles  $\theta_1$ ,  $\theta_2$  and  $\theta_3$ , and can reach a set of task positions.

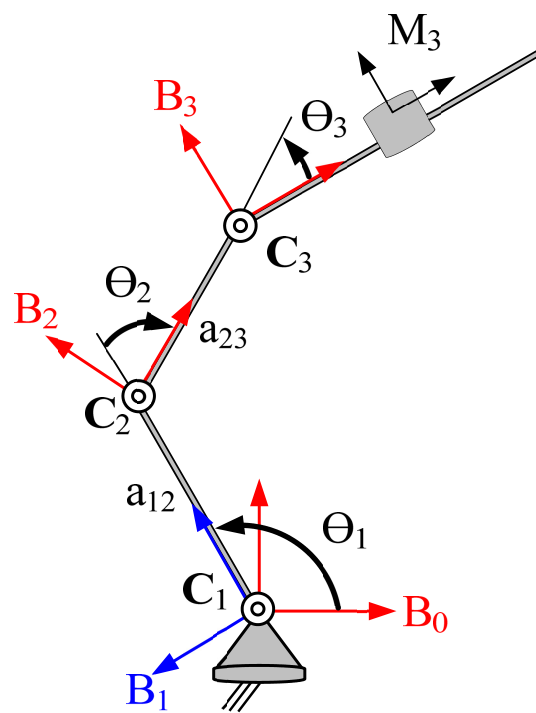


Figure 2: A schematic of a planar 3R serial chain. The graph of this chain forms a straight line with a vertex for each link in the manipulator.

The goal is to add constraints consistent with the task positions. While any of the constraints PR, RP, and RR can be used, our focus is on RR constraints, Fig. 3.

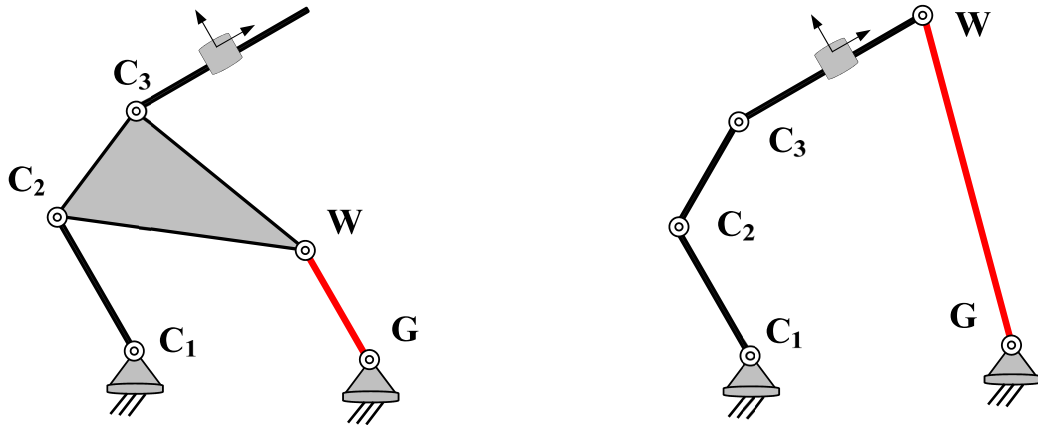


Figure 3: Examples of constrained 3R serial chain.

A planar six-bar linkage consists of six links and seven joints and has two topologically distinct structures. These are called the Watt and Stephenson six-bar chains, Fig. 4. Inversions of these chains yield the Watt I, Watt II, Stephenson I, Stephenson II, and Stephenson III linkages.

In order to identify the ways to add RR constraints to a 3R serial chain, we denote links of the 3R chain, as  $B_i$ ,  $i = 0, 1, 2$  and  $3$ . An RR chain cannot constrain consecutive links, therefore the two links that can be connected by the first RR constraint are (i)  $B_0B_2$ , (ii)  $B_0B_3$ , or (iii)  $B_1B_3$ . Once the first constraint is attached, the second RR constraint can be connected either to one of the original links, or to the link created by the first RR constraint. Figure 5 shows the various systems that result from independent RR constraints applied to a 3R chain. Notice that while two RR chains can connect  $B_3$  to ground, there are no other cases in which the two RR cranks are connected to the same bodies. The result is three six-bar linkages, the Stephenson IIb, Stephenson IIIa, and Stephenson IIIb. The notation a and b is used to distinguish the input crank, which we consider to be the first link of the 3R chain.

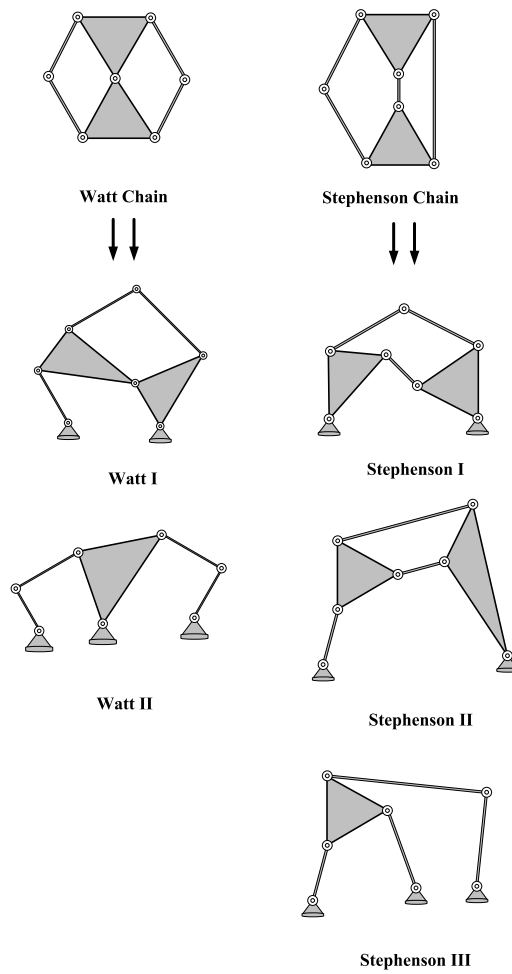
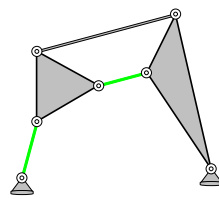
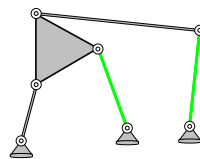


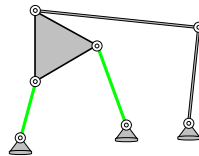
Figure 4: The Watt and Stephenson six-bar chains, and the different forms obtained by selecting different links as the base.



**Stephenson IIb**



**Stephenson IIIa**



**Stephenson IIIb**

Figure 5: The linkage graphs show the synthesis sequence for the three constrained 3R chains in which the two RR chains are attached independently.

We now consider the case in which the second RR chain is connected to the new link  $B_4$  of the first RR chain. Figure 6 shows that we obtain the following four topologies, which can be identified as (i)  $(B_0B_2;B_3B_4)$  known as a Watt Ia linkage, (ii)  $(B_0B_3;B_1B_4)$ , the Stephenson I, (iii)  $(B_0B_3;B_2B_4)$ , the Stephenson IIa, and (iv)  $(B_1B_3;B_0B_4)$ , the Watt Ib linkage.

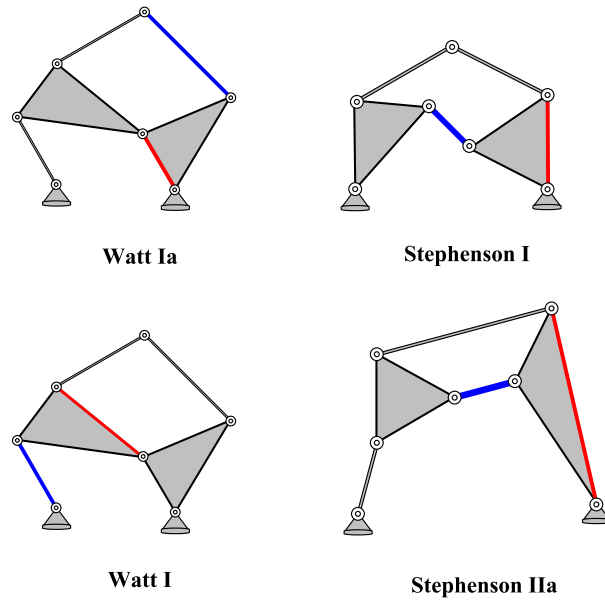


Figure 6: The linkage graphs show the synthesis sequence for the four constrained 3R chains in which the second RR chain connects to the first RR chain.

In order to size the two RR constraints for the 3R backbone chain, we generalize the RR synthesis equations. Let  $[B_{l,j}]$ ,  $j = 1, \dots, 5$ , be the five positions of the  $l$ -th moving link, and  $[B_{k,j}]$ ,  $j = 1; \dots, 5$ , the five positions of the  $k$ -th moving link measured in a world frame  $F$ . Let  $g$  be the coordinates of the R joint attached to the  $l$ -th link measured in the link frame  $B_l$ . Similarly, let  $w$  be the coordinates of the other R joint measured in the link frame  $B_k$ . The five positions assumed by these points of the moving frame as the two bodies move relative to each other are given by:

$$G^j = [B_{l,j}]g, \quad W^j = [B_{k,j}]w \quad (1)$$

Where  $[B_{l,j}]$  is the position of the l-th moving link and  $[B_{k,j}]$  is the position of the k-th moving link. Now introduce the relative displacements ( $[R_{l,j}]$  and  $[S_{l,j}]$ ):

$$[R_{1j}] = [B_{l,j}][B_{l,1}]^{-1}, [S_{1j}] = [B_{k,j}][B_{k,1}]^{-1} \quad (2)$$

then these equations become:

$$G^j = [R_{1j}]G^1, W^j = [S_{1j}]W^1 \quad (3)$$

where  $[R_{11}] = [S_{11}] = [I]$  are the identity transformations. The points  $G^j$  and  $W^j$  define the ends of a binary rigid link of length R; therefore we have the constraint equations:

$$([S_{1j}]W^1 - [R_{1j}]G^1)([S_{1j}]W^1 - [R_{1j}]G^1) = R^2 \quad (4)$$

These five equations 4 can be solved to determine the five design parameters of the RR constraint,  $G^1 = (u, v, 1)^T$ ,  $W^1 = (x, y, 1)^T$ , and R. We will refer to these equations as the general synthesis equations for the planar RR link. To solve the general synthesis equations, it is convenient to introduce the displacements:

$$[D_{1j}] = [R_{1j}]^{-1}[S_{1j}] = [B_{l1}][B_{l,j}]^{-1}[B_{k,j}][B_{k1}]^{-1} \quad (5)$$

then we obtain

$$([D_{1j}]W^1 - G^1)([D_{1j}]W^1 - G^1) = R^2, j = 1, 2, 3, 4, 5 \quad (6)$$

Subtract the first of these equations from the remaining ones to cancel  $R^2$  and the square terms in the variables  $u, v$  and  $x, y$ . The resulting four bi-linear equations can be solved algebraically to obtain the desired pivots. The general synthesis equations 6 can be solved using an algebraic elimination procedure. Recall that this consists of constructing four bi-linear equations and extracting four  $3 \times 3$  minors  $M_j$  to obtain four cubic polynomials in  $x$  and  $y$ , given by:

$$\Lambda_j : d_{j0}y^3 + d_{j1}y^2 + d_{j2}y^1 + d_{j3}y^0 = 0, j = 1, 2, 3, 4 \quad (7)$$

where the coefficient  $d_{kj}$  is a polynomial in  $x$  of degree  $k$ . The four polynomials  $\Lambda_j$  are assembled into the matrix equation:

$$\Lambda = [D(x)]m = 0 \quad (8)$$

where:

$$[D(x)] = \begin{bmatrix} d_{10}(x) & d_{11}(x) & d_{12}(x) & d_{13}(x) \\ \vdots & \vdots & \vdots & \vdots \\ d_{40}(x) & d_{41}(x) & d_{42}(x) & d_{43}(x) \end{bmatrix}, m = \begin{bmatrix} y^3 \\ y^2 \\ y \\ 1 \end{bmatrix} \quad (9)$$

This equation can be solved for a non-zero  $m = (y^3; y^2; y; 1)$ , only if the resultant matrix  $[D(x)]$  has a determinant equal to zero. Here we present a method to compute the roots of  $\det[D(x)] = 0$  using the eigenvalue technique described in [Manocha and Krishnan \[1996\]](#). For convenience, rename  $x$  as  $\lambda$ , and expand

$[D(\lambda)]$  in matrix polynomial form as:

$$[D(\lambda)] = [D_0] + [D_1]\lambda + [D_2]\lambda^2 + [D_3]\lambda^3 \quad (10)$$

where  $D_0$ ,  $D_1$ ,  $D_2$ , and  $D_3$  are  $4 \times 4$  matrices. The roots of  $\det D(\lambda) = 0$  are the finite eigenvalues of the generalized system:

$$[B]x = \lambda[A]x \quad (11)$$

where  $A$ ,  $B$ , and  $x$  are given by:

$$[A] = \begin{bmatrix} I_4 & 0 & 0 \\ 0 & I_4 & 0 \\ 0 & 0 & D_3 \end{bmatrix}, [B] = \begin{bmatrix} 0 & I_4 & 0 \\ 0 & 0 & I_4 \\ -D_0 & -D_1 & -D_2 \end{bmatrix}, x = \begin{bmatrix} m \\ \lambda m \\ \lambda^2 m \end{bmatrix} \quad (12)$$

where  $I_4$  is the  $4 \times 4$  identity matrix and  $0$  is a  $4 \times 4$  matrix of zeros. The solution of this eigenvalue problem yields four finite solutions. For each real value of  $\lambda$  we compute its eigenvector and obtain a value for  $y$ . Notice that each eigenvector  $x$  is defined up to a constant multiple  $\mu$ , therefore, it is convenient to determine the coordinate of  $y$  by computing the ratio of elements of  $x$ , such as:

$$y = \frac{x_3}{x_4} = \frac{\mu y}{\mu} \quad (13)$$

The remaining variables  $u$  and  $v$  are obtained by solving two of the four bilinear synthesis equations formulated from equation 6. The synthesis of an RR constraint yields as many as four different geometries, therefore two constraints can yield 16 different geometries. However, our process always has one link of the 3R chain as one of the solutions, so there are at most 12 different geometries.

The Stephenson I structure has all 12 different geometries. The Stephenson II has two different sets of different geometries that differ in the workpiece link, and so yields 24 different geometries. The Stephenson III also has two ways to connect to the end effector, one of which yields 12 different geometries and the other six, a total of 18. The Watt I has two different sets of different geometries that differ in the input crank, and both sets include a link on the 3R chain for both RR constraints, so there are  $2 \times 9$  candidates. The result is as many as 72 different six-bar linkage geometries obtained using this process (McCarthy [2000]).

Given any six-bar linkage, we can perform closed-form kinematic analysis to simulate its movement using complex vectors and the Dixon determinant (see McCarthy [2000]). Our focus in this section is on the Watt Ia six-bar, but the approach can be applied to all of the six-bar linkages obtained from our synthesis methodology. All that is needed are the loop equations for the linkage. Consider the general Watt Ia linkage shown in Fig. 7. Introduce a Cartesian frame such that the base pivot of the 3R chain,  $C_1$ , is the origin with its x-axis directed toward  $G_1$ . Let the configuration angles  $\theta_i$ ,  $i = 1, 2, 3, 4, 5$  be as shown in Fig. 7. Using the notation in Fig. 7, we formulate the vector equations of the loops formed by  $C_1 C_2 W_1 G_1$  and  $C_1 C_2 C_3 W_2 G_2 G_1$ , that is:

$$\mathfrak{F}1 : l_1 \cos(\theta_1) + b_1 \cos(\theta_2 - \gamma) - b_2 \cos(\theta_4 - \eta) - l_0 = 0 \quad (14)$$

$$\mathfrak{F}2 : l_1 \sin(\theta_1) + b_1 \sin(\theta_2 - \gamma) - b_2 \sin(\theta_4 - \eta) = 0 \quad (15)$$

$$\mathfrak{F}3 : l_1 \cos(\theta_1) + l_2 \cos(\theta_2) - l_3 \cos(\theta_3) - l_4 \cos(\theta_4) - l_5 \cos(\theta_5) - l_0 = 0 \quad (16)$$

$$\mathfrak{F}4 : l_1 \sin(\theta_1) + l_2 \sin(\theta_2) - l_3 \sin(\theta_3) - l_4 \sin(\theta_4) - l_5 \sin(\theta_5) = 0 \quad (17)$$

Select the angle  $\theta_1$  as the input to the six-bar linkage, then these four equa-

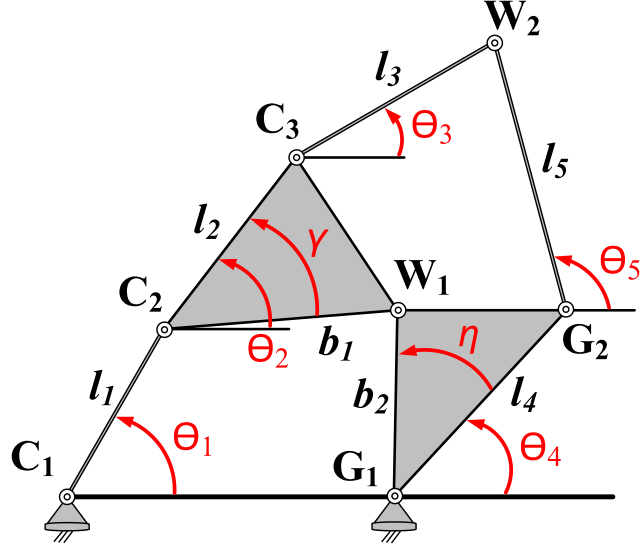


Figure 7: The joint angle and link length parameters for the Watt Ia six-bar linkage.

tions  $\mathfrak{F}_i$  determine the joint angles  $\theta_j$ ;  $j = 2,3,4,5$ . Now introduce the complex numbers  $\Theta_j = e^{i\theta_j}$ , so the four loop equations 14, 15, 16 and 17 become two complex loop equations:

$$l_1 : l_1\Theta_1 + b_1\Theta_2e^{-i\gamma} - b_2\Theta_4e^{i\eta} - l_0 = 0 \quad (18)$$

$$l_2 : l_1\Theta_1 + l_2\Theta_2 + l_3\Theta_3 - l_4\Theta_4 - l_5\Theta_5 - l_0 = 0 \quad (19)$$

Take the complex conjugate of these two equations:

$$l_1^* : l_1\Theta_1^{-1} + b_1\Theta_2^{-1}e^{i\gamma} - b_2\Theta_4^{-1}e^{-i\eta} - l_0 = 0 \quad (20)$$

$$\ell_2^* : l_1\Theta_1^{-1} + l_2\Theta_2^{-1} + l_3\Theta_3^{-1} - l_4\Theta_4^{-1} - l_5\Theta_5^{-1} - l_0 = 0 \quad (21)$$

We now solve the four complex loop equations (18), (19), (20) and (21) for the complex configuration angles  $\Theta_j$ ,  $j = 2,3,4,5$  by using the Dixon determinant. Suppress  $\Theta_3$ , so we have four complex equations in the three variables  $\Theta_2$ ,  $\Theta_4$  and  $\Theta_5$ . We formulate the Dixon determinant by inserting each of the four functions  $\ell_1, \ell_1^*, \ell_2$  and  $\ell_2^*$  as the first row, and then sequentially replacing the three variables by  $\alpha_j$  ( $j=2,4$  and  $5$  respectively) in the remaining rows, to obtain:

$$\Delta(\ell_1, \ell_1^*, \ell_2, \ell_2^*) = \begin{vmatrix} \ell_1(\Theta_2, \Theta_4, \Theta_5) & \ell_1^*(\Theta_2, \Theta_4, \Theta_5) & \ell_2(\Theta_2, \Theta_4, \Theta_5) & \ell_2^*(\Theta_2, \Theta_4, \Theta_5) \\ \ell_1(\alpha_2, \Theta_4, \Theta_5) & \ell_1^*(\alpha_2, \Theta_4, \Theta_5) & \ell_2(\alpha_2, \Theta_4, \Theta_5) & \ell_2^*(\alpha_2, \Theta_4, \Theta_5) \\ \ell_1(\alpha_2, \alpha_4, \Theta_5) & \ell_1^*(\alpha_2, \alpha_4, \Theta_5) & \ell_2(\alpha_2, \alpha_4, \Theta_5) & \ell_2^*(\alpha_2, \alpha_4, \Theta_5) \\ \ell_1(\alpha_2, \alpha_4, \alpha_5) & \ell_1^*(\alpha_2, \alpha_4, \alpha_5) & \ell_2(\alpha_2, \alpha_4, \alpha_5) & \ell_2^*(\alpha_2, \alpha_4, \alpha_5) \end{vmatrix} \quad (22)$$

This determinant is zero when  $\Theta_j$ ,  $j=2,4,5$ , satisfy the loop equations, because the elements of the first row become zero. Notice that each complex loop equation has the form:

$$\ell_k : c_{k0} + c_{k3}x + \sum_{j=2,4,5} c_{k,j}\Theta_j \quad (23)$$

$$\ell_1^* : c_{k0}^* + c_{k0}^*x^{-1} + \sum_{j=2,4,5} c_{k,j}^*\Theta_j^{-1} \quad (24)$$

where  $x$  denotes the suppressed variable  $\Theta_3$ . Clearly, the equations maintain this form when  $\alpha_j$  replaces  $\Theta_j$ . Now row reduce  $\Delta$  by subtracting the second row from the first row, then the third from the second, and the fourth from the

third, to obtain:

$$\begin{vmatrix} c_{12}(\Theta_2 - \alpha_2) & c_{12}^*(\Theta_2^{-1} - \alpha_2^{-1}) & c_{22}(\Theta_2 - \alpha_2) & c_{22}^*(\Theta_2^{-1} - \alpha_2^{-1}) \\ c_{14}(\Theta_4 - \alpha_4) & c_{14}^*(\Theta_4^{-1} - \alpha_4^{-1}) & c_{24}(\Theta_4 - \alpha_4) & c_{24}^*(\Theta_4^{-1} - \alpha_4^{-1}) \\ c_{15}(\Theta_5 - \alpha_5) & c_{15}^*(\Theta_5^{-1} - \alpha_5^{-1}) & c_{25}(\Theta_5 - \alpha_5) & c_{25}^*(\Theta_5^{-1} - \alpha_5^{-1}) \\ \ell_1(\alpha_2, \alpha_4, \alpha_5) & \ell_1^*(\alpha_2, \alpha_4, \alpha_5) & \ell_2(\alpha_2, \alpha_4, \alpha_5) & \ell_2^*(\alpha_2, \alpha_4, \alpha_5) \end{vmatrix} \quad (25)$$

This determinant contains extraneous roots of the form  $\Theta_j = \alpha_j$ , which we can remove by dividing out the factor  $(\Theta_j^{-1} - \alpha_j^{-1})$  using  $\Theta_j - \alpha_j = -\Theta_j \alpha_j (\Theta_j^{-1} - \alpha_j^{-1})$ , in order to define the determinant:

$$\delta = \frac{\Delta(\ell_1, \ell_1^*, \ell_2, \ell_2^*)}{(\Theta_2^{-1} - \alpha_2^{-1})(\Theta_4^{-1} - \alpha_4^{-1})(\Theta_5^{-1} - \alpha_5^{-1})} \quad (26)$$

that is:

$$\delta = \begin{bmatrix} -c_{12}\Theta_2\alpha_2 & c_{12}^* & -c_{22}\Theta_2\alpha_2 & c_{22}^* \\ -c_{14}\Theta_4\alpha_4 & c_{14}^* & -c_{24}\Theta_4\alpha_4 & c_{24}^* \\ -c_{15}\Theta_5\alpha_5 & c_{15}^* & -c_{25}\Theta_5\alpha_5 & c_{25}^* \\ \ell_1(\alpha_2, \alpha_4, \alpha_5) & \ell_1^*(\alpha_2, \alpha_4, \alpha_5) & \ell_2(\alpha_2, \alpha_4, \alpha_5) & \ell_2^*(\alpha_2, \alpha_4, \alpha_5) \end{bmatrix} \quad (27)$$

This determinant expands to form a polynomial of the form:

$$\delta = a^T[W]t = 0 \quad (28)$$

where  $a$  and  $t$  are vectors of monomials:

$$a = \begin{bmatrix} \alpha_2 \\ \alpha_4 \\ \alpha_5 \\ \alpha_4\alpha_5 \\ \alpha_2\alpha_5 \\ \alpha_2\alpha_4 \end{bmatrix}, t = \begin{bmatrix} \Theta_2 \\ \Theta_4 \\ \Theta_5 \\ \Theta_4\Theta_5 \\ \Theta_2\Theta_5 \\ \Theta_2\Theta_4 \end{bmatrix} \quad (29)$$

the  $6 \times 6$  matrix  $[W]$  is given by:

$$[W] = \begin{bmatrix} D_1 x + D_2 & A^T \\ A & -(D_1^* x^{-1} + D_2^*) \end{bmatrix} \quad (30)$$

and the matrices  $[D_1]$  and  $[D_2]$  are  $3 \times 3$  diagonal matrices, given by:

$$[D_1] = \begin{bmatrix} b_1 b_2 l_3 l_5 e^{-i(\gamma+\eta)} & 0 & 0 \\ 0 & -b_1 b_2 l_3 l_5 e^{i(\gamma+\eta)} & 0 \\ 0 & 0 & 0 \end{bmatrix}, [D_2] = \begin{bmatrix} d_1 & 0 & 0 \\ 0 & d_2 & 0 \\ 0 & 0 & d_3 \end{bmatrix} \quad (31)$$

Where:

$$d_1 = (l_1 \Theta_1 - l_0)(b_1 b_2 l_5 e^{-i(\gamma+\eta)} - b_2 l_2 l_5 e^{-i(\eta)}) \quad (32)$$

$$d_2 = (-l_1 \Theta_1 + l_0)(b_1 b_2 l_5 e^{i(\gamma+\eta)} - b_2 l_2 l_5 e^{i(\gamma)}) \quad (33)$$

$$d_3 = (l_1\Theta_1 - l_0)(b_2l_2l_5e^{-i(\eta)} - b_1l_4l_5e^{i(\gamma)}) \quad (34)$$

and the  $3 \times 3$  matrix  $[A]$  is given by:

$$[A] = \begin{bmatrix} 0 & b_1b_2l_5^2e^{i(\gamma+\eta)} & -b_2^2l_2l_5 + b_1b_2l_4l_5e^{i(\gamma+\eta)} \\ -b_1b_2l_5^2e^{-i(\gamma+\eta)} & 0 & -b_1^2l_4l_5 + b_1b_2l_2l_5e^{-i(\gamma+\eta)} \\ b_2^2l_2l_5 - b_1b_2l_4l_5e^{-i(\gamma+\eta)} & b_1^2l_4l_5 - b_1b_2l_2l_5e^{i(\gamma+\eta)} & 0 \end{bmatrix} \quad (35)$$

A set of values  $\Theta_j$  that satisfy the loop equations (18), 19, 20 and 21 will also yield  $\delta_j = 0$ , which will be true for arbitrary values of the auxiliary variables  $\alpha_j$ . Thus, solutions for these loop equations must also satisfy the matrix equation:

$$[W]t = 0 \quad (36)$$

The matrix  $[W]$  has the structure:

$$[W]t = [Mx - N]t = 0 \quad (37)$$

where:

$$M = \begin{bmatrix} D_1 & 0 \\ A & D_2^* \end{bmatrix}, N = \begin{bmatrix} -D_2 & -A^T \\ 0 & D_1^* \end{bmatrix} \quad (38)$$

Because  $[W]$  is a square matrix, this equation has non-zero solutions only if  $\det[W] = 0$ . Expanding this determinant, we obtain a polynomial in  $x = \Theta_3$ .

Notice that the values of  $x=\Theta_3$  that satisfy  $\det[W] = 0$  are also eigenvalues of the characteristic polynomial  $p(x)=\det(Mx-N)$  of the generalized eigenvalue problem:

$$[N]t = x[M]t \quad (39)$$

Each value of  $x=\Theta_3$  has an associated eigenvector  $t$ , which yields the values of the remaining joint angles  $\Theta_j$ ;  $j=2,4,5$ . It is useful to notice that an eigenvector  $t = (t_1, t_2, t_3, t_4, t_5, t_6)^T$  is defined only up to a constant multiple,  $\mu$ . Therefore, it is convenient to determine the values  $\Theta_j$  by the computing the ratios,

$$\Theta_2 = \frac{t_5}{t_3} = \frac{\mu\Theta_2\Theta_5}{\mu\Theta_5}, \Theta_4 = \frac{t_6}{t_1} = \frac{\mu\Theta_2\Theta_4}{\mu\Theta_2}, \Theta_5 = \frac{t_4}{t_2} = \frac{\mu\Theta_4\Theta_5}{\mu\Theta_4} \quad (40)$$

For a given input angle, a six-bar linkage can have as many as six roots for the configuration variables  $\Theta_j$ ,  $j=2,3,4,5$ . Each of these roots defines an assembly of the six-bar linkage. As we analyze a six-bar linkage for a sequence of input angles  $\Theta_1^k$ , there are as many as six sets of configuration angles  $\vec{\Theta} = (\Theta_2, \Theta_3, \Theta_4, \Theta_5)_i$ ,  $i=1, \dots, 6$  that define the assemblies of the linkage associated with each input angle. In order to sort the roots among the assemblies, we use the Jacobian of the loop equations. Compute the derivative of the loop equations (18), (19), (20) and (21) to obtain:

$$\Delta\ell_1 : l_1\dot{\Theta}_1 + b_1\dot{\Theta}_2e^{-i\gamma} - b_2\dot{\Theta}_4e^{i\eta} = 0 \quad (41)$$

$$\Delta\ell_2 : l_1\dot{\Theta}_1 + l_2\dot{\Theta}_2 + l_3\dot{\Theta}_3 - l_4\dot{\Theta}_4 - l_5\dot{\Theta}_5 = 0 \quad (42)$$

$$\Delta\ell_1^* : l_1\dot{\Theta}_1\Theta_1^{-2} + b_1\dot{\Theta}_2\Theta_2^{-2}e^{i\gamma} - b_2\dot{\Theta}_4\Theta_4^{-2}e^{-i\eta} = 0 \quad (43)$$

$$\Delta\ell_2^* : l_1\dot{\Theta}_1\Theta_1^{-2} + l_2\dot{\Theta}_2\Theta_2^{-2} + l_3\dot{\Theta}_3\Theta_3^{-2} - l_4\dot{\Theta}_4\Theta_4^{-2} - l_5\dot{\Theta}_5\Theta_5^{-2} = 0 \quad (44)$$

Factor out the derivative vector  $\dot{\Theta} = (\dot{\Theta}_1, \dot{\Theta}_2, \dot{\Theta}_3, \dot{\Theta}_4, \dot{\Theta}_5)$ , and obtain the Jacobian matrix:

$$[\Delta\ell(\Theta_k)] = \begin{bmatrix} l_1 & b_1e^{-i\gamma} & 0 & -b_2e^{i\eta} & 0 \\ l_1 & l_2 & l_3 & -l_4 & -l_5 \\ -l_1\Theta_1^{-2} & -b_1e^{i\gamma}\Theta_2^{-2} & 0 & b_2e^{-i\eta}\Theta_4^{-2} & 0 \\ -l_1\Theta_1^{-2} & -l_2\Theta_2^{-2} & -l_3\Theta_3^{-2} & l_4\Theta_4^{-2} & l_5\Theta_5^{-2} \end{bmatrix} \quad (45)$$

In order to sort the roots among the assemblies of the six-bar linkage, we approximate the complex loop equations using the Jacobian, and obtain:

$$[\Delta\ell(\Theta_i^k)](\Psi - \Theta_i^k) = 0 \quad (46)$$

where  $\Psi$  approximates the value  $\Theta_i^{k+1}$  associated with the input angle  $\Theta_1^{k+1}$  and is near to the assembly defined by  $\Theta_i^k$ . It is then a matter of identifying which of the root  $\Theta_i^{k+1}$  is closest to  $\Psi$  on the i-th circuit, in order to match the assemblies. This provides a rapid and exact method to determine a sequence of configuration angles for each assembly in order to animate the six-bar linkage.

# References

- S. Balasubramanian, J. Klein, and E. Burdet. Robot-assisted rehabilitation of hand function. *Current opinion in neurology*, 23(6):661, 2010. [3](#), [11](#)
- M. Bouzit, G. Burdea, G. Popescu, and R. Boian. The rutgers master ii-new design force-feedback glove. *Mechatronics, IEEE/ASME Transactions on*, 7(2):256–263, 2002. [3](#), [30](#), [38](#)
- B.R. Brewer, S.K. McDowell, and L.C. Worthen-Chaudhari. Poststroke upper extremity rehabilitation: a review of robotic systems and clinical results. *Topics in stroke rehabilitation*, 14(6):22–44, 2007. [2](#)
- E.B. Brokaw, I. Black, R.J. Holley, and P.S. Lum. Hand spring operated movement enhancer (handsome): a portable, passive hand exoskeleton for stroke rehabilitation. *Neural Systems and Rehabilitation Engineering, IEEE Transactions on*, 19(4):391–399, 2011. [13](#), [19](#), [20](#), [29](#), [30](#)
- T.S Buchanan, D.G Lloyd, K. Manal, and T.F Besier. Neuromusculoskeletal modeling: estimation of muscle forces and joint moments and movements from measurements of neural command. *Journal of applied biomechanics*, 20(4):367, 2004. [84](#)
- B. Buchholz and T.J. Armstrong. A kinematic model of the human hand to evaluate its prehensile capabilities. *Journal of biomechanics*, 25(2):149–162, 1992. [44](#)
- TMW Burton, R. Vaidyanathan, SC Burgess, AJ Turton, and C. Melhuish. Development of a parametric kinematic model of the human hand and a novel

## REFERENCES

---

- robotic exoskeleton. In *Rehabilitation Robotics (ICORR), 2011 IEEE International Conference on*, pages 1–7. IEEE, 2011. [3](#), [19](#), [23](#), [30](#)
- C. Bütefisch, H. Hummelsheim, P. Denzler, and K.H. Mauritz. Repetitive training of isolated movements improves the outcome of motor rehabilitation of the centrally paretic hand. *Journal of the neurological sciences*, 130(1):59–68, 1995. [1](#)
- L.S. Cardoso, R.M.E.M. da Costa, A. Piovesana, M. Costa, L. Penna, AC Crispin, J. Carvalho, H. Ferreira, M.L. Lopes, G. Brandao, et al. Using virtual environments for stroke rehabilitation. In *Virtual Rehabilitation, 2006 International Workshop on*, pages 1–5. IEEE, 2006. [4](#)
- A. Chiri, F. Giovacchini, N. Vitiello, E. Cattin, S. Roccella, F. Vecchi, and MC Carrozza. Handexos: towards an exoskeleton device for the rehabilitation of the hand. In *Intelligent Robots and Systems, 2009. IROS 2009. IEEE/RSJ International Conference on*, pages 1106–1111. IEEE, 2009. [3](#), [10](#), [19](#), [21](#), [27](#), [30](#)
- BH Choi and HR Choi. A semi-direct drive hand exoskeleton using ultrasonic motor. In *Robot and Human Interaction, 1999. RO-MAN'99. 8th IEEE International Workshop on*, pages 285–290. IEEE, 1999. [3](#), [39](#)
- R. Datta and K. Deb. Multi-objective design and analysis of robot gripper configurations using an evolutionary-classical approach. In *Proceedings of the 13th annual conference on Genetic and evolutionary computation*, pages 1843–1850. ACM, 2011. [60](#)
- Carlo J. De, L. The use of surface electromyography in biomechanics. *Journal of applied biomechanics*, 13:135–163, 1997. [84](#)
- L. Diller. Post-stroke rehabilitation practice guidelines. *International handbook of neuropsychological rehabilitation. Critical issues in neurorehabilitation*, pages 167–182, 2000. [1](#)
- R. Drillis, R. Contini, and M. Bluestein. Body segment parameters. *Artificial limbs*, 8(1):44–66, 1964. [44](#)

## REFERENCES

---

- A.G. Erdman. Three and four precision point kinematic synthesis of planar linkages. *Mechanism and Machine Theory*, 16(3):227–245, 1981. 60
- I.H. Ertas, E. Hocaoglu, D.E. Barkana, and V. Patoglu. Finger exoskeleton for treatment of tendon injuries. In *Rehabilitation Robotics, 2009. ICORR 2009. IEEE International Conference on*, pages 194–201. IEEE, 2009. 3, 10, 19, 22, 30
- H. Fang, Z. Xie, and H. Liu. An exoskeleton master hand for controlling dlr/hit hand. In *Intelligent Robots and Systems, 2009. IROS 2009. IEEE/RSJ International Conference on*, pages 3703–3708. IEEE, 2009. 3
- Festo-Company. Festo exohand. <http://www.festo.com/cms/encorp/12713.htm>, 2012. 15, 19, 24, 27, 28, 30
- M. Fontana, A. Dettori, F. Salsedo, and M. Bergamasco. Mechanical design of a novel hand exoskeleton for accurate force displaying. In *Robotics and Automation, 2009. ICRA '09. IEEE International Conference on*, pages 1704–1709. IEEE, 2009. 3, 38
- A. Frisoli, F. Salsedo, M. Bergamasco, B. Rossi, and M.C. Carboncini. A force-feedback exoskeleton for upper-limb rehabilitation in virtual reality. *Applied Bionics and Biomechanics*, 6(2):115–126, 2009. 6, 90
- A. Frisoli, C. Loconsole, R. Bartalucci, and M. Bergamasco. A new bounded jerk on-line trajectory planning for mimicking human movements in robot-aided neurorehabilitation. *Robotics and Autonomous Systems*, 2012. 90
- Y. Fu, P. Wang, and S. Wang. Development of a multi-dof exoskeleton based machine for injured fingers. In *Intelligent Robots and Systems, 2008. IROS 2008. IEEE/RSJ International Conference on*, pages 1946–1951. IEEE, 2008. 3, 18, 19, 22, 27, 29
- Y. Fu, Q. Zhang, F. Zhang, and Z. Gan. Design and development of a hand rehabilitation robot for patient-cooperative therapy following stroke. In *Mechatronics and Automation (ICMA), 2011 International Conference on*, pages 112–117. IEEE, 2011. 25, 27, 29

## REFERENCES

---

- J. Gülke, N.J. Wachter, T. Geyer, H. Schöll, G. Apic, M. Mentzel, et al. Motion coordination patterns during cylinder grip analyzed with a sensor glove. *The Journal of hand surgery*, 35(5):797, 2010. [41](#), [42](#), [43](#), [44](#), [45](#), [47](#), [53](#), [55](#), [60](#), [61](#), [76](#)
- Y. Hasegawa, Y. Mikami, K. Watanabe, and Y. Sankai. Five-fingered assistive hand with mechanical compliance of human finger. In *Robotics and Automation, 2008. ICRA 2008. IEEE International Conference on*, pages 718–724. IEEE, 2008. [3](#), [4](#)
- P. Heo, G.M Gu, S.j Lee, K. Rhee, and J. Kim. Current hand exoskeleton technologies for rehabilitation and assistive engineering. *International Journal of Precision Engineering and Manufacturing*, 13(5):807–824, 2012. [10](#), [11](#)
- NSK Ho, KY Tong, XL Hu, KL Fung, XJ Wei, W. Rong, and EA Susanto. An emg-driven exoskeleton hand robotic training device on chronic stroke subjects: Task training system for stroke rehabilitation. In *Rehabilitation Robotics (ICORR), 2011 IEEE International Conference on*, pages 1–5. IEEE, 2011. [3](#), [18](#), [19](#), [21](#), [27](#), [29](#)
- H.K. In, K.J. Cho, K.R. Kim, and B.S. Lee. Jointless structure and under-actuation mechanism for compact hand exoskeleton. In *Rehabilitation Robotics (ICORR), 2011 IEEE International Conference on*, pages 1–6. IEEE, 2011. [4](#)
- J. Iqbal, N.G Tsagarakis, A.E Fiorilla, and D.G Caldwell. A portable rehabilitation device for the hand. In *Engineering in Medicine and Biology Society (EMBC), 2010 Annual International Conference of the IEEE*, pages 3694–3697. IEEE, 2010. [10](#), [17](#), [19](#), [21](#), [27](#), [29](#)
- S. Ito, H. Kawasaki, Y. Ishigure, M. Natsume, T. Mouri, and Y. Nishimoto. A design of fine motion assist equipment for disabled hand in robotic rehabilitation system. *Journal of the Franklin Institute*, 348(1):79–89, 2011. [17](#), [24](#), [27](#), [29](#)
- D. Jack, R. Boian, A.S. Merians, M. Tremaine, G.C. Burdea, S.V. Adamovich, M. Recce, and H. Poizner. Virtual reality-enhanced stroke rehabilitation. *Neu-*

## REFERENCES

---

- ral Systems and Rehabilitation Engineering, IEEE Transactions on*, 9(3):308–318, 2001. 4
- H. Kawasaki, S. Ito, Y. Ishigure, Y. Nishimoto, T. Aoki, T. Mouri, H. Sakaeda, and M. Abe. Development of a hand motion assist robot for rehabilitation therapy by patient self-motion control. In *Rehabilitation Robotics, 2007. ICORR 2007. IEEE 10th International Conference on*, pages 234–240. IEEE, 2007. 3
- Kinetec-Maestra-Hand. Kinetec maestra portable hand. <http://www.pattersonmedical.com/app.aspx?cmd=getProduct>, 2011. 10, 19, 20, 27, 28, 29
- T. Kitada, Y. Kunii, and H. Hashimoto. 20 dof five fingered glove type haptic interface-sensor glove ii. *Journal of Robotics and Mechatronics*, 9:171–176, 1997. 3, 38, 54
- T. Kline, D. Kamper, and B. Schmit. Control system for pneumatically controlled glove to assist in grasp activities. In *Rehabilitation Robotics, 2005. ICORR 2005. 9th International Conference on*, pages 78–81. IEEE, 2005. 4
- A. Konak, D.W. Coit, and A.E. Smith. Multi-objective optimization using genetic algorithms: A tutorial. *Reliability Engineering & System Safety*, 91(9):992–1007, 2006. 60
- H.I. Krebs, S. Mernoff, S.E. Fasoli, R. Hughes, J. Stein, and N. Hogan. A comparison of functional and impairment-based robotic training in severe to moderate chronic stroke: a pilot study. *NeuroRehabilitation*, 23(1):81–87, 2008. 2
- N.G. Kutner, R. Zhang, A.J. Butler, S.L. Wolf, and J.L. Alberts. Quality-of-life change associated with robotic-assisted therapy to improve hand motor function in patients with subacute stroke: a randomized clinical trial. *Physical therapy*, 90(4):493–504, 2010. 10, 19, 27, 28, 30
- G. Kwakkel, B.J. Kollen, and H.I. Krebs. Effects of robot-assisted therapy on upper limb recovery after stroke: a systematic review. *Neurorehabilitation and neural repair*, 22(2):111–121, 2008. 2

## REFERENCES

---

- M.J. Lelieveld and T. Maeno. Design and development of a 4 dof portable haptic interface with multi-point passive force feedback for the index finger. In *Robotics and Automation, 2006. ICRA 2006. Proceedings 2006 IEEE International Conference on*, pages 3134–3139. IEEE, 2006. [3](#)
- J. Li, R. Zheng, Y. Zhang, and J. Yao. ihandrehab: An interactive hand exoskeleton for active and passive rehabilitation. In *Rehabilitation Robotics (ICORR), 2011 IEEE International Conference on*, pages 1–6. IEEE, 2011. [3](#), [25](#), [27](#), [29](#)
- C. Loconsole, A. Frisoli, M. Bergamasco, M. Mozaffari-Foumashi, M. Troncossi, and V. Parenti-Castelli. An emg-based robotic hand exoskeleton for bilateral training of grasp. *IEEE WHC 2013, World Haptics Conference 2013, and The 5th Joint Eurohaptics Conference and IEEE Haptics Symposium, Daejeon, Korea, April 14-17, 2013*, 2013a. [90](#)
- C. Loconsole, A. Frisoli, M. Bergamasco, M. Mozaffari-Foumashi, M. Troncossi, and V. Parenti-Castelli. A motor imagery bci approach to robotic-assisted neuro-motor rehabilitation of reaching and hand grasping in stroke. *13th International Conference on Rehabilitation Robotics (ICORR), University of Washington campus, June 24-26, 2013*, 2013b. [92](#)
- T.J. Lord, D.M. Keefe, Y. Li, N. Stoykov, and D. Kamper. Development of a haptic keypad for training finger individuation after stroke. In *Virtual Rehabilitation (ICVR), 2011 International Conference on*, pages 1–2. IEEE, 2011. [3](#)
- R.C.V. Loureiro and W.S. Harwin. Reach & grasp therapy: design and control of a 9-dof robotic neuro-rehabilitation system. In *Rehabilitation Robotics, 2007. ICORR 2007. IEEE 10th International Conference on*, pages 757–763. IEEE, 2007. [3](#), [19](#), [23](#), [27](#), [30](#)
- L. Lucas, M. DiCicco, and Y. Matsuoka. An emg-controlled hand exoskeleton for natural pinching. *Journal of Robotics and Mechatronics*, 16:482–488, 2004. [3](#)
- D. Manocha and S. Krishnan. Solving algebraic systems using matrix computations. *ACM SIGSAM Bulletin*, 30(4):4–21, 1996. [108](#)

## REFERENCES

---

- J.M. McCarthy. *Geometric design of linkages*, volume 11. Springer Verlag, 2000. [46](#), [101](#), [110](#)
- J. Mehrholz, T. Platz, J. Kugler, and M. Pohl. Electromechanical and robot-assisted arm training for improving arm function and activities of daily living after stroke. *Stroke*, 40(5):e392–e393, 2009. [2](#)
- M. Mozaffari-Foumashi, M. Troncossi, and V. Parenti-Castelli. A study on the rehabilitation hand exoskeletons. *Ettore Funaioli Workshop*, 2010. [3](#)
- M. Mozaffari-Foumashi, M. Troncossi, and V. Parenti-Castelli. State-of-the-art of hand exoskeleton systems. *DIEM Technical Report*, pages 1–54, 2011. [3](#)
- M. Mozaffari-Foumashi, M. Troncossi, and V. Parenti-Castelli. Design of a new hand exoskeleton for rehabilitation of post-stroke patients. *Romansy 19-Robot Design, Dynamics and Control*, page 159, 2013. [6](#), [90](#)
- M. Mulas, M. Folgheraiter, and G. Gini. An emg-controlled exoskeleton for hand rehabilitation. In *Rehabilitation Robotics, 2005. ICORR 2005. 9th International Conference on*, pages 371–374. IEEE, 2005. [3](#), [10](#), [17](#), [19](#), [20](#), [27](#), [29](#)
- A. Muzumdar. *Powered upper limb prostheses: control, implementation and clinical application*. Springer, 2004. [84](#)
- S. Nakagawara, H. Kajimoto, N. Kawakami, S. Tachi, and I. Kawabuchi. An encounter-type multi-fingered master hand using circuitous joints. In *Robotics and Automation, 2005. ICRA 2005. Proceedings of the 2005 IEEE International Conference on*, pages 2667–2672. IEEE, 2005. [3](#), [38](#)
- R. Oboe, O.A. Daud, S. Masiero, F. Oscari, and G. Rosati. Development of a haptic teleoperation system for remote motor and functional evaluation of hand in patients with neurological impairments. In *Advanced Motion Control, 2010 11th IEEE International Workshop on*, pages 518–523. IEEE, 2010. [22](#)
- T.S. Olsen. Arm and leg paresis as outcome predictors in stroke rehabilitation. *Stroke*, 21(2):247–251, 1990. [1](#)

## REFERENCES

---

- G. Pfurtscheller and FH Lopes da Silva. Event-related eeg/meg synchronization and desynchronization: basic principles. *Clinical neurophysiology*, 110(11):1842–1857, 1999. [5](#)
- G.B. Prange, M.J.A. Jannink, C.G.M. Groothuis-Oudshoorn, H.J. Hermens, M.J. IJzerman, et al. Systematic review of the effect of robot-aided therapy on recovery of the hemiparetic arm after stroke. *Journal of rehabilitation research and development*, 43(2):171, 2006. [2](#)
- Y. Ren, H. Park, and L. Zhang. Developing a whole-arm exoskeleton robot with hand opening and closing mechanism for upper limb stroke rehabilitation. In *Rehabilitation Robotics, 2009. ICORR 2009. IEEE International Conference on*, pages 761–765. IEEE, 2009. [10](#), [19](#), [25](#), [27](#), [30](#)
- G. Rosati, S. Cenci, G. Boschetti, D. Zanotto, and S. Masiero. Design of a single-dof active hand orthosis for neurorehabilitation. In *Rehabilitation Robotics, 2009. ICORR 2009. IEEE International Conference on*, pages 161–166. IEEE, 2009. [10](#), [19](#), [27](#), [29](#)
- L. Rosenstein, A.L. Ridgel, A. Thota, B. Samame, and J.L Alberts. Effects of combined robotic therapy and repetitive task practice on upper-extremity function in a patient with chronic stroke. *Therapy*, 62:000–000, 2008. [22](#)
- I. Sarakoglou, N.G. Tsagarakis, and D.G. Caldwell. Occupational and physical therapy using a hand exoskeleton based exerciser. In *Intelligent Robots and Systems, 2004. (IROS 2004). Proceedings. 2004 IEEE/RSJ International Conference on*, volume 3, pages 2973–2978. IEEE, 2004. [17](#), [19](#), [25](#), [27](#), [29](#)
- D. Sasaki, T. Noritsugu, M. Takaiwa, and H. Yamamoto. Wearable power assist device for hand grasping using pneumatic artificial rubber muscle. In *Robot and Human Interactive Communication, 2004. ROMAN 2004. 13th IEEE International Workshop on*, pages 655–660. IEEE, 2004. [4](#)
- C.N Schabowsky, S.B Godfrey, R.J Holley, and P.S Lum. Development and pilot testing of hexorr: hand exoskeleton rehabilitation robot. *Journal of neuroengineering and rehabilitation*, 7(1):36, 2010. [10](#), [17](#), [19](#), [21](#), [27](#), [29](#)

## REFERENCES

---

- B.L. Shields, J.A. Main, S.W. Peterson, and A.M. Strauss. An anthropomorphic hand exoskeleton to prevent astronaut hand fatigue during extravehicular activities. *Systems, Man and Cybernetics, Part A: Systems and Humans, IEEE Transactions on*, 27(5):668–673, 1997. [4](#)
- F. Simoncini, M. Bergamasco, and F. Salsedo. Kinematic design of a two contact points haptic interface for the thumb and index fingers of the hand. *Journal of Mechanical Design*, 129:521, 2007. [3](#)
- G.S. Soh and J.M. McCarthy. The synthesis of six-bar linkages as constrained planar 3r chains. *Mechanism and Machine Theory*, 43(2):160–170, 2008. [46](#), [101](#)
- P. Stergiopoulos, P. Fuchs, and C. Laugeau. Design of a 2-finger hand exoskeleton for vr grasping simulation. *Eurohaptics, Dublin, Ireland*, pages 80–93, 2003. [3](#)
- Z. Sun, X. Miao, and X. Li. Design of a bidirectional force feedback dataglove based on pneumatic artificial muscles. In *Mechatronics and Automation, 2009. ICMA 2009. International Conference on*, pages 1767–1771. IEEE, 2009. [3](#)
- K. Tadano, M. Akai, K. Kadota, and K. Kawashima. Development of grip amplified glove using bi-articular mechanism with pneumatic artificial rubber muscle. In *Robotics and Automation (ICRA), 2010 IEEE International Conference on*, pages 2363–2368. IEEE, 2010. [4](#)
- CD Takahashi, L. Der-Yeghiaian, VH Le, and SC Cramer. A robotic device for hand motor therapy after stroke. In *Rehabilitation Robotics, 2005. ICORR 2005. 9th International Conference on*, pages 17–20. IEEE, 2005. [3](#), [22](#)
- C.D Takahashi, L. Der-Yeghiaian, V. Le, R.R Motiwala, and S.C Cramer. Robot-based hand motor therapy after stroke. *Brain*, 131(2):425–437, 2008. [3](#), [10](#), [19](#), [27](#), [30](#)
- M. Troncossi, M. Mozaffari-Foumashi, M. Carricato, and V. Parenti-Castelli. Feasibility study of a hand exoskeleton for rehabilitation of post-stroke patients. *Proceedings of ESDA 2012 - 11th Biennial ASME Conference on Engineering Systems Design and Analysis*, Nantes(France), 2012. [11](#)

- L. Turki and P. Coiffet. Dextrous telemanipulation with force feedback in virtual reality. In *Proc. International Conference on Artificial Reality and Tele-Existence*, volume 95, pages 193–202, 1995. 3
- J. Wang, J. Li, Y. Zhang, and S. Wang. Design of an exoskeleton for index finger rehabilitation. In *Engineering in Medicine and Biology Society, 2009. EMBC 2009. Annual International Conference of the IEEE*, pages 5957–5960. IEEE, 2009. 3, 17, 18, 25, 27, 29
- WaveFlex-Hand. Waveflex hand cpm device. <http://www.ottobock.ca/cps/rde/xchg/obusen/hs.xsl/15712.html>, 2011. 10, 19, 20, 28, 29
- A. Wege and G. Hommel. Development and control of a hand exoskeleton for rehabilitation of hand injuries. In *Intelligent Robots and Systems, 2005. (IROS 2005). 2005 IEEE/RSJ International Conference on*, pages 3046–3051. IEEE, 2005. 3, 10, 13, 17, 24, 27, 29
- E.T. Wollbrecht, D.J. Reinkensmeyer, and A. Perez-Gracia. Single degree-of-freedom exoskeleton mechanism design for finger rehabilitation. In *Rehabilitation Robotics (ICORR), 2011 IEEE International Conference on*, pages 1–6. IEEE, 2011. 3, 10, 18, 19, 22, 27, 29
- TT Worsnopp, MA Peshkin, JE Colgate, and DG Kamper. An actuated finger exoskeleton for hand rehabilitation following stroke. In *Rehabilitation Robotics, 2007. ICORR 2007. IEEE 10th International Conference on*, pages 896–901. IEEE, 2007. 3, 24, 27
- J. Wu, J. Huang, Y. Wang, and K. Xing. A wearable rehabilitation robotic hand driven by pm-ts actuators. *Intelligent Robotics and Applications*, pages 440–450, 2010. 10, 18, 19, 23, 27, 29
- H. Yamaura, K. Matsushita, R. Kato, and H. Yokoi. Development of hand rehabilitation system for paralysis patient–universal design using wire-driven mechanism–. In *Engineering in Medicine and Biology Society, 2009. EMBC 2009. Annual International Conference of the IEEE*, pages 7122–7125. IEEE, 2009. 3, 10, 17, 19, 23, 29

## REFERENCES

---

- G. Zong, X. Pei, J. Yu, and S. Bi. Classification and type synthesis of 1-dof remote center of motion mechanisms. *Mechanism and Machine Theory*, 43 (12):1585–1595, 2008. [18](#)